

Antti Saikko

POSITIONING METHODS IN DECT-2020 NR NETWORKS

Master of Science Thesis
Faculty of Information Technology and Communication Sciences
Examiners: Jukka Talvitie, Prof. Mikko Valkama
March 2024

ABSTRACT

Antti Saikko: Positioning Methods in DECT-2020 NR Networks
Master of Science Thesis
Tampere University
Electrical Engineering
March 2024

DECT-2020 NR is a wireless communication technology which is developed to support especially various Internet of Things (IoT) applications. DECT-2020 NR is part of the official 5G standards, and it meets the performance requirements of massive machine type communications (mMTC) and ultra reliable and low latency communications (URLLC) set for 5G technologies. DECT-2020 NR supports mesh networking which enables direct communication between devices. The mesh networking capabilities of DECT-2020 NR support high density of devices and autonomous routing which enables massive scale of network.

Device positioning in DECT-2020 NR networks is an important feature to enable wide-ranging use cases. DECT-2020 NR offers interesting possibilities regarding to positioning because the device density may be high. Positioning is based on different measurable characteristics of the network and signals, and the device positions are estimated based on these measurements. Wireless communication networks contain a wealth of measurable information, for example, signal strength, distance, or angle, and this information can be used for positioning. However, support for high density of devices and requirements for power-efficiency cause some challenges for positioning.

The goal of this master's thesis is to study the possibilities of efficient device positioning in DECT-2020 NR mesh networks. The thesis is divided into two parts: literary review and simulated positioning results. Internet of Things, DECT-2020 NR, and positioning in a general level are discussed in the literature review part. Based on the literature review, potential positioning methods in DECT-2020 NR networks are methods based on time and angle measurements, as well as methods based on signal strength. The simulation part of the thesis focuses on the study of time-based and angle-based positioning methods. The positioning results based on DECT-2020 NR signal characteristics show that it is possible to achieve good positioning accuracies with the methods studied in the thesis. However, there are some challenges in practice which affect the positioning accuracies, for example, clock error in time-based methods.

The optimization of efficient positioning is based on methods that would enable to select the most useful measurements for positioning. Using these methods, positioning would be efficient in terms of computation and power consumption, but good positioning accuracy should still be achievable. We found from the simulated results that it has an influence for the positioning accuracy how the selection of measurements is done. Based on the results, with an optimal method of measurement selection, it is possible to achieve positioning accuracies near the ideal method. The ideal method requires, for example, more power and increases the computational load. Further development of measurement selection method studied in this thesis is a potential option for implementing effective positioning capabilities in DECT-2020 NR networks.

Keywords: DECT-2020 NR, positioning, localization, mesh network, Internet of Things

The originality of this thesis has been checked using the Turnitin OriginalityCheck service.

TIIVISTELMÄ

Antti Saikko: Paikannusmenetelmät DECT-2020 NR -verkoissa

Diplomityö

Tampereen yliopisto

Sähkötekniikka

Maaliskuu 2024

DECT-2020 NR on langattoman viestinnän verkkoteknologia, joka on kehitetty erityisesti tukemaan erilaisia esineiden internetin sovelluksia. DECT-2020 NR on virallisesti hyväksytty 5G-standardien joukkoon, ja se täyttää 5G-teknologioiden suorituskyvyvaatimukset massiivisen koneiden välisen viestinnän (mMTC, massive machine type communications) sekä ultraluotettavan ja pienen viiveen (URLLC, ultra reliable and low latency communications) käytötapausten osalta. DECT-2020 NR tukee mesh-verkkotekniikkaa, jossa laitteet voivat kommunikoida suoraan keskenään. DECT-2020 NR:n mesh-tekniikka tukee suurta laitemäärää ja itsenäistä reititystä, jotka mahdollistavat verkon massiivisen skaalautumisen.

Laitteiden paikannus on yksi tärkeä ominaisuus DECT-2020 NR -verkoissa monipuolisten käyttökohteiden mahdollistamiseksi. DECT-2020 NR tarjoaa mielenkiintoisia mahdollisuuksia paikannusta ajatellen, koska verkon laitetiheys voi olla suuri. Paikannus perustuu erilaisiin verkon ja signaalien mitattaviin ominaisuuksiin, joihin perustuen laitteen sijaintia voidaan arvioida. Verkoissa on saatavilla reilusti tarkan laitepaikannuksen mahdollistavaa informaatiota, kuten signaalin voimakkuus, etäisyys tai kulma. DECT-2020 NR:n tuki suurelle määrälle laitteita ja vaatimukset energiatehokkuudelle aiheuttavat kuitenkin myös omat haasteensa paikannukseen.

Tämän diplomityön tavoitteena on tutkia tehokkaan laitepaikannuksen mahdollisuuksia DECT-2020 NR mesh-verkossa. Työ jakaantuu kahteen osaan: kirjallisuustutkimukseen ja simuloituihin paikannustuloksiin. Työn kirjallisuustutkimuksessa käsitellään esineiden internetiä, DECT-2020 NR -teknologiaa sekä paikannusta yleisesti. Työn kirjallisuustutkimuksen perusteella potentiaalisia paikannusmenetelmiä DECT-2020 NR -verkoissa ovat aika- ja kulmamittauksiin perustuvat menetelmät sekä signaalin voimakkuuteen perustuvat menetelmät. Työn simulaatio-osiossa keskitytään tutkimaan aika- ja kulmaperusteisia menetelmiä. DECT-2020 NR signaalien ominaisuuksiin perustuvat simuloitut paikannustulokset osoittavat, että hyvien paikannustarkkuuksien saavuttaminen on mahdollista työssä tutkituilla menetelmillä. Käytännön toteutuksessa on kuitenkin joitakin paikannustarkkuuksiin vaikuttavia haasteita, kuten kellovirhe aikamittausmenetelmässä.

Paikannusmenetelmien tehokkuuden optimointi perustuu menetelmiin, joilla pystyttäisiin valitsemaan paikannuksen kannalta hyödyllisimmät mittaukset. Tällä tavoin paikannus olisi tehokasta esimerkiksi laskennan ja virrankulutuksen kannalta, mutta hyvä paikannustarkkuus olisi kuitenkin saavutettavissa. Simuloiduista tuloksista huomattiin, että ankkureiden valinnalla on merkitystä saavutettaviin paikannustarkkuuksiin. Tulosten perusteella ankkureiden valinnan optimaalisesti valitsevalla menetelmällä on teoreettisesti mahdollista saavuttaa paikannustarkkuuksia, jotka eivät juuri poikkea ideaalisesta, esimerkiksi laskenta- ja energiatehokkaimmista vaatimammasta, vertailutapauksesta. Työssä tutkitun ankkurien valintamenetelmän jatkokehittäminen on potentiaalinen vaihtoehto tehokkaan laitepaikannuksen ominaisuuden toteuttamiseen DECT-2020 NR -verkoissa.

Avainsanat: DECT-2020 NR, paikannus, mesh-verkko, esineiden internet

Tämän julkaisun alkuperäisyys on tarkastettu Turnitin OriginalityCheck -ohjelmalla.

PREFACE

Writing the master's thesis has been an extensive process, and my university studies as a whole have led me to this goal. I have combined my studies with the sport I love: orienteering. Training as a part of my everyday life and competitions on weekends have gone hand in hand with my studies, and I am pleased that this combination of study and sport has worked out so well.

In orienteering, I navigate through the forest, moving from control point to another, from start to finish, as quickly as possible, challenging my physical capacity. My goal is to navigate smoothly based on a plan created from a map. However, sometimes I also need to stop and locate myself by comparing my position with the landmarks on the map and the surrounding terrain. This very similar principle forms the basis of the positioning covered in my thesis, although the perspective is completely different.

I would like to express my gratitude to Tampere University for providing me the opportunity to work as a part-time research assistant in the Unit of Electrical Engineering, and additionally, for allowing me to pursue this thesis on the topic of positioning. Through this experience, I have also gained valuable insights into the cooperation between the university and companies.

I am deeply grateful to my supervisor and examiner Jukka Talvitie, who helped me to find this interesting topic for thesis and supported me throughout the thesis process. I would also like to express my appreciation to Professor Mikko Valkama, the second examiner of the thesis.

During my thesis work, my supervisor Jukka has guided me deeper into the world of positioning theory. His assistance in understanding both the basic principles of positioning and more complex issues has been invaluable. Jukka's inspiring guidance has increased my interest in the subject, and he has also provided essential feedback to improve the structure and content of my thesis.

Lastly, I want to express my deepest gratitude to my family, whose support has been essential. They have made it possible for me to reach this and other important milestones in my life. Thank you!

Tampere, 22nd March 2024

Antti Saikko

CONTENTS

1.	Introduction	1
1.1	Background	1
1.2	Objective of the Thesis and Research Method	2
1.3	Structure of the Thesis	3
2.	Internet of Things (IoT)	5
2.1	General Aspects of Internet of Things.	5
2.1.1	Definition	5
2.1.2	Classification.	6
2.1.3	Architecture and Layers	7
2.1.4	Main Topologies	8
2.2	Non-cellular Internet of Things	8
2.3	Cellular Internet of Things	10
2.4	Characteristics of Non-cellular and Cellular IoT Technologies	12
3.	DECT-2020 New Radio (NR)	13
3.1	Benefits and Opportunities	13
3.2	Key Organizations Related to DECT-2020 NR Standardization and Development.	14
3.2.1	ITU	15
3.2.2	ETSI	15
3.2.3	DECT Forum.	16
3.3	DECT-2020 NR Development and Standardization Process	16
3.4	DECT-2020 NR Technology Overview	20
3.4.1	Technical Specifications	20
3.4.2	Terminology	20
3.4.3	System and Network Architectures	21
3.4.4	Mesh System Operation	21
3.4.5	Mesh Routing	22
3.4.6	Interworking with 3GPP 5G Networks	23
4.	Positioning	24
4.1	Positioning Use Cases and Applications.	24
4.2	Related Work	25
4.3	Positioning methods	26
4.3.1	Time of Arrival (ToA).	27
4.3.2	Time Difference of Arrival (TDoA)	31

4.3.3	Received Signal Strength (RSS)	32
4.3.4	Angle of Arrival (AoA)	33
4.4	Theoretical Positioning Bounds	35
4.4.1	Cramér-Rao Lower Bound (CRLB)	35
4.4.2	Cramér-Rao Lower Bound for Time Estimation	38
4.4.3	Cramér-Rao Lower Bound for Angle Estimation	40
4.4.4	Position Error Bound (PEB)	41
4.5	Positioning Tracking and Kalman Filter	41
4.5.1	Commonly Used Filters for Position Tracking	42
4.5.2	Structure of Kalman Filter and Extended Kalman Filter	43
5.	Methodology	47
5.1	Cramér-Rao Lower Bound with DECT-2020 NR Numerologies	47
5.2	Selecting the Best Anchors for Positioning	48
6.	Results and Analysis	54
6.1	Cramér-Rao Lower Bounds for Time of Arrival	54
6.2	Cramér-Rao Lower Bounds for Angle of Arrival	56
6.3	Position Error Bound and Selecting the Best Anchors for Positioning	60
7.	Conclusion	67
	References	70

LIST OF FIGURES

4.1	ToA trilateration in the theoretical error-free 2D case. The intersection of the circles defines the position of the user device.	29
4.2	ToA trilateration in the 2D case with error. The intersection of the circles defines the area with high probability for the user device position.	30
4.3	TDoA in the theoretical error-free 2D case. The intersection of the hyperbolas defines the position of the user device.	32
4.4	AoA in the theoretical error-free 2D case. The intersection of the angle measurements defines the position of the user device.	34
5.1	Example of a confidence ellipse for positioning using ToA measurements with errors.	49
5.2	Choosing the best anchors in the AoA positioning. Examples of different anchor selections.	51
5.3	Choosing the best anchors in the AoA. All 5 possible anchors selected. . .	52
6.1	CRLBs for ToA based range estimation with DECT-2020 NR subcarrier spacing of 108 kHz.	55
6.2	Comparison of CRLBs for ToA based range estimation with DECT-2020 NR numerologies.	56
6.3	CRLBs for AoA based angle estimation with different numbers of antenna elements. Parameters used: antenna spacing $d = \frac{\lambda}{2}$ and antenna direction angle $\alpha = 60^\circ$	57
6.4	CRLBs for AoA based angle estimation with different antenna spacing values. Parameters used: number of antenna elements $L = 4$ and antenna direction angle $\alpha = 60^\circ$	58
6.5	CRLBs for AoA based angle estimation with different antenna direction angles. Parameters used: number of antenna elements $L = 4$ and antenna spacing $d = \frac{\lambda}{2}$	58
6.6	CRLBs for AoA based angle estimation with different parameter combinations.	59
6.7	Comparison of methods for selecting the best anchors in the AoA positioning. Mean of PEB values from 1 000 simulation rounds. The grid edge length of the observation area is 100 m.	61

6.8	Comparison of methods for selecting the best anchors in the AoA positioning. 95th percentile of PEB values from 1 000 simulation rounds. The grid edge length of the observation area is 100 m.	62
6.9	Comparison of methods for selecting the best anchors in the AoA positioning. Standard deviation of PEB values from 1 000 simulation rounds. The grid edge length of the observation area is 100 m.	63
6.10	Comparison of methods for selecting the best anchors in the ToA positioning. Mean of PEB values from 1 000 simulation rounds. The grid edge length of the observation area is 100 m.	64
6.11	Comparison of methods for selecting the best anchors in the AoA positioning. Mean of PEB values from 1 000 simulation rounds. The grid edge length of the observation area is 150 m.	64
6.12	Comparison of methods for selecting the best anchors in the AoA positioning. Standard deviation of PEB values from 1 000 simulation rounds. The grid edge length of the observation area is 150 m.	65
6.13	Comparison of methods for selecting the best anchors in the AoA positioning. Mean of PEB values from 1 000 simulation rounds. The grid edge length of the observation area is 150 m.	66

LIST OF TABLES

2.1	Characteristics of non-cellular and cellular IoT technologies.	12
3.1	IMT-2020 technical performance requirements.	18
3.2	Timeline for the development of DECT-2020 NR.	19
5.1	Supported transmission numerologies in DECT-2020 NR, adapted from [66, pp. 9–10].	48
6.1	Values used in anchor selection simulations.	60

LIST OF ABBREVIATIONS

2D	two-dimensional
3D	three-dimensional
3G	third generation
3GPP	3rd Generation Partnership Project
4G	fourth generation
5G	fifth generation
AoA	angle of arrival
AWGN	additive white Gaussian noise
BLE	Bluetooth Low Energy
CDB	correlation database
CEN	European Committee for Standardization
CENELEC	European Committee for Electrotechnical Standardization
CRLB	Cramér-Rao lower bound
CSA	Connectivity Standards Alliance
CSS	chirp spread spectrum
CVG	convergence
D2D	device-to-device
DBPSK	differential binary phase-shift keying
DC	direct current
DECT	Digital Enhanced Cordless Telecommunications
DECT 5G-SRIT	DECT 5G-SRIT consists of two RIT components: DECT-2020 NR and 3GPP 5G NR. This term is used in particular by the ITU.
DECT-2020 NR	DECT-2020 New Radio. ETSI standard.
DL	downlink
DLC	data link control
DoA	direction of arrival
EC-GSM-IoT	extended coverage GSM IoT

EGPRS	Enhanced General Packet Radio Service
EKF	extended Kalman filter
eMBB	enhanced mobile broadband
EN	European Standard
ES	ETSI Standard
ESO	European Standards Organization
ETSI	European Telecommunications Standards Institute
EU	European Union
FDM	frequency division multiplexing
FIM	Fisher information matrix
FSK	frequency shift keying
FT	Fixed Termination point
GFSK	Gaussian frequency shift keying
GNSS	Global Navigation Satellite System
GPRS	General Packet Radio Service
GSM	Global System for Mobile Communications
HARQ	hybrid automatic repeat request
ICT	Information and Communications Technology
IEEE	Institute of Electrical and Electronics Engineers
IMT-2000	International Mobile Telecommunications-2000
IMT-2020	International Mobile Telecommunications-2020
IoE	Internet of Everything
IoT	Internet of Things
ISM	industrial, scientific and medical
ITU	International Telecommunication Union
ITU-R	International Telecommunication Union Radiocommunication Sector
KF	Kalman filter
LoS	line of sight
LPWA	low-power wide-area
LPWAN	low-power wide-area network
LTE-M	Long-Term Evolution Machine Type Communication

M2M	machine-to-machine
MAC	medium access control
MATLAB	MATrix LABoratory. Programming language and numeric computing software developed by MathWorks.
mMTC	massive machine type communications
N3IWF	non-3GPP interworking function
NB-IoT	Narrowband Internet of Things
NG-DECT	New Generation DECT
NG-RAN	Next Generation Radio Access Network
NLoS	non-line of sight
NR	New Radio
NR+	Abbreviation for DECT NR+. Basically a synonym for the DECT-2020 NR. This term is used in particular by the DECT Forum.
OFDM	orthogonal frequency division multiplexing
P2M	point-to-multipoint
P2P	point-to-point
PDF	probability density function
PEB	position error bound
PF	particle filter
PHY	physical layer
PL	path loss
PMF	probability mass function
PT	Portable Termination point
RD	Radio Device
RF	radio frequency
RFID	radio frequency identification
RIT	radio interface technology
RSS	received signal strength
RSSI	received signal strength indicator
RX	receiver
SNR	signal-to-noise ratio
SRIT	set of radio interface technologies

TC	Technical Committee
TDoA	time difference of arrival
TNGF	trusted non-3GPP gateway function
ToA	time of arrival
ToF	time of flight
ToT	time of transmission
TR	Technical Report
TS	Technical Specification
TX	transmitter
UE	user equipment
UKF	unscented Kalman filter
UL	uplink
ULE	Ultra Low Energy
UNB	ultra narrowband
URLLC	ultra reliable and low latency communications
WSN	wireless sensor network

1. INTRODUCTION

This Master of Science thesis introduces potential positioning methods in DECT-2020 NR. Therefore, one main topic to be considered is DECT-2020 NR, the first non-cellular 5G technology, which is specially designed for Internet of Things (IoT) environment. This thesis is done from the positioning perspective, and therefore, we will study the possible positioning bounds with DECT-2020 NR numerologies, and the possibilities to develop accurate and efficient positioning features in the related environment.

1.1 Background

DECT-2020 NR is a new wireless communication technology which is developed especially for local area networks and IoT use cases. DECT-2020 NR is part of the fifth generation (5G) mobile network standards. DECT-2020 NR is designed to meet the requirements of high reliability, low latency, and massive device density. [1] One key feature in DECT-2020 NR is mesh network topology that allows devices to form an autonomous network without the need for base stations or core network. That improves, for example, reliability and scalability of IoT applications. [2]

As in many other wireless communications systems, also in DECT-2020 NR it is possible to localize devices based on the signal measurements in the network. Positioning in the network enables many different use cases and applications. DECT-2020 NR offers a great environment for positioning due to its typical structure with dense network of nodes or devices. General positioning methods are suitable for positioning also in DECT-2020 NR networks, but this topic have not been covered much yet and not much public research is available yet. Mainly positioning based on received signal strength (RSS), or received signal strength indicator (RSSI), in DECT-2020 NR networks is addressed in some sources. Advantages with RSS-based positioning is that the RSS information is easily available and it is used for other purposes such as analysing network characteristics. Therefore, positioning based on this same information does not require much extra effort. However, the challenge with the RSS-based positioning is that the positioning accuracy is limited, especially in varying environments, because it is not so straightforward to identify the impact of objects for the distance estimation between the transmitter and receiver. Therefore, the other common positioning methods could offer better position-

ing performance. However, the positioning methods besides the RSS-based positioning, such as time of arrival (ToA) and angle of arrival (AoA), have not been widely studied in DECT-2020 NR environment because the technology is so new.

The features of DECT-2020 NR, such as dense network and energy efficiency, motivates to study positioning possibilities with different methods, for example ToA and AoA, and the optimization of positioning with these methods. Also, positioning capability with excellent accuracy is offering many possibilities for different use cases and applications, and is therefore important topic to study. Because potential positioning methods are based on signal measurements from the known reference points, called anchors, we will focus on the methods for selecting anchors for positioning in this work. We do not need to take measurements from all anchors which are accessible, but in theory, with a higher number of measurements we could achieve better positioning accuracy. However, to achieve other goals, such as energy efficiency, the positioning algorithm needs to be optimized. We assume that if the anchors used for positioning are chosen wisely, good positioning results can be achieved with fewer measurements from different anchors. Our objective is to provide some simulated results to answer this hypothesis in this work. We will also present the best potential positioning accuracy results with DECT-2020 NR numerologies based on general positioning theories, such as Cramér-Rao lower bound (CRLB) and position error bound (PEB).

1.2 Objective of the Thesis and Research Method

One key objective of the thesis is to study the best potential positioning accuracies for DECT-2020 NR networks with its physical waveform characteristics, for example, with different bandwidths and subcarrier spacings. Another key topic is to consider different methods for selecting anchors for efficient positioning, and to analyze the accuracy of the considered methods compared to the ideal selection. Therefore, we are interested in determining whether efficient user device positioning is possible in DECT-2020 NR mesh networks. The following research questions are answered in this thesis:

1. What are the potential positioning methods in DECT-2020 NR mesh networks?
2. What positioning accuracies can be achieved with the potential positioning methods in DECT-2020 NR networks in theory?
3. What positioning accuracies can be achieved with different anchor selection methods compared to the ideal results in DECT-2020 NR networks?

The first research question is answered by studying the theoretical background and academic literature of DECT-2020 NR technology and potential positioning methods. The main sources are, for example, DECT-2020 NR standard documents, scientific publications related to DECT-2020 NR, publications related to positioning in different types of

networks, and positioning books.

The second research question is answered by simulating the best possible positioning accuracies with the chosen positioning methods. The results are presented by values of CRLB, and therefore, the results are based on the principle of CRLB. The theory of CRLB is presented in the theory part of thesis. The simulation results are generated using the computer software MATLAB.

The third research question is answered by simulating the different methods of selecting anchors and comparing the simulated results. The results are presented by PEB values. PEB results are generated in different scenarios, and the different numbers of selected anchors are considered and compared. Therefore, we can analyze the gained positioning accuracy results with efficient positioning methods compared to ideal results. Simulation is done using the MATLAB.

As a result of answering to the research questions above, we should have better understanding of positioning possibilities in DECT-2020 NR networks. The objective is also to gain perspectives and support for possible further research on the topic related to positioning in DECT-2020 NR.

1.3 Structure of the Thesis

The structure of the thesis is as follows: the theoretical background is presented first, and the theoretical part starts with Chapter 2, where we study the key aspects of IoT. We present the definition and background of IoT, discuss how the IoT can be classified, and briefly familiarize main architectures and topologies in IoT. We also present some common non-cellular and cellular IoT technologies, and compare differences between them.

In Chapter 3, we study different aspects of the standardized technology DECT-2020 NR. For example, we will present the benefits and opportunities, standardization and development process, and technology overview of DECT-2020 NR.

Theoretical background for positioning is presented in Chapter 4. We will consider possible positioning use cases and applications, and take a look for related work from the positioning point of view. We present potential positioning methods: ToA, time difference of arrival (TDoA), RSS, and AoA. Also positioning bounds, CRLB and PEB, and their theoretical basis are presented in this chapter. Finally, basics of Kalman filter (KF) is presented to be considered as a method for positioning tracking.

After theoretical background, the research methodology is presented in Chapter 5. There are two main areas to study with the MATLAB simulations in this thesis: CRLB with DECT-2020 NR numerologies, and selecting the best anchors for positioning in DECT-2020 NR

network. The methodology for getting the results are presented in this chapter.

Chapter 6 presents the simulated results of CRLB for ToA, CRLB for AoA, and results for anchor selection methods in positioning, including the PEB results for the simulated anchor selection scenarios. Also, the analysis based on the gained numerical results are presented in this chapter.

Finally, the thesis concludes with Chapter 7, which collects the main results and draws conclusions based on the results. Also, further research possibilities are briefly considered in this chapter.

2. INTERNET OF THINGS (IOT)

In recent years, the use of IoT has become increasingly widespread and the technology has undergone significant development. New IoT technologies and concepts will be developed continuously, and the development of the wireless networks enables that even more IoT applications will appear in the near future. In this section, we will present general aspects of IoT. We also have a look for the key points of non-cellular and cellular IoT, and compare the main differences between them.

2.1 General Aspects of Internet of Things

General aspects of IoT are studied using different literature references. In this section, we present IoT related basic information, such as definition, classification, architecture and layers, and main topologies used in IoT networks.

2.1.1 Definition

The term IoT was established by Kevin Ashton in a presentation in 1999 to describe a network that connects not only people but also the things and objects around them [3], [4], [5]. Radio frequency identification (RFID) was the key technology behind Ashton's idea for connecting things [6]. Technology in general has improved a lot after that time. The current availability of faster and more reliable data connections with low latency has enabled numerous possibilities for IoT technologies and applications to integrate things and devices into everyday life.

In [6], the evolution of IoT is presented with different phases. First, approximately in 1999, RFID was a key technology and it offered passive identification with help of wireless networks. Second phase can be considered as a time of wireless sensor networks (WSNs) around in 2005. Third, a term Smart Things could be used from the time approximately in 2012 when mobile computing and better connection and operation between devices enabled a step towards IoT nowadays. The years around 2017 was time when the term IoT got also more practical meaning due to advanced sensor fusion, improvements in mobile networks and higher data rates in communication networks in general. They have been some enablers also for better analytics. [6]

In the literature, IoT has been defined in various ways, but the main idea remains the same. In [7, pp. 1–17], the term IoT is used to describe embedded devices – things – with Internet connectivity that enables interaction with other devices, services, and people on a global scale. According to [8], IoT can be understood as a closed loop system. A set of sensors is connected by a network to servers, and the data from sensors are stored in a database. The collected data is then analyzed by IoT analytics and the results are used to inform decision-making.

In the summary of the challenges of IoT presented in [7, pp. 1–17], the following issues are identified: the availability of free and widespread internet access, security concerns, the development of low-cost smart sensing systems, energy consumption, computational ability, scalability, fault tolerance, power consumption, and societal acceptance. IoT professionals are actively working to address these challenges due to the significant benefits that functional IoT technology can provide. However, it is important to always consider the challenges and ensure that technology is up-to-date in all sectors. For example, security is a crucial aspect of IoT. If there are any security issues with the IoT application, the technology becomes unsafe and unusable.

Currently, the term Internet of Everything (IoE) is sometimes used in certain contexts. This term highlights the connectivity of all entities, including things, data, processes, and people, through the Internet. IoE defines this extensively connected system. [9]

2.1.2 Classification

IoT systems can be divided roughly into two groups: non-cellular IoT and cellular IoT. Next we will address a short overview of non-cellular IoT and cellular IoT and the main IoT technologies at the moment. We will address also some differences between non-cellular IoT and cellular IoT.

IoT can be divided into cellular and non-cellular systems based on the spectrum used. In other words, if the IoT system is using infrastructure of cellular networks which are mainly in licensed spectrum, it is called cellular IoT. Cellular IoT relies on existing cellular infrastructure, while non-cellular IoT uses mainly unlicensed spectrum. It is important to note that cellular IoT has restrictions for adaptations. In non-cellular systems, building the system from the ground up may be necessary, but this approach allows better customization. Some IoT technologies may have support for both cellular and non-cellular systems. [4]

In addition to the spectrum separation of licensed and unlicensed spectrum, IoT technologies can also be classified based on different characteristics. Some examples of possible classifications could be range (short–medium–long), power consumption (low–high), data rate (low–high) and latency (low–high). [4]

The definitions for the range of IoT are varying a bit in the literature between different

authors and manufacturers. Short range is typically defined as a distance ranging from centimetres to tens of meters. Medium range means often ranges between a hundred meters to about 5 kilometers. Long range or wide range are ranges higher than 5 kilometers. Cellular networks can cover ranges about 100 kilometers. In addition, non-terrestrial IoT can reach a range up to 700 kilometers. [4]

The definitions of low and high power, rate, and latency may vary depending on the author, making it challenging to determine the limits. However, the definition of low power is often used if the IoT device has target battery life of several years. Similarly, low rate is typically used for IoT technologies which are operating with data rates below 1 Mbps. In the case of latency, it may vary even more depending on the application, but in general, latencies measured in milliseconds can be considered as low latency applications and latency with a second or longer can be said high latency applications.

IoT types in terms of applications are Massive IoT, Critical IoT, Industrial IoT, and Broadband IoT. These application types may have different requirements for data rate, latency, range, and other characteristics of the IoT technology. [4]

IoT technologies can be classified also in standard-wise, if they are IoT specific protocols or IoT enablers. For example, IoT specific protocols are Narrowband Internet of Things (NB-IoT), LoRa and Sigfox while Bluetooth Low Energy (BLE), WiFi and 5G can be considered as IoT enablers. [10] For instance, WiFi solutions can enable IoT applications which do not require low power or which are operated plugged-in. However, WiFi is not planned originally for the IoT use cases so it is not specific IoT technology but can be considered as IoT enabler. WiFi can be used to implement high-power high-rate IoT solutions. [4], [11]

2.1.3 Architecture and Layers

IoT architecture definitions, layer names and number of layers are varying in different contexts. There are several different versions of IoT layer architectures. Here we address three example protocol architectures based on [12], one of each with three, four and five layers.

In an example of three-layer architecture, the names of layers are perception layer, network layer and application layer. In perception layer the sensors are collecting the information. Network layer works as a bridge between perception layer and application layer and is working as a transmission layer. As the name indicates, IoT applications are working in application layer. [12]

In four-layer architecture, support layer is additional compared to the three layer, and it is working between application layer and network layer. The main target with support layer is to improve the security of IoT system. For example, support layer confirms that the

users are authenticated, and threads are protected. [12]

Five-layer architectures layer names from bottom to up are perception layer, transport layer, processing layer, application layer, and business layer. In comparison to three-layer architecture, processing layer and business layer are additional layers and other three layers are rather similar to the three-layer architecture. In five-layer architecture, the main idea is also to better the security issues in IoT systems. [12]

2.1.4 Main Topologies

IoT utilizes different topologies, and the three main topologies are point-to-point (P2P), star and mesh. Each topology has advantages and disadvantages, often related to the complexity and the functionality of the IoT technology.

P2P topology is very simple topology where two devices have straight link between each other. However, P2P is not very useful for IoT applications, because it enables only device-to-device (D2D) or machine-to-machine (M2M) type of networks. [13], [14]

In star topology, central node controls the data transmission and distribution, and all other nodes are connected to central node. Star topology is quite simple because the central node carries the main complexity and other nodes have very low complexity and power. However, the downside in star topology is that the resource is limited, because all traffic is going through the central node. [13]

Mesh topology allows all nodes to be connected to each other with straight links, resulting in shorter links, lower transmit power and lower latency. However, the range between the nodes is limited if straight transmission is required. Multi-hop techniques can be used to increase the range, but this also increases complexity. Mesh topology is commonly used in IoT technologies. [13], [14]

In the world of IoT, the data is collected through sensors and other devices. However, this data needs to be processed also to be useful. Therefore, the computation is important part of IoT applications. The computation can be performed in smart objects themselves, in fog, or in cloud. When computation is performed in smart objects, the method is referred as edge computing. Fog computing means that computations are done at the local area network level. In cloud computing, the computations are performed on a remote cloud server. [15]

2.2 Non-cellular Internet of Things

Non-cellular IoT technologies are often designed to be power-efficient, cost-effective, and flexible. However, the coverage of non-cellular IoT system might be limited, and the interoperability between different systems can be a challenge. Examples of non-cellular

IoT technologies include LoRa, Sigfox, Zigbee, Z-Wave, and DECT-2020 NR.

In general, non-cellular IoT has both advantages and disadvantages. The advantages of non-cellular IoT include lower power consumption, lower cost, and greater flexibility. In terms of power consumption, many non-cellular technologies are designed to be power-efficient, enabling long battery life for IoT devices. Additionally, non-cellular IoT technologies often require less complex hardware and have lower power consumption, resulting in cheaper devices and lower infrastructure costs. Non-cellular technologies often operate on unlicensed or shared spectrum bands, which do not require subscription fees. Non-cellular IoT networks are generally easier to customize to fit specific use cases, offering better flexibility. Non-cellular IoT technologies are also often more accessible to smaller organizations and individuals for creating their own IoT applications.

The disadvantages of non-cellular IoT are primarily limited coverage and compatibility challenges. Non-cellular technologies typically have shorter operating ranges compared to cellular networks. Additionally, compatibility between devices using different protocols can be a challenge.

LoRa technology is designed for long-range, low-power IoT applications. LoRaWAN is built on top of LoRa technology. LoRa is the physical layer technology and LoRaWAN is the protocol and network infrastructure that facilitates the connection of IoT devices to the internet. LoRa was originally developed by Semtech but is now developed by LoRa Alliance. LoRa Alliance consists of several contributing member organizations. LoRa is operating in unlicensed industrial, scientific and medical (ISM) bands, which makes it suitable for various regions globally. LoRa has good energy efficiency, which enables long battery life for IoT devices. LoRa uses the proprietary chirp spread spectrum (CSS) modulation. LoRa technology can be utilized to develop low-cost positioning systems, such as indoor positioning. However, it is important to note that the positioning accuracy of LoRa-based systems is relatively poor, with the best accuracies being limited to around 20 metres. [16]

Sigfox is proprietary IoT technology developed by Sigfox company. Sigfox is low-power wide-area network (LPWAN) technology that enables devices to communicate efficiently over long distances with low energy consumption. Sigfox uses ultra narrowband (UNB) signals and modulation schemes are differential binary phase-shift keying (DBPSK) in the uplink and Gaussian frequency shift keying (GFSK) in the downlink. Sigfox can also be used for positioning devices, with positioning based on RSSI measurements. Its advantages as a positioning system are low cost, long battery life and resilience to interference and jamming. However, the positioning accuracy is limited, with an accuracy range of 1 to 10 km for over 80% of cases. [17]

Zigbee is an open IoT standard that operates in ISM bands. Zigbee technology was originally developed by the Zigbee Alliance, now known as the Connectivity Standards

Alliance (CSA). According to the CSA, Zigbee is a globally adopted and interoperable IoT solution. Zigbee operates on the IEEE 802.15.4 physical radio standard and uses mesh topology, making it a reliable solution that can eliminate single points of failure. Additionally, Zigbee is a low-power, low-rate network with low-cost. Zigbee is considered as a short-range IoT technology. Zigbee facilitates interoperability among devices from different manufacturers, making it a widely used option for smart home ecosystems and industrial automation systems. [18]

Z-Wave is an open wireless IoT standard and technology designed primarily for home automation and smart devices. Z-Wave was developed in 1999 by a Danish start-up company Zen-SYS. The Z-Wave Alliance is a consortium of companies and organizations that collaborate to develop and promote Z-Wave technology in the smart home and IoT market. The Z-Wave Alliance was established in 2005 and re-incorporated as a non-profit organization in 2020. Z-Wave operates on low-power radio waves in the sub-GHz frequency range, enabling efficient and reliable communication between various smart devices, such as lights, thermostats, locks, and sensors. Z-Wave uses a mesh network topology, which enhances the range of network and reliability. Z-Wave devices are energy-efficient, enabling long battery life for battery-powered devices. Z-Wave utilizes frequency shift keying (FSK) and GFSK modulations. [19], [20]

DECT-2020 NR is the world's first non-cellular 5G technology standard designed especially for IoT. DECT-2020 NR has been standardized by the European Telecommunications Standards Institute (ETSI), and DECT-2020 NR has a high potential as a massive IoT technology connecting big number of smart devices. [14, pp. 7–8], [21], [22], [23], [24] Chapter 3 will present a more detailed overview of the DECT-2020 NR.

2.3 Cellular Internet of Things

Cellular IoT systems utilize existing cellular networks to connect IoT devices and typically operate in licensed bands, which is the main difference compared to non-cellular IoT. Cellular IoT offers wide coverage, scalability, and robust security, making it suitable for large-scale deployments and critical IoT applications. However, cellular IoT may consume more power, cause additional data subscription costs, and require more complex integration between the IoT systems. [4]

The 3rd Generation Partnership Project (3GPP) has standardized technologies and protocols used for cellular IoT. 3GPP offers radio technologies especially for long-range and power efficient massive machine type communications (mMTC). In [25], it is described that 3GPP standardized IoT solutions have a high value compared to proprietary competitors in the low-power wide-area (LPWA) segment. It is also noted that in comparison to technologies operating in the unlicensed frequency domain, the licensed spectrum provides better control and quality assurance.

Also cellular IoT has both advantages and disadvantages. The advantages of cellular IoT include wide coverage, scalability, reliability, and security. Cellular networks have extensive coverage, making cellular IoT suitable for applications in both urban and rural areas. Additionally, cellular IoT networks can support a large number of devices, making cellular IoT suitable for applications and use cases that require a vast network of interconnected devices. Cellular networks often provide robust security and reliable connectivity, which is crucial for critical IoT applications and industries. [4]

The drawbacks of cellular IoT in general are higher power consumption, complexity, and cost. Cellular modules can consume more power than non-cellular alternatives, and therefore, non-cellular IoT technologies may be a better choice for battery-powered IoT devices. However, the energy efficiency aspect can be also taken into account with cellular IoT applications. Implementing cellular connectivity in IoT devices may require more complex hardware and software integration compared to non-cellular alternatives. Cellular IoT connectivity must meet the requirements and architecture of cellular technologies, such as fourth generation (4G) or 5G. Typically, cellular connectivity involves data subscription plans or data charges, which can increase the costs of cellular IoT systems. [4], [26]

Some examples of cellular IoT technologies are extended coverage GSM IoT (EC-GSM-IoT), Long-Term Evolution Machine Type Communication (LTE-M), and NB-IoT. Also, IoT aspects has taken into account in the development of 5G New Radio (NR), and therefore, 5G has significant potential for IoT use cases. [4], [26]

EC-GSM-IoT is a LPWA technology based on Enhanced General Packet Radio Service (EGPRS). It is designed as a high capacity, long range, low energy, and low complexity cellular system for IoT communications. EC-GSM-IoT operates within the Global System for Mobile Communications (GSM) network, which has extensive coverage worldwide. EC-GSM-IoT has low device cost compared to General Packet Radio Service (GPRS) and GSM devices. [26]

LTE-M is a LPWAN standard developed by 3GPP. It is designed specially for M2M and IoT applications, and it has support for end-to-end secure connection. Device costs are low in LTE-M. LTE-M supports also higher data rates and has high mobility. [26]

NB-IoT is a LPWAN radio communication technology standard developed by 3GPP. It is designed specially for low-power, wide-area IoT applications. NB-IoT offers long battery life for devices, and has even lower cost than LTE-M, because the hardware is very simple and cheap. NB-IoT is 5G ready technology. [26]

The 5G network can be used for various IoT use cases and applications. 5G has several IoT-related features, which are already in use. For example, reduced capacity, reduced latency and support for a massive number of connected devices. [4]

2.4 Characteristics of Non-cellular and Cellular IoT Technologies

Table 2.1 presents common cellular and non-cellular IoT technologies and lists their main characteristics. The information in Table 2.1 is collected from several references, which are [4], [10], [14], [21], [26], [27], [28], [29], [30], [31], [32]. It is important to note that the specific values of some factors may depend on the implementations, use cases, applications, and techniques used by IoT device manufacturers or application developers. In addition, there are often trade-offs between data rate, range, energy consumption, and latency, that affect the specific values. There are also some differences in the information in the references. Nevertheless, Table 2.1 provides an indicative classification based on the references.

Table 2.1. Characteristics of non-cellular and cellular IoT technologies.

IoT technology	Typical range	Frequency bands	Data rate	Target battery life	Main topology	
Non-cellular IoT	LoRa	1 km (urban) / 20 km (rural)	Sub-GHz	0.3-50 kbps	1-10 years	Star
	Sigfox	10 km (urban) / 40 km (rural)	Sub-GHz	100 bps (UL) / 600 bps (DL)	6-10 years	Star
	Zigbee	10-100 m	Sub-GHz & GHz	250 kbps	20 years	Mesh
	Z-Wave	up to 30m	Sub-GHz	100 kbps	10 years	Mesh
	DECT-2020 NR	>100 m (indoor) / 2 km (outdoor)	Sub-GHz & GHz	3.4 Mbps (or even higher)	10 years	Mesh
Cellular IoT	EC-GSM-IoT	<25 km	Sub-GHz	474 kbps (UL) / 2 Mbps (DL)	10 years	Star
	LTE-M	11 km	Sub-GHz & GHz	3-7 Mbps (UL) / 4 Mbps (DL)	10 years	Star
	NB-IoT	15 km	Sub-GHz & GHz	127 kbps (UL) / 159 kbps (DL)	10 years	Star

As we can see from Table 2.1, there are some similarities and differences between the different IoT technologies. For example, typical ranges are shown here as distances, but the ranges could also be divided into three categories: long, medium and short. Sub-GHz and GHz frequency bands are supported by the listed IoT technologies. Data rates can vary, but are generally low on non-cellular IoT, and higher data rates can be achieved on cellular IoT. DECT-2020 NR is an exception in this sense. Target battery life is calculated in years, with a target of 10 years being typical. Both mesh and star topologies are commonly used in different IoT technologies, and some of the technologies may have support for multiple topologies. In this table, the main topology based on the references is listed. All IoT technologies aim to minimize power consumption, and the all IoT technologies in Table 2.1 are low or ultra-low power, and therefore this information is not listed in here. Latency can vary widely between technologies, and can be highly dependent on the use case, and therefore not listed in the table.

3. DECT-2020 NEW RADIO (NR)

DECT-2020 NR is the world's first non-cellular 5G connection, which is designed to enable especially the massive IoT. One of the key advantages of DECT-2020 NR is the possibility for anyone to deploy and connect license-exempt private 5G networks. DECT-2020 NR aims to solve the connectivity problem in large-scale IoT deployment, which has been a major challenge in previous solutions due to lack of cost-efficiency and reliability. [14, pp. 7–8], [21], [22], [23], [24], [33]

This section covers the benefits and opportunities of DECT-2020 NR. We then discuss the standardization and development process of technology at a general level. Finally, we delve into the technical details of DECT-2020 NR.

3.1 Benefits and Opportunities

DECT-2020 NR is designed to address future digitalization needs in the future. DECT-2020 NR is optimized for local area wireless applications that can be deployed by any one, anywhere, anytime. Possible applications and use cases for DECT-2020 NR technology include Industry 4.0, public services and media industry. [1], [34]

One of the main advantages in DECT-2020 NR is its ability to connect thousands of devices on a single access point, which enables massive IoT. DECT-2020 NR also offers low-latency and high-reliable connections through a streamlined message protocol. Ultra reliable and low latency communications (URLLC) and mMTC are important aspects of DECT-2020 NR. [21]

According to [21], the key capabilities and benefits of DECT-2020 NR are:

- Flexible mesh network architecture
- Unlicensed and global shared spectrum
- Low latency and dense massive network
- Automatic configuration and self-healing topology
- Possibility for high data throughput and medium range
- Low power consumption
- Security

In [21], DECT-2020 NR and its features are compared to other IoT technologies, such as LoRa. For example, the spectral efficiency of DECT-2020 NR radio protocols is very high, making it possible to provide the same quality of service at a higher node densities. The throughput of DECT-2020 NR is also relatively high for an IoT technology. The DECT-2020 NR throughput is 3.4 Mbps with a channel bandwidth of 1.728 MHz in a global 1.9 GHz frequency band. The frequency band around 1.9 GHz is a licence-free and available in most parts of the world. Because of the mesh network topology used in DECT-2020 NR, the radio protocol has greater flexibility for high density of nodes, offering higher spectral efficiency and throughput capabilities. DECT-2020 NR is an open ETSI standard that allows all chip manufacturers to offer DECT-2020 NR chips. To summarise these points, DECT-2020 NR provides a more reliable network for dense node connections and massive IoT scalability. [21]

The DECT-2020 NR standard is an example of future connectivity. DECT-2020 NR is an infrastructure-less, autonomous and decentralised network that enables different types of existing and new IoT applications and use cases. In a decentralized mesh network, each device can operate as a node or a router, enabling short hop distances and therefore small transmission power. This type of network also eliminates single points of failure. [24]

According to [35], DECT-2020 NR is an attractive option for the IoT networks of local-area, low-latency and self-hosted mMTC. Also, the mesh network in DECT-2020 NR allows significantly higher node densities for the same delay and loss performance bounds compared to operator-driven cellular IoT solutions. DECT-2020 NR is a potential technology especially for smart IoT applications, such as smart home or smart buildings. The biggest challenges are seen in the extremely high mobility scenarios where the mesh network is not the most stable with the performance. [35]

3.2 Key Organizations Related to DECT-2020 NR Standardization and Development

Technology development and standardization in wireless communication systems requires collaboration between industry organisations, research partners, regulatory bodies and standardization organisations. The standardization process typically starts with research and development, where companies, institutions and research organisations explore new concepts and technologies. An industry consortium and standardization organisations, such as 3GPP, Institute of Electrical and Electronics Engineers (IEEE), and ETSI, play important roles in developing and defining global standards. The different phases in the technology development and standardization process may include, for example, proposal submission, technical evaluation, drafting and different types of publication. Regulatory bodies ensure compliance with legal and technical regulations. Overall, standardization

enables interoperability, compatibility and the commercialisation of wireless technologies, which is important for global connectivity. Without precisely defined, common standards, communication systems would not work together and would not be useful.

Some key organizations linked to the development and standardization process of DECT-2020 NR technology are presented in this section. The shortly presented organizations are International Telecommunication Union (ITU), ETSI and DECT Forum.

3.2.1 ITU

ITU is the United Nations specialised agency for Information and Communications Technology (ICT). ITU was founded in 1865, and its headquarter is located in Geneva, Switzerland. [36]

ITU is divided into three sectors:

- Radiocommunication Sector (ITU-R)
- Standardization Sector (ITU-T)
- Development Sector (ITU-D)

The ITU Radiocommunication Sector manages the global allocation of radio frequency spectrum and satellite orbits. The ITU Standardization Sector standardizes and develops global technical standards for ICT. Standardization is important to ensure interoperability and seamless communication between different devices and networks. The ITU Development Sector promotes the development of ICT infrastructure and services, particularly in underserved and developing regions, and bridges the digital divide. [36]

3.2.2 ETSI

ETSI is a standardization organisation in the field of information and communications, established in 1988. ETSI provides an open environment for the development and testing of global technical standards for ICT systems and services. ETSI is a not-for-profit organisation with over 900 member organizations from over 60 countries and 5 continents. ETSI is one of the three European Standards Organizations (ESOs) recognised by the European Union (EU). [37] As stated on the official website of the EU, the ESOs are officially recognised as providers of European standards by Regulation (EU) No 1025/2012. The other two ESOs are European Committee for Standardization (CEN) and European Committee for Electrotechnical Standardization (CENELEC). [38], [39]

ETSI Technical Committee (TC) Digital Enhanced Cordless Telecommunications (DECT) is responsible for the development and maintenance of DECT standards. DECT-2020 NR is the latest standard developed by the committee. [40]

3.2.3 DECT Forum

The DECT Forum is an international non-profit industry organisation that promotes and develops the DECT standard. The DECT Forum was founded in 1997 and is based in Bern, Switzerland. There are many organisations that are full or associate members of the DECT Forum. [41] Based on the DECT Forum website, the mission of the DECT Forum is to support the DECT industry by creating a collaborative environment helping to develop and improve DECT wireless technology through various projects. The goal of organisation is to exceed expectations for wireless communications and meet the needs of a technology-shifting world. The mission of DECT Forum is also to ensure that both consumers and forum members benefit from the different activities that the DECT Forum undertakes. Consumers may gain confidence in the technology and its capabilities. Member organisations may gain a collaborative community where they can develop and improve DECT technology and better reach consumers with high quality technology. [42]

The DECT Forum has several working groups and one of them is the NR+ Working Group. The DECT Forum uses the name DECT NR+ from the DECT-2020 NR. The NR+ Working Group has some main tasks and missions. For example, it aims to improve the awareness of DECT-2020 NR standard and to promote different use cases, applications and benefits of the technology. The contribution to the further development of the DECT-2020 NR standard and open collaboration with the ETSI TC is also important for them. The NR+ Working Group also acts as a facilitator between industry participants. [43]

3.3 DECT-2020 NR Development and Standardization Process

DECT-2020 NR is a radio interface technology (RIT) standardized by ETSI. The original DECT standard was developed already in the 1990s, but the new modern DECT-2020 NR technology provides many new possibilities, particularly for IoT applications, especially related to URLLC and mMTC. [14, p. 8], [23]

The DECT standard, originally published in 1990s, is now referred to as 'original' or 'classic' DECT to distinguish it from the DECT-2020 NR, which has significant difference in the features. [1], [44]. However, the classic DECT has been updated over time to meet the evolving requirements of communication systems. Additional DECT specifications have been introduced over the years, such as New Generation DECT (NG-DECT) and DECT Ultra Low Energy (ULE). However, these specifications can be considered as updates to classic DECT. DECT-2020 NR can be considered totally new technology with a background in classic DECT.

Classic DECT is part of the global International Mobile Telecommunications-2000 (IMT-2000) standard for third generation (3G) wireless telecommunications technology. IMT-2000 is defined by the International Telecommunication Union Radiocommunication Sec-

tor (ITU-R). Classic DECT has been included in IMT-2000 since the first publication of the detailed specifications of the radio interfaces of IMT-2000. [45] ITU-R Working Party 5D has been updating IMT frameworks and the latest defined framework is International Mobile Telecommunications-2020 (IMT-2020). IMT-2020 includes the standardized 5G technologies that meet the requirements. [46]

DECT-2020 NR technology has gone through standardization process of the ITU-R, which consists of multiple stages and precisely defined criteria. The IMT-2020 standardization process is based on three ITU-R reports in particular:

- Report ITU-R M.2410-0 Requirements related to technical performance for IMT-2020 radio interface(s) [47]
- Report ITU-R M.2411-0 Requirements, evaluation criteria and submission templates for the development of IMT-2020 [48]
- Report ITU-R M.2412-0 Guidelines for evaluation of radio interface technologies for IMT-2020 [49]

In November 2017 ITU-R published the above mentioned reports. Report M.2410-0 ([47]) defines the minimum requirements. The purpose of the requirements in report M.2410-0 is to support 5G use cases involving URLLC, mMTC and enhanced mobile broadband (eMBB). Reports M.2411-0 ([48]) and M.2412-0 ([49]) provide definitions for the evaluation process. DECT-2020 NR has attempted to meet two out of the three concepts of the requirements set for 5G, which are URLLC and mMTC. Multiple evaluations have been made and the results can be seen, for example, in publications [27], [50], [51], [52], [53], [54].

The minimum technical performance requirements in M.2410-0 for IMT-2020 5G candidate technologies are collected in Table 3.1 from [47]. As we can see from Table 3.1, the requirement quantities for URLLC are latency, control plane latency, reliability, mobility interruption time and bandwidth. The requirement quantities for mMTC are connection density and bandwidth. Other requirement quantities are only relevant for the eMBB usage scenario.

In June 2017, ETSI published a Technical Report (TR) with a title *DECT evolution technical study; Requirements and technical analysis for the further evolution of DECT and DECT ULE*. This was a step towards DECT-2020 NR. In July 2018, the first TR of DECT-2020 NR was published with the title *DECT-2020 New Radio (NR) interface; Study on Physical (PHY) layer*. In 2019, the IMT-2020 submission proposal was published by ITU-R.

In July 2020, ETSI launched the new DECT-2020 NR standard. DECT-2020 NR was presented as an advanced radio interface to support a wide range of different wireless IoT applications requiring ultra-reliable, low-latency and massive machine-type communica-

Table 3.1. IMT-2020 technical performance requirements.

Minimum technical performance requirements	Usage scenario	Required value		Note
		Downlink	Uplink	
Connection density	mMTC	1 000 000 devices/km ²		
Bandwidth	mMTC, URLLC & eMBB	At least 100 MHz		
Reliability	URLLC	1–10 ⁻⁵ success probability of transmitting a layer 2 PDU (protocol data unit) of size 32 bytes within 1 ms in channel quality of coverage edge		Urban Macro
Latency	URLLC & eMBB	1 ms for URLLC 4 ms for eMBB	1 ms for URLLC 4 ms for eMBB	
Control plane latency	URLLC & eMBB	20 ms		
Mobility interruption time	URLLC & eMBB	0 ms		
Area traffic capacity	eMBB	10 Mbit/s/m ²	-	Indoor Hotspot
Peak data rate	eMBB	20 Gbit/s	10 Gbit/s	
User experienced data rates	eMBB	100 Mbit/s	50 Mbit/s	Dense Urban
Peak spectrum efficiency	eMBB	30 bit/s/Hz	15 bit/s/Hz	
Average spectral efficiency	eMBB	9 bit/s/Hz/TRxP	6.75 bit/s/Hz/TRxP	Indoor Hotspot
		7.8 bit/s/Hz/TRxP	5.4 bit/s/Hz/TRxP	Dense Urban
		3.3 bit/s/Hz/TRxP	1.6 bit/s/Hz/TRxP	Rural
5th percentile user spectral efficiency	eMBB	0.3 bit/s/Hz	0.21 bit/s/Hz	Indoor Hotspot
		0.225 bit/s/Hz	0.15 bit/s/Hz	Dense Urban
		0.12 bit/s/Hz	0.045 bit/s/Hz	Rural
Energy efficiency	eMBB	capability to support a high sleep ratio and long sleep duration		
Mobility: Normalized traffic channel link data rate	eMBB	1.5 bit/s/Hz		• Indoor Hotspot • Mobility: 10 km/h
		1.12 bit/s/Hz		• Dense Urban • Mobility: 30 km/h
		0.8 bit/s/Hz		• Rural • Mobility: 120 km/h
		0.45 bit/s/Hz		• Rural • Mobility: 500 km/h

tions. DECT-2020 NR aimed to meet the IMT-2020 requirements of URLLC and mMTC with its technology. [23] DECT-2020 NR was one of the candidate technologies being evaluated to meet IMT-2020 requirements. The set of radio interface technologies (SRIT) proposal submitted by ETSI (TC DECT) and DECT Forum, called DECT 5G-SRIT, included two RIT components: DECT-2020 NR RIT component and 3GPP NR RIT component [54], [55]. The target with the DECT-2020 NR RIT component was to meet IMT-2020 URLLC and mMTC requirements [27]. The requirements overall was planned to meet

with the DECT 5G-SRIT as a whole [55].

In the first evaluation round in 2020, DECT-2020 NR did not meet all the requirements set for the URLLC and mMTC. ITU-R extended the evaluation of ETSI DECT-2020 NR [50], [54], [56]. In 2021, ITU-R Working Party 5D confirmed that DECT-2020 NR meets 5G IMT-2020 performance requirements for URLLC and mMTC. ITU-R included it as a part of the 5G NR standards within the IMT-2020 technology recommendation ITU-R M.2150-1 in February 2022 [21], [24], [54], [55], [57]. The introduction of DECT-2020 NR commercial systems is planned to start in 2024. The DECT-2020 NR development timeline is also shown in Table 3.2.

Table 3.2. *Timeline for the development of DECT-2020 NR.*

Year	Month	Activity
1988–1992		<ul style="list-style-type: none"> • DECT technology was developed (nowadays called also the original or classic DECT) • First round of DECT standards were published in 1992
2000	May	<ul style="list-style-type: none"> • The IMT-2000 published, DECT standard included as one 3G technology
2007		<ul style="list-style-type: none"> • The New Generation DECT (NG-DECT) was published
2011	January	<ul style="list-style-type: none"> • DECT Ultra Low Energy (DECT ULE) was published • First commercial products based on DECT ULE were launched later in 2011
2017	June November	<ul style="list-style-type: none"> • Technical Report "<i>DECT evolution technical study</i>" published (<i>Requirements and technical analysis for the further evolution of DECT and DECT ULE</i>) • ITU-R published the IMT-2020 reports related to the technology requirements and the evaluation process
2018	July	<ul style="list-style-type: none"> • First Technical Report of DECT-2020 NR published (<i>DECT-2020 New Radio (NR) interface; Study on Physical (PHY) layer</i>)
2019	June	<ul style="list-style-type: none"> • IMT-2020 submission proposal (<i>Acknowledgement of candidate SRIT submission from ETSI (TC DECT) and DECT Forum under Step 3 of the IMT-2020 process</i>)
2020	July	<ul style="list-style-type: none"> • DECT-2020 New Radio (TS103.636 Parts 1–4) was published • SRIT submission to ITU-R • ITU-R extends evaluation of ETSI DECT-2020 NR
2021	October December	<ul style="list-style-type: none"> • ITU-R (Working Party 5D) confirms that DECT-2020 NR meets 5G IMT-2020 performance requirements for URLLC and mMTC • ETSI TS103.636 V1.3.1 (Parts 1–5) published
2022	February	<ul style="list-style-type: none"> • DECT-2020 NR officially recognized as an IMT-2020 5G technology and added to 5G standards by ITU-R • Harmonised European Standard EN 301 406 was split into two parts <ul style="list-style-type: none"> - Part 1: traditional DECT (published in October 2022) - Part 2: essential requirements for the DECT-2020 NR (published in August 2023)
2023	January	<ul style="list-style-type: none"> • Latest updates to the first release of DECT-2020 NR specifications (V.1.4.1) was published
2024		<ul style="list-style-type: none"> • Plan: Update of DECT-2020 NR specifications and introduction of commercial systems

ETSI DECT standards can be accessed from the ETSI's website [58]. There are different types of specifications, standards, reports and guides available with different purposes.

European Standard (EN), ETSI Standard (ES), Technical Specification (TS) and TR are some examples of the different types of standards. [59]

The development of DECT-2020 NR can be studied from the published technical specifications, technical reports and other standard related documents. Based on these and other related sources, the main activities related to the development of DECT-2020 NR are presented in Table 3.2. The main sources used in Table 3.2 and the relevant ETSI standards are [1], [55], [60], [61], [62], [63], [64].

3.4 DECT-2020 NR Technology Overview

In this section we will get an overview of DECT-2020 NR technology, including the list of DECT-2020 NR specifications, overview of terminology and overview of the system and network architectures. Mesh network is in an important part of the DECT-2020 NR technology and the main idea of the DECT-2020 NR the mesh system operation and mesh routing will be presented. The interaction with 3GPP 5G networks will be considered. The overview is mainly based on DECT-2020 NR TS 103 636 Part 1 [14].

3.4.1 Technical Specifications

The DECT-2020 NR technology is defined in a five part standard series called ETSI TS 103 636 [23]. The parts of the DECT-2020 NR Technical Specifications are:

- Part 1: Overview [14]
- Part 2: Radio reception and transmission requirements [65]
- Part 3: Physical layer [66]
- Part 4: MAC layer [67]
- Part 5: DLC and Convergence layers [68]

As we can see, the ETSI TS 103 636 specification set consists of the overview and the radio reception and transmission requirements, and furthermore the four protocol layers defined in the three different parts. The DECT-2020 NR protocol layers from bottom to top are physical layer (PHY), medium access control (MAC) layer, data link control (DLC) layer and convergence (CVG) layer.

3.4.2 Terminology

DECT-2020 NR has its own terminology for the communicating devices and their modes to differ from, for example, cellular mobile network systems. DECT-2020 NR does not follow the typical cellular structure. [14], [54]

In the ETSI specifications of DECT-2020 NR it is defined that Radio Device (RD) is a device with radio transmission and reception capability which can operate in two modes: Fixed Termination point (FT) and/or Portable Termination point (PT). In FT operational mode, RD initiates coordinates local radio resources and provides information how other RDs can communicate with it. In PT, RD selects another RD, which is in FT mode, for association. RD can also operate in FT and PT modes simultaneously. [14]

3.4.3 System and Network Architectures

DECT-2020 NR supports several different types of connections and topologies. For example, DECT-2020 NR can operate as a local area network with a star topology or carry out RD to RD communication based on a mesh topology. Direct P2P and point-to-multipoint (P2M) connections are also possible in DECT-2020 NR. [14]

The mesh network topology is an essential part of the DECT-2020 NR operation. The mesh network allows devices to communicate directly with each other. This extends the range of the network and increases the reliability of communications. Each RD can act as a node transmitting, forwarding or receiving a message. Different communication routes can be established between the radios, minimising the probability of outage. Mesh operation can support high densities of devices and the routing is based on cost value to achieve mMTC operation. This eliminates the need to maintain routing tables in each device. Autonomous routing allows dynamic adaptation mobile users and interference. [14, p. 10]

Massive scalability can be achieved if the key requirements can be met. The key requirements are presented next. First, all radio devices can route data. Second, radio devices make local decisions about radio resources, such as the choice of modulation and coding, and how the devices use hybrid automatic repeat request (HARQ). Third, radio devices have the ability to switch between the operating modes individually in radio devices. The operating modes are FT, PT or modes FT&PT together. Furthermore, no central coordinators are used, which makes it possible to have a massive scale in the network. Local radio resource coordination should also be possible from a radio device operating in FT or FT&PT mode. It is important to have a support of multiple backend connected RDs operating in FT mode. Finally, the operation of radio devices could be done with multiple radio channels. [14, p. 10]

3.4.4 Mesh System Operation

The mesh system operation in DECT-2020 NR is based on a clustered tree topology, where each radio device independently decides its next hop by using available routes to the RD operating in FT mode and connected to the external internet. This RD can

be called as a sink. Each RD has knowledge of the next uplink and downlink hops in the clustered tree. Every cluster has a RD in FT or FT&PT mode, which independently controls radio resources and transmissions. [14, pp. 10–12]

The clustered tree topology is formatted in several steps. The steps include the selection of operating frequencies, beacon transmissions by RDs with internet connectivity, and association processes between RDs. RDs evaluate connection quality and signal strength to make autonomous decisions about association with other RDs based on routing costs. This process extends to the next hops. Once a RD has connectivity to the next hop, it can start transmitting data towards the RD in FT mode, using specific addressing to indicate data destined for a backend system. The network can support multiple backends sharing the same mesh network connection. The beaconing and association procedures in mesh and star topologies are similar, with beacon transmission intervals adjusted for power efficiency. The operation of multiple RDs in FT mode is also outlined, allowing RDs to change their associations to different RDs in FT mode as required. [14, pp. 10–12]

3.4.5 Mesh Routing

Mesh routing in DECT-2020 NR is utilized with three routing parameters. The parameters are route cost, sink address, and application sequence number. [14, p. 12]

In the mesh routing, a RD makes the decision about the next hop based on quality attributes, such as RSSI measurements from a beacon signal. RSSI can be used to determine the path loss. If both downlink (DL) and uplink (UL) path losses are at a level where a connection could be established, the RD that transmitted this beacon is considered as a potential next hop. If multiple beacons from multiple RDs meet the criteria of a reliable connection, the cost of the routing is considered in the RD. Route cost means the cost of delivering the data to the sink. Some examples of potential variables in the route cost calculation are data rate, interference and available battery power. The route with the lowest cost may be selected by the RD. [14, p. 12]

The sink address is also an important routing information. The sink address is a 32-bit long RD ID and it represents the RD in FT mode which has the backend connection. If there are multiple FTs, the RD can send a short packet to the backend to update backend's knowledge of the locations in the mesh network for the different RDs. This allows DL traffic to be sent only to the correct FT. [14, p. 12]

The application sequence number provides identification for the network level application data that is distributed in the DL direction to all network members. RDs uses this number to determine if the application data has changed. If the sequence number has increased, RD requests updated data from the next hop. [14, p. 12]

3.4.6 Interworking with 3GPP 5G Networks

DECT-2020 NR interoperates with 3GPP 5G networks through interworking profiles. DECT-2020 NR can connect to the 5G Core Network in two different modes: as an untrusted non-3GPP access network using the non-3GPP interworking function (N3IWF), or as a trusted non-3GPP access network using the trusted non-3GPP gateway function (TNGF). FT can act as intelligent gateways to the 3GPP network. When dealing with untrusted non-3GPP access, FT establishes a connection through N3IWF, while for trusted non-3GPP access, the FT will connect via TNGF. If PT supports both technologies, it can act as a user equipment (UE) within the 3GPP network. DECT-2020 NR provides "standalone" non-3GPP access to the 5G core network. This means that a DECT-2020 NR network operates completely independently and outside of 3GPP Next Generation Radio Access Network (NG-RAN). [14, p. 13]

4. POSITIONING

In this chapter, we present different positioning methods and theoretical positioning accuracy theories. The following positioning aspects are generally applicable in different communication systems and positioning environments. However, we will focus on them especially from the perspective of DECT-2020 NR. We will consider which positioning methods and algorithms could be potential alternatives in the DECT-2020 NR standard.

4.1 Positioning Use Cases and Applications

Positioning systems can offer a variety of use cases and applications for the user. These use cases are based on three main concepts: positioning, tracking and navigation. Positioning refers to the determination of a person or object with reference coordinates. Tracking is monitoring the movement of a person or object. Navigation is routing and guidance from the current location to destination. Tracking combines the determination of the current position with position history data. In navigation, the knowledge of the current position or travelled route is the background information and it is combined with information about the environment. For example, a map could provide additional information. With this information, it is possible to navigate a route from the current location to the destination. [69, pp. 1–3]

Positioning, tracking and navigation are interesting because the information and knowledge about locations or assistance with navigation from one place to another can offer new possibilities and make life easier on both individual and societal levels. For example, transport can be made easier, faster, and safer. On the other hand, positioning makes it easier to search of objects. It is also easier to generate information related to a specific location is easier when an accurate and reliable positioning system is in use.

Positioning, tracking and navigation are strongly present in our everyday lives. Some of the positioning use cases for positioning are so common that we may not realise the importance of positioning. For example, finding your position after getting lost while picking berries in a forest or navigating through the streets of a city you are visiting for the first time using Global Navigation Satellite System (GNSS) and a background map on your mobile phone. A constantly updated public transport timetable or live tracking of buses and trams could be other applications to utilize the real-time positioning systems, with

mobile phone and map application. GNSS positioning works well outdoors with good accuracy, but narrow streets with tall buildings are already a challenge for GNSS systems. There are also many interesting indoor positioning use cases where GNSS positioning does not work. Therefore, different positioning systems are needed for indoor positioning. For example, indoor positioning systems can be based on WiFi or Bluetooth signals, or on mobile communication systems, like 5G. So it can be any radio communication system where we can measure signals and use the measurements for a positioning solution with specific positioning methods.

IoT is growing significantly, and the location data of IoT devices is important. For example, the location data can be used to combine the environmental information measured by the IoT sensors with the exact location, to locate objects or to track their movements. Precise positioning of IoT devices or devices with tag can also enable many modern and innovative applications, such as remote control or automation. Devices in IoT systems transmit and receive radio signals. Therefore, IoT systems have a high potential for both indoor and outdoor positioning. Especially IoT systems in mMTC areas have dense networks of IoT devices, and the information about the locations of the devices is interesting and important. There are also a lot of radio signals that could be used for positioning. One challenge with IoT positioning is that we would want to have accurate positioning, but we also want to have very low power consumption. Combining these two aspects is not easy and it requires trade-offs. Therefore, in this thesis we will study the potential positioning methods that can be used with DECT-2020 NR technology. We will also theoretically study the best possible positioning accuracy and the lowest possible possible positioning errors with DECT-2020 NR numerologies. To obtain these results, we will first present the theory and basic principles of different positioning methods.

Some examples of potential positioning related use cases and applications could be smart cities, safe and smart transportation, smart buildings, smart home, smart agriculture, Industry 4.0, factory automation, process automation, asset and people tracking, asset management, smart electricity metering, and radio resource management. For example, traffic management and optimization of street lightning or finding parking spaces are possible scenarios for a smart city where accurate positioning could be a key enabler. IoT also plays an important role in many of these applications and use cases. The DECT-2020 NR technology aims to cover at least some of the related use cases. For some DECT-2020 NR features already seem to respond to requirements, such as smart home and smart city [35].

4.2 Related Work

Public research on positioning in the DECT-2020 NR environment is not yet widely available, but there has been done research on positioning in other IoT environments. For ex-

ample, positioning related aspects for different IoT protocols have been presented and the rough accuracies are compared in [10]. In the same study, the positioning performance of the Wirepas IoT mesh solution is also studied with experimental measurements. Wirepas IoT is based on the DECT-2020 NR standard. The positioning domain studied is RSS and is therefore based on power domain measurements. The study concluded that, at that moment, the best trade-off between implementation cost and positioning accuracy for low-power systems was offered by power-domain positioning. [10]

There is a lot of research positioning techniques in WSN. For example publications [70], [71], [72], [73], [74] deal with the topic of WSN localization. The positioning principles and operating environments of wireless sensor networks covered in these publications are generally similar to those covered in DECT-2020 NR. These and other references used provide some basis for considering the potential positioning methods for DECT-2020 NR. For example, AoA, ToA, TDoA and RSS are positioning techniques that are considered in many sources, and the main points of these positioning methods are also presented in this work. As mentioned above, the same positioning principles are broadly applicable in different environments and systems.

Some evaluation aspects for different positioning methods could be accuracy, power consumption, energy efficiency, system cost and hardware cost. For example, different positioning techniques in these terms are compared in [74]. However, in this work we will focus on the possibilities of different positioning methods in the DECT-2020 NR environment using the DECT-2020 NR numerologies.

4.3 Positioning methods

Positioning can be used in many different ways and from many different information sources. First, we need to have measurements or other information related to the position. Then, with the information we have, we can calculate an estimate for the unknown position using different calculation methods. The more unique and recognizable the information is, the better the accuracy of position estimate is. Different errors in the measurements make positioning more challenging and reduce the accuracy of the localization.

Positioning techniques can be divided into different positioning domains based on the type of physical quantities used. The main positioning domains are time-based, space-based and power or signal strength based positioning. Also other position domains exist and they may provide new possibilities especially in the future. For example, light, sound, smell and geomagnetic field can be used for positioning, but the three domains mentioned earlier are more general and easier to measure. [10]

In radio localization methods, we need to have a signal transmission between a transmitter (TX) and a receiver (RX). As presented in [69, pp. 21–22], there are two main

approaches for the radio location methods that differ in the direction how the positioning happens: self-positioning and network-positioning. In self-positioning, the transmitter is at a known position and the position of the receiver is determined. The unknown position is often calculated on device to be located. In network positioning, the transmitter is at an unknown position and the position of the receiver is known. The position is calculated at the receiver or at the network from the RX side. [69, pp. 21–22] There may also be some errors or inaccuracies in the known device positions. This could be the case with a mesh network, for example. Then the position solution is more challenging to obtain, but not impossible. More complex and efficient algorithms can be used in these cases.

In this section, we will consider the position methods ToA and TDoA as time-based domain solutions, AoA as a space-based solution with angle measurements, and RSS as a power or signal strength solution. It is also possible to combine different positioning methods, and thus potentially improve positioning accuracy. However, this can increase power consumption and complexity. An appropriate method or combination of methods should be selected for each situation.

4.3.1 Time of Arrival (ToA)

ToA is a propagation time based positioning method [69, pp. 22–26]. In certain contexts, ToA may refer specifically to the exact time of signal arrival. Then, time of transmission (ToT) denotes the moment when the signal is transmitted, and time of flight (ToF) represents the elapsed time between ToT and ToA, the propagation delay. Nevertheless, in here we use the term ToA to describe the position method based on the one-way propagation time between a transmitter and a receiver.

ToA is based on trilateration. Trilateration is a technique used to determine the position of a device or other object by measuring its distance from three known reference points. The ranges used in trilateration can be defined in different ways. ToA is one general trilateration-based positioning method, but trilateration can also be performed based on RSS measurements, for example. In two-dimensional (2D) trilateration, at least three reference points are needed to locate a device if the timing error is not known. In the case of three-dimensional (3D), at least four reference points are needed for positioning. However, in 3D case, if the positions of three anchors are fixed and known, and all measurements are fully synchronized, the unknown user position in 3D can be solved with only these three reference points [10]. When more than three reference points are used for positioning, the term multilateration can be used instead of trilateration to emphasise the number of distance measurements. If more than three reference points are used in a 2D case, the accuracy should be theoretically better. This is because error sources (i.e. noise or obstructions) can be better detected and more measurements with a better quality can be used for positioning.

There are several possible computational methods and algorithms to solve the trilateration problem. For example, approximation, iterative or linear algebraic solutions can be used. They differ in computational complexity and estimation error. The computational requirements for trilateration are not significant, but any reduction in the computation time and complexity can increase battery life. [75] Energy-efficiency and low battery consumption are especially desirable in IoT systems.

We consider the ToA method in a basic situation where two assumptions are made: [69, pp. 22–26]

- The signal propagation speed is known.
- Line of sight (LoS) circumstances exist, which means that the signal can propagate along the shortest path. For example, there is no reflection, refraction, diffraction, shadowing or scattering that could cause diversion for the signal.

Let's consider a self-positioning situation where the position of the receiver is solved. The distance between transmitter (TX) and receiver (RX) can be defined as

$$d_i = c(T_{\text{RX}} - T_{\text{TX}}) = c(T_i - T_0), \quad (4.1)$$

where c is light speed, $T_{\text{RX}} = T_i$ is the absolute moment of time when the radio signal is received in the RX, and $T_{\text{TX}} = T_0$ is the moment of time when the signal is transmitted in the TX. In here, LoS is assumed. [69, pp. 23–26] The same equation applies in both directions. The important factor is the elapsed time between the transmitter and receiver, which represents the propagation delay.

Equation 4.1 gives a radius of a circle in the 2D situation, and the unknown device can be anywhere on the circumference. In the 3D case, the distance between TX and RX represents a radius of a sphere, and the user device with unknown position can be anywhere on the surface of a sphere. To solve the user position, we need more measurements from other transmitters to use the trilateration principle. At least three known reference points in 2D and four in the 3D situation.

The distance measurements to N known radio devices form a system of N non-linear equations. In the 3D case, the coordinates of the user device (x, y, z) are unknown, and the system of equations can be written as [69, pp. 23–26]

$$\begin{aligned} d_1 &= c(T_1 - T_0) = \sqrt{(x - x_1)^2 + (y - y_1)^2 + (z - z_1)^2}, \\ d_2 &= c(T_2 - T_0) = \sqrt{(x - x_2)^2 + (y - y_2)^2 + (z - z_2)^2}, \\ &\vdots \\ d_N &= c(T_N - T_0) = \sqrt{(x - x_N)^2 + (y - y_N)^2 + (z - z_N)^2}. \end{aligned} \quad (4.2)$$

In the 2D scenario, the equation is otherwise the same, but the z coordinates can be

omitted. Once we have all these distance measurements, we also get all these circles (2D) or spheres (3D) with these radii. The intersection of all these circles or spheres defines the location of the unknown radio device. The trilateration principle in ToA in the theoretical case of 2D without error is shown in Figure 4.1.

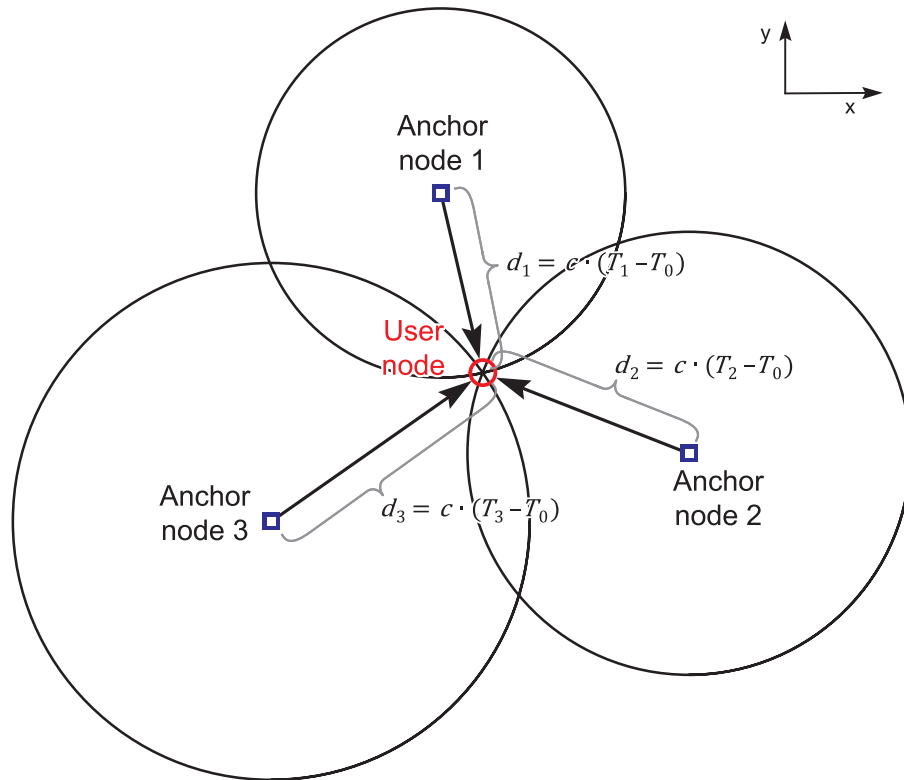


Figure 4.1. ToA trilateration in the theoretical error-free 2D case. The intersection of the circles defines the position of the user device.

In practical systems, the distance measurements d_i are generally noisy. There can also be other sources of error, such as clock errors, and therefore the distance between the user and the anchor will be estimated incorrectly. This means that there is no single-valued solution and the circles or spheres do not intersect at an exact point. An error can be marked by ϵ in the equations. [69, pp. 23–26] The position of user can be estimated with various calculation methods. The position can be presented with error bounds or confidence ellipses in 2D visualisations. One example of a ToA trilateration with error is shown in Figure 4.2.

If the system of equations is over-determined, for example, there are more equations than unknowns, finding a solution requires more sophisticated computational methods. It can be considered as an equivalent system of equations

$$(x - x_i)^2 + (y - y_i)^2 + (z - z_i)^2 - c^2(T_i - T_0)^2 = \epsilon_i^2, \quad i = 1, \dots, N \quad (4.3)$$

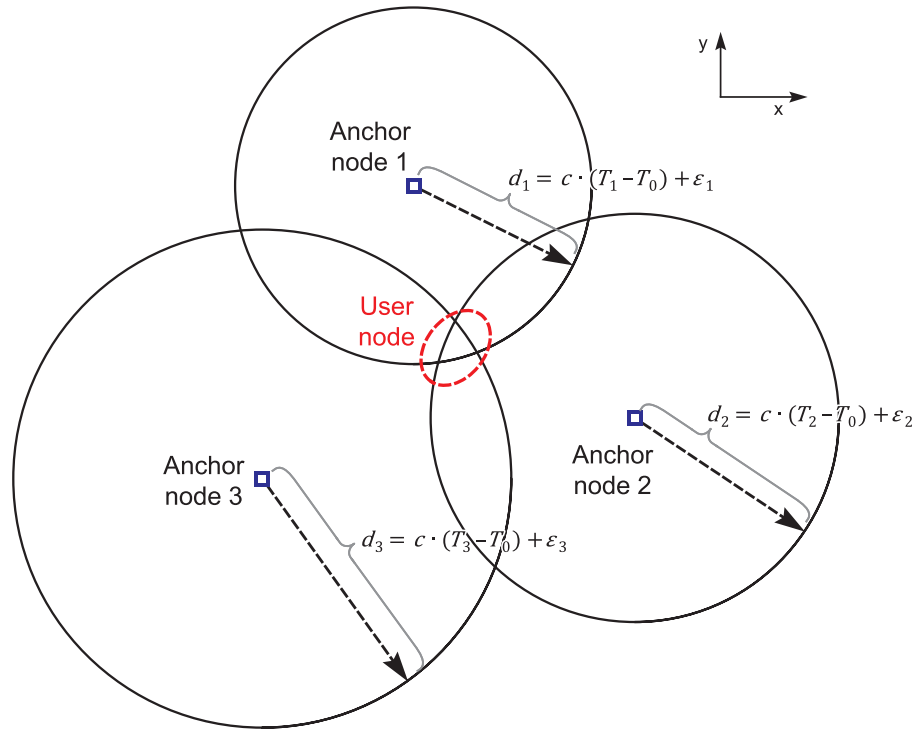


Figure 4.2. ToA trilateration in the 2D case with error. The intersection of the circles defines the area with high probability for the user device position.

that shows an error value ϵ_i per equation. An estimation

$$(\hat{x}, \hat{y}, \hat{z}) = \arg \min_{(x,y,z)} \sum_{i=1}^N \epsilon_i^2 \quad (4.4)$$

of the unknown radio device position can be solved by minimizing the total quadratic error. [69, pp. 23-26]

There are some clear challenges with ToA positioning. In theory, ToA is a really accurate positioning method, but with all the small details and limitations in the real physical world makes it more error-sensitive. Some of the challenges can be overcome, but it is necessary to take them into account when designing and developing the system with positioning. Some of the challenges are presented below.

The time bases in all the anchor devices and the user device must be the same. However, this requirement is difficult to achieve because the devices have low cost oscillators as clocks, and the clocks are not stable enough during the measurement. Also, synchronization between the devices would be necessary to avoid the synchronization error. In positioning, synchronization often means that the difference between the clocks is known, not necessarily that the clocks are synchronized to the same time. [69, pp. 24–26]

The measurement of signal propagation delay is affected by thermal noise. It is often modelled as an additive white Gaussian noise (AWGN) process and is therefore a so-

called unbiased error. [69, pp. 24–26]

Non-line of sight (NLoS) propagation is a significant source of error and is caused by reflection, refraction or diffraction. This means that signals do not propagate the shortest possible way from transmitter to receiver. In practice, NLoS is likely to happen, and it is important to consider both NLoS and LoS propagation. [69, pp. 24–26]

4.3.2 Time Difference of Arrival (TDoA)

TDoA positioning method is based on the propagation delay differences. TDoA is a useful method to eliminate clock synchronization differences between anchor devices. However, TDoA positioning also assumes that the clocks between the devices are stable. In other words, the duration of a unit of time (e.g. second) should be the same between the clocks, but it does not matter if the clocks show different times. [69, pp. 26–28]

In TDoA, two signals are transmitted synchronously from two different anchor devices i and j at the same time moment T_0 , and the signals are received in the user device at two different time instances T_i and T_j . Because the radio signals travel at the speed of light c , the difference in propagation distance can be calculated by multiplying the signal propagation time differences by the speed of light. Thus, the TDoA equation can be written as

$$\Delta d_{i,j} = d_i - d_j = c(T_i - T_0) - c(T_j - T_0) = c(T_i - T_j) = c\Delta T_{i,j}. \quad (4.5)$$

The TDoA equation system consists of $N - 1$ equations, where N is the number of anchors for which we have measurements. The distances between the transmitter and the receiver d_i and d_j are Euclidean distances in 3D, which can be presented as

$$d_i = \sqrt{(x - x_i)^2 + (y - y_i)^2 + (z - z_i)^2}, \quad (4.6)$$

$$d_j = \sqrt{(x - x_j)^2 + (y - y_j)^2 + (z - z_j)^2}. \quad (4.7)$$

In 2D case, only two coordinate planes (x and y in general) are considered. As we can see from the Equation 4.1 and Equation 4.5, TDoA is the time difference between the two ToA radio signal measurements. We get rid of T_0 and the both T_i and T_j are measured in the user device. Thus, we do not have the problem with the different time scales between the user device and the anchors. This is a big advantage of TDoA compared to ToA. However, like ToA, also TDoA measurements are noisy in reality. This must be taken into account during the positioning process. There may also be more equations than unknowns. For example, a least squares algorithm can be used to solve the system of equations. [69, pp. 26–28]

Propagation delay measurements of TDoA create hyperbolas in 2D and hyperboloids

in 3D with the foci of the anchors involved. The intersection of the hyperbolas (2D) or hyperboloids (3D) provides the position of the user device. Therefore, TDoA positioning is called as hyperbolic positioning. [69, pp. 26–28] An example of TDoA positioning in the error-free 2D case is presented in Figure 4.3, where the hyperbolas are presented by purple lines.

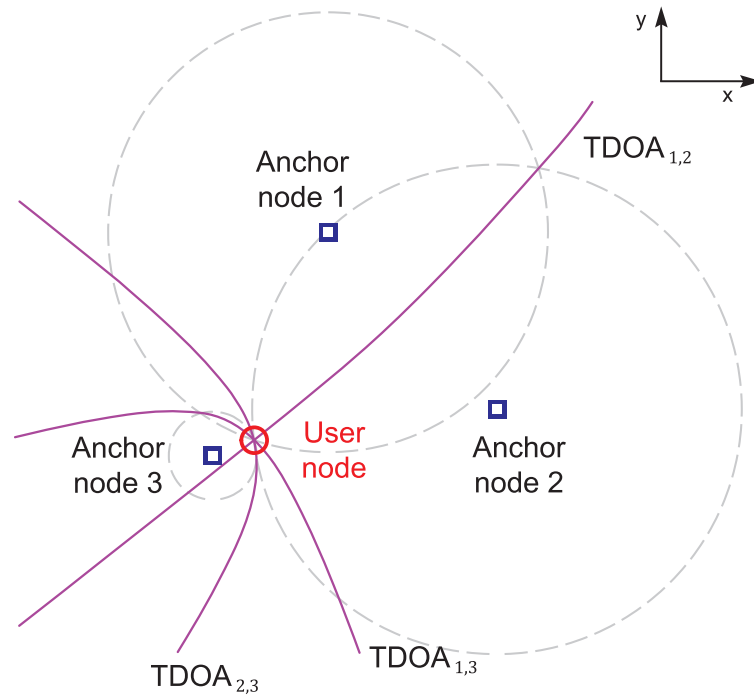


Figure 4.3. TDoA in the theoretical error-free 2D case. The intersection of the hyperbolas defines the position of the user device.

The necessary assumptions for TDoA are similar to those for ToA. The propagation velocity must be known and LoS propagation is assumed. In the case of NLoS, the positions of reflectors or obstacles causing refraction or diffraction are required to be known, or these are further unknowns in the TDoA system equations. [69, pp. 26–28]

4.3.3 Received Signal Strength (RSS)

RSS -based positioning is potential method especially for IoT applications. RSSI measurements are relative easily available. So, the power consumption is not increased or separate extensions are not needed due to the RSSI measurements which makes possible to keep the system development costs low. However, the RSS-based positioning is relatively inaccurate or it requires a lot of time to build the database. [76, pp. 46–55] It is necessary to consider whether the accuracy can meet the position accuracy requirements set for the system. There are a few different possible position methods that can be used with RSS measurements [76, pp. 46–55].

Trilateration can be used in RSS-based positioning in a similar way than in ToA position-

ing. Instead of using the time measurements, the signal strength measurements in the user device are taken from multiple anchors. The distances between the unknown device and the anchors are estimated based on the received signal strength information. Then the basic principle of trilateration is used and the location of the user device can be estimated. In general, RSS-based distance estimation is not as accurate as ToA-based estimation with synchronized clocks because there are many environmental factors that can affect the signal strength and cause variations in the measurements.

Signal power is attenuated during transmission from the transmitter to the receiver. In addition to signal power measurements, path loss models can be used to determine the signal power at a certain point. A classical path loss (PL) model can be written as

$$P_r(d) = P_r(d_0) - 10\eta \log_{10}\left(\frac{d}{d_0}\right) + \omega, \quad (4.8)$$

where $P_r(d)$ is the received signal power on a logarithmic scale as a function of distance d , $P_r(d_0)$ is the reference signal power on a logarithmic scale at a reference distance d_0 , $\eta > 0$ is the path loss exponent and $\omega \sim \log(\mathcal{N}(0, \sigma^2))$ is a logarithmic normally distributed random variable. [10], [77]

Another method that can be used for RSS-based positioning is fingerprinting. However, fingerprint-based positioning requires more base work before the actual position estimation. Fingerprints are position-dependent signal parameters. Radio frequency (RF) fingerprints are stored in a database, also called as a correlation database (CDB), which makes possible to estimate the positions by comparing received measurements to values in the database. CDB can be collected in field tests or RSS values can be generated by simulation models. Fingerprinting techniques have two phases: training phase and a test/operational phase. In the first phase the CDB is built and in the second phase the position estimate for the device is produced. [78]

4.3.4 Angle of Arrival (AoA)

AoA is a space-based positioning method which is based on the angle measurement of the signal [10]. In other words, in the AoA positioning the direction of the signal arriving to the receiver is measured and with multiple angle measurements the user position can be solved [69]. The term direction of arrival (DoA) is also used in some sources from direction based positioning [78]. We consider here a scenario where the receiver is user device with unknown location and the transmitting devices are anchors, and they have known locations. Also the other direction would work. If the orientation of receiver is known, it makes the AoA equations simpler [69]. In the following equations, LoS propagation is assumed to simplify the problem. As in the ToA positioning method, NLoS cause challenges to the positioning and the NLoS must be identified and processed to obtain

undistorted positioning results [79]. In Equation 4.9, the orientation of the user device is known.

First, we consider AoA positioning in the 2D case. If we have two transmitters with known location, we can solve the position (x, y) of the receiver in the 2D case with the linear equation system

$$\begin{aligned} y - y_1 &= \tan(\varphi_1)(x - x_1) \\ y - y_2 &= \tan(\varphi_2)(x - x_2), \end{aligned} \quad (4.9)$$

where x_1 and y_1 are the coordinates of transmitter 1, φ_1 is the angle of arrival from transmitter 1 and (x_2, y_2) , φ_2 are the same variables of transmitter 2 [69, pp. 32–35]. An example of AoA positioning in the error-free 2D case is shown in Figure 4.4. Measurements from two different anchors would be enough for positioning solution in the error-free 2D case, but Figure 4.4 shows measurements from three different anchors.

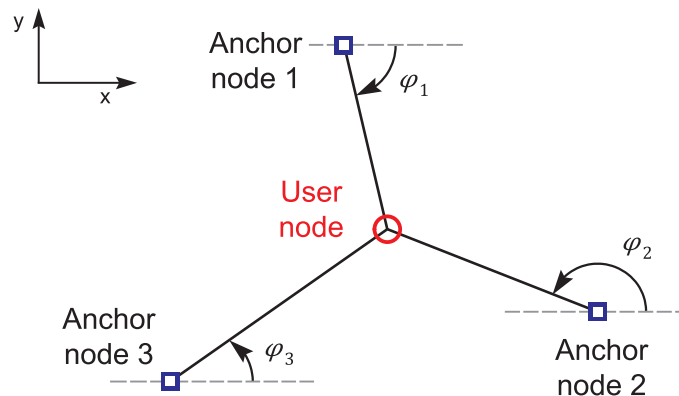


Figure 4.4. AoA in the theoretical error-free 2D case. The intersection of the angle measurements defines the position of the user device.

If the orientation of the user device is not known, another unknown term is added to the equation. In this case, we obtain a set of equations

$$y - y_i = \tan(\varphi_i + \varphi)(x - x_i), \quad i = 1, \dots, N, \quad (4.10)$$

where the φ is the unknown orientation. The set of equations is non-linear. [69] To eliminate the unknown position of the user device, the angle is typically measured at the anchor instead of the user device since the orientation of the anchor is usually known.

Next, we will extend the consideration to a 3D AoA positioning scenario. The same main principles apply to 3D AoA positioning as in 2D. However, in addition to observing the signal direction azimuth angle φ_i , it is also necessary to know the direction elevation angle ϑ_i to solve position with the AoA measurements. Also in here, the orientation of the user device is needed to be known as it will affect the AoA solution. For simplicity, we assume that the orientation of the located device is known. [69, pp. 33–35]

The signal is transmitted from the anchor device i and received in the user device. If we use spherical coordinates (x, y, z) with azimuth angle φ and elevation angle ϑ , the equation can be written as

$$\begin{pmatrix} x - x_i \\ y - y_i \\ z - z_i \end{pmatrix} = r_i \begin{pmatrix} \cos(\vartheta_i + \vartheta) \cos(\varphi_i + \varphi) \\ \cos(\vartheta_i + \vartheta) \sin(\varphi_i + \varphi) \\ \sin(\vartheta_i + \vartheta) \end{pmatrix},$$

where (x_i, y_i, z_i) are the coordinates of the anchor i , φ_i is the azimuth of the received signal and ϑ_i is the elevation of the received signal. The above equation can be written as

$$\begin{aligned} (y - y_i) &= \tan(\varphi_i + \varphi)(x - x_i) \\ \cos(\varphi_i + \varphi)(z - z_i) &= \tan(\vartheta_i + \vartheta)(x - x_i), \end{aligned} \tag{4.11}$$

where we have eliminated the radius r . This set of two equations presented in 4.11 can be obtained from any anchor. In Equation 4.11, there are five unknown components: x_i, y_i, z_i, φ_i and ϑ_i . Therefore, we need at least five equations, which means azimuth and elevation measurements to at least three anchors. [69, pp. 33–35]

4.4 Theoretical Positioning Bounds

In the various fields of technology it is generally interesting to evaluate the performance of the system with numerical values. In the field of positioning and localization, positioning bounds are key concepts to obtain practical values to illustrate how accurate the positioning system is. For example, CRLB and PEB are practical approaches that have been widely used in different researches. CRLB and PEB can be used to obtain theoretical bounds on positioning accuracies. These concepts are also used in this thesis to analyze possible positioning accuracies in DECT-2020 NR technology. The theoretical and simulated results are presented in Chapter 6. In this section, the fundamental background of CRLB and PEB is described.

4.4.1 Cramér-Rao Lower Bound (CRLB)

CRLB is a fundamental concept in information theory and statistics. CRLB defines a performance lower bound on the variance of an unbiased estimator in a statistical model. CRLB can be used to estimate the best possible theoretical performance of the system with the given parameters. [80], [81]

CRLB is widely used in the field of positioning and localization. The concept of CRLB is described and the CRLB equations are presented and derived in many books on signal

processing and positioning theory, for example [69], [78], [80], [81].

The variance of an estimate given by CRLB can be used to describe the accuracy of the positioning estimator if we have the necessary information about the signal properties through measurements or theoretical values together with the knowledge of the system parameters and numerologies. The lower the variance, the better the accuracy of the estimator. CRLB gives the lowest value of the variance of an estimate, and unbiased estimation algorithm cannot perform better than CRLB defines. [69, pp. 41–43] In other words, CRLB is a limit beyond which performance cannot be improved without modifying the system.

CRLB is based on a probability density function (PDF). PDF describes how the values of a random variable are likely to be distributed over a specific range of values. PDF can be considered as a mathematical representation of the likelihood of observing certain values of a continuous random variable within a given range. [80]

One type of continuous probability distribution is the normal distribution, also known as the Gaussian distribution. The general notation for a Gaussian distribution is

$$\mathcal{N}(\mu, \sigma^2),$$

where μ is the mean or expectation of the distribution and σ^2 is the variance. Moreover, σ , the square root of variance, is called the standard deviation. The general form of the probability density function for a Gaussian distribution is

$$p(x) = \frac{1}{\sigma\sqrt{2\pi}} \exp\left(-\frac{1}{2}\left(\frac{x-\mu}{\sigma}\right)^2\right). \quad (4.12)$$

Probability mass function (PMF) could be described as a discrete version of PDF. In PMF the random variables are discrete values.

In positioning we are interested to know the location in the two or three dimensions and use the coordinates, such as (x, y) or (x, y, z) . The concept of univariate normal distribution can be generalized to two dimensions or more and it is then called as multivariate normal distribution. The general notation for the Gaussian distribution is

$$\mathcal{N}_k(\mu, \Sigma),$$

where μ is the k -dimensional mean vector and Σ is the $k \times k$ covariance matrix.

The PDF of the multivariate normal distribution \mathbf{x} is

$$p(\mathbf{x}) = \frac{1}{(2\pi)^{\frac{n}{2}} |\Sigma|^{\frac{1}{2}}} \exp\left(-\frac{1}{2}(\mathbf{x}-\mu)^T \Sigma^{-1}(\mathbf{x}-\mu)\right), \quad (4.13)$$

where \mathbf{x} is a vector of random values.

Another example of different probability density functions is the uniform distribution. In a uniform distribution, all values within a given range or set of elements have the same probability of being observed. The general form of a continuous uniform distribution function is

$$f(x) = \begin{cases} \frac{1}{b-a} & \text{for } x \in [a, b], \\ 0 & \text{else,} \end{cases} \quad (4.14)$$

where a is the lower bound and b is the upper bound of the observed values.

The CRLB applies to unbiased estimators. It means that the expected value of the estimator is equal to the true value of the parameter being estimated. [80]

It is assumed that the PDF $p(\mathbf{x}, \theta)$ satisfies the regularity condition. The variance of any unbiased estimator $\hat{\theta}$ must satisfy

$$\text{Var}(\hat{\theta}) \geq \frac{1}{-\text{E} \left[\frac{\partial^2 \ln p(\mathbf{x}, \theta)}{\partial \theta^2} \right]}, \quad (4.15)$$

where $\hat{\theta}$ is an unbiased estimator, $\text{E}[X]$ is the expected value of X , $\frac{\partial^2 f}{\partial x^2}$ is the second order partial derivative, $\ln p(\mathbf{x}, \theta)$ is the natural logarithm of the likelihood function of θ , that is, the measurement set and θ is the true value. [80] [78, pp. 36–39]

The denominator in Equation 4.15 is called Fisher information and it can be written as [80]

$$I(\theta) = -\text{E} \left[\frac{\partial^2 \ln p(\mathbf{x}, \theta)}{\partial \theta^2} \right]. \quad (4.16)$$

As we can see from Equation 4.15 and Equation 4.16, the general form for the CRLB for an unbiased estimator can be stated as

$$\text{CRLB} = \text{Var}(\hat{\theta}) \geq \frac{1}{I(\theta)}, \quad (4.17)$$

where $I(\theta)$ is the Fisher information. The parameter θ is estimated from a set of independent and identically distributed observations or measurements. [80, pp. 30–31], [78, pp. 36–39]

The Fisher information measures the amount of information that the probability distribution of a random variable carries about an unknown parameter. It indicates how sensitive the likelihood function of a statistical model is to changes in the parameter being estimated. If the Fisher information is high, it means that small changes in the parameter value will lead to noticeable changes in the likelihood function and in that way, making it easier to estimate the parameter accurately. If the Fisher information is low, it is more difficult to make accurate estimates.

We use the Fisher information in positioning related cases in 2D or 3D dimensions, which means that there are certainly multiple parameters in the system. The Fisher information takes the form of matrix of size $N \times N$. In the 2D case the size of a matrix would be 2×2 and in the 3D case the size would be 3×3 . The Fisher information matrix (FIM) is defined as

$$\mathbf{I}(\boldsymbol{\theta}) = \text{E} \left[\left(\frac{\partial}{\partial \boldsymbol{\theta}} \ln f(\mathbf{x}, \boldsymbol{\theta}) \right) \left(\frac{\partial}{\partial \boldsymbol{\theta}} \ln f(\mathbf{x}, \boldsymbol{\theta}) \right)^T \right], \quad (4.18)$$

where $f(\mathbf{x}, \boldsymbol{\theta})$ is the PDF of the random vector \mathbf{x} conditioned on $\boldsymbol{\theta}$ [82]. The parameter vector $\boldsymbol{\theta}$ contains the unknown parameters. For example, these could be the position coordinates (x, y) in 2D and (x, y, z) in 3D. [69, pp. 95–96]

An example of a simple FIM with two parameters $\boldsymbol{\theta} = (\theta_1, \theta_2)$ could be presented as

$$\mathbf{I}(\boldsymbol{\theta}) = \begin{bmatrix} I_{1,1} & I_{1,2} \\ I_{2,1} & I_{2,2} \end{bmatrix},$$

where $I_{i,j}$ is the Fisher information between the individual parameters i and j . Since the order has no effect on the result, we can see that $I_{1,2} = I_{2,1}$.

The elements of the FIM are calculated as follows:

$$I_{1,1} = -\text{E} \left[\frac{\partial^2}{\partial \theta_1^2} \ln f(x, \theta) \right]$$

$$I_{1,2} = I_{2,1} = -\text{E} \left[\frac{\partial^2}{\partial \theta_1 \partial \theta_2} \ln f(x, \theta) \right]$$

$$I_{2,2} = -\text{E} \left[\frac{\partial^2}{\partial \theta_2^2} \ln f(x, \theta) \right]$$

The diagonal elements of the FIM represent the Fisher information for each individual parameter. These diagonal elements quantify how much information the data set provides about each parameter separately. The off-diagonal elements show the correlation between the different parameters. If the element is close to zero, it indicates that the related parameters in the data set are not strongly correlated. If they are significantly different from zero, it indicates that the parameters are interdependent and a change in one parameter affects for the estimation of another.

4.4.2 Cramér-Rao Lower Bound for Time Estimation

Position can be estimated by measuring the propagation time of the signal. For example, ToA and TDoA are propagation time based methods, as presented in Section 4.3. Next we

will look at the equations for ToA positioning in the multicarrier modulation scheme orthogonal frequency division multiplexing (OFDM). OFDM can be defined as frequency division multiplexing (FDM) with overlapping subchannels without interfering with others. Avoiding the interference is possible because the subcarriers are orthogonal to each other. [83]

We assume uniformly distributed energy, i.e. the signal energy is equally distributed among the subcarriers $-M, \dots, M$ and the subcarriers are located symmetrically around the central subcarrier (also called subcarrier zero). Therefore, the signal energy is

$$|S_n|^2 = \begin{cases} |S|^2 & n \leq \frac{N}{2} \\ 0, & \text{else} \end{cases}$$

and the number of used subcarriers is $N_u = 2M + 1$. Here we get $M = \frac{N_u - 1}{2}$. [69, pp. 50–51]

The CRLB for time estimation with the assumptions mentioned above is

$$\text{Var}\{\hat{\tau}(\mathbf{r})\} \geq \frac{\sigma^2}{8\pi^2 f_{\text{SC}}^2 |S|^2 \sum_{m=-M}^M n^2} = \frac{1}{8\pi^2 f_{\text{SC}}^2 \frac{|S|^2}{\sigma^2} \frac{M(M+1)(2M+1)}{3}}, \quad (4.19)$$

where σ^2 is the noise variance, f_{SC} is the subcarrier spacing, $|S|^2$ is the signal energy and M is the number of used subcarrier pairs around the subcarrier zero [69, pp. 46–58].

Occupied bandwidth can be written as

$$B = N_u f_{\text{SC}},$$

where N_u is the number of used subcarriers [69, pp. 46–58].

With Equation 4.19, we will get the result for time estimation. However, we are often interested in the positioning accuracy as a distance estimation. The CRLB for distance estimation in form of the standard deviation can be written as

$$\text{std dev} = c\sqrt{\text{Var}\{\hat{\tau}(\mathbf{r})\}},$$

where $c = 2.998... * 10^8 \frac{\text{m}}{\text{s}}$ is the speed of light [69, pp. 50–51].

If we use the definition of signal-to-noise ratio (SNR) [69, p. 50]

$$\text{SNR} = \frac{|S|^2}{\sigma^2}$$

and will combine it with Equation 4.19, we can simplify the equation as

$$\text{Var}\{\hat{\tau}(\mathbf{r})\} \geq \frac{1}{8\pi^2 f_{\text{SC}}^2 \text{SNR} \frac{M(M+1)(2M+1)}{3}}. \quad (4.20)$$

Therefore, in order to estimate CRLB for time measurements, we need to know the signal-to-noise ratio, the subcarrier spacing and either the number of used subcarriers or the effective bandwidth. As can be seen from this equation in [29], wide bandwidth signals with high SNR make positioning based on time estimation more accurate.

The standard deviation for time estimation CRLB can be obtained as the square root of the variance

$$\text{std dev} = \sqrt{\text{Var}\{\hat{\tau}(\mathbf{r})\}}, \quad (4.21)$$

where std dev is the standard deviation and $\text{Var}\{\hat{\tau}(\mathbf{r})\}$ is the time estimation variance.

4.4.3 Cramér-Rao Lower Bound for Angle Estimation

Another way to estimate position is to measure the angle of signals. AoA is a positioning method which is based on angle measurements.

CRLB for angular estimation in radians can be written as

$$\text{Var}\{\hat{\alpha}(\mathbf{r})\} \geq \frac{6}{L(L^2 - 1) \text{SNR } k^2 d^2 \cos^2(\alpha)}, \quad (4.22)$$

where L is the number of antenna elements, SNR is the signal-to-noise ratio, k is the wave number, d is the antenna element spacing (the distance between adjacent elements) and α is the received angle of a planar wavefront [69, pp. 59–68].

Equation 4.22 assumes AWGN, which can only be considered as a good approximation for high SNRs only [69, pp. 59–68].

The wave number is defined as $k = \frac{2\pi}{\lambda}$ and in order to observe only one amplitude maximum, the antenna element spacing have to be restricted $d < \frac{\lambda}{2}$. As we can see, in this scenario the wave number and the antenna element are related to π , since

$$k^2 d^2 = (kd)^2 = \left(\frac{2\pi}{\lambda} * \frac{\lambda}{2}\right)^2 = \pi^2.$$

If we want to have a unique amplitude maximum, the antenna element spacing is up to half of the wavelength, and therefore, Equation 4.22 gets its minimum value here. Thus, the 4.22 can be simplified as

$$\text{Var}\{\hat{\alpha}(\mathbf{r})\} \geq \frac{6}{L(L^2 - 1) \text{SNR } \pi^2 \cos^2(\alpha)}. \quad (4.23)$$

As we can see from Equation 4.23, in this simplified case, we need to know the system parameters L , SNR and α in order to estimate the location using angular CRLB.

CRLB in radians can be converted to degrees using the equation

$$\text{Var}\{\hat{\alpha}(\mathbf{r})\}_{\text{deg}} = \text{Var}\{\hat{\alpha}(\mathbf{r})\}_{\text{rad}} * \left(\frac{180^\circ}{\pi}\right)^2, \quad (4.24)$$

where $\text{Var}\{\hat{\alpha}(\mathbf{r})\}_{\text{deg}}$ is the variance in degrees and $\text{Var}\{\hat{\alpha}(\mathbf{r})\}_{\text{rad}}$ is the variance in radians.

The standard deviation for angle estimation CRLB can be obtained as the square root of the variance

$$\text{std dev} = \sqrt{\text{Var}\{\hat{\alpha}(\mathbf{r})\}}, \quad (4.25)$$

where std dev is the standard deviation and $\text{Var}\{\hat{\alpha}(\mathbf{r})\}$ is the variance of the angle estimation.

4.4.4 Position Error Bound (PEB)

PEB is a quantity that can be used to analyze and compare the positioning accuracies. PEB gives positioning accuracies in a more understandable way because the PEB can be presented as a distance of accuracy when the CRLB gives a variance.

PEB is called to be the square-root of the CRLB of the position and can be written as

$$\text{PEB} = \sqrt{\text{trace}(\text{CRLB})} = \sqrt{\text{trace}(\mathbf{I}(\boldsymbol{\theta})^{-1})}, \quad (4.26)$$

where $\mathbf{I}(\boldsymbol{\theta})$ is FIM. [84], [85], [86] The calculation of PEB can be done indirectly by transforming the bounds of the channel parameters, such as AoA and ToA [84].

PEB can be used to compare positioning errors in different cases. For example, positioning accuracy depends on the location of the device and PEB can be used to compare the accuracies in different locations. For example, in this thesis we have studied how the positioning accuracy varies with different numbers of used anchors in AoA.

4.5 Positioning Tracking and Kalman Filter

The positioning methods and theories presented earlier are considered in a static position estimation. Static estimation assumes that the user device with unknown position does not move during the estimation process. The static case is a good way to present the basics of positioning theory, but in practice, devices move either in a short or a long term, and it is more interesting to locate the position of a moving device over time period. One snapshot from a static moment gives only a momentary position for the localized device. [69, pp. 101–104]

There are several methods and algorithms that can be used for position tracking. If we

have some estimates or even exact knowledge from the past position estimates, it is much easier to estimate the new position. This is due to the physical limitations that different objects have on their movement, and it gives a smaller probability area for the new position. For example, changes in speed and heading are limited in practice. Appropriate mobility or movement models and the history of previous estimates can be used to solve the unknown position. [69, pp. 101–104]

4.5.1 Commonly Used Filters for Position Tracking

Some examples of commonly used filters for position tracking are KF, extended Kalman filter (EKF), unscented Kalman filter (UKF) and particle filters (PFs). The classic Kalman filter approach to position tracking assumes linear models and noise distributions. The EKF approximates non-linear models in a linearization phase based on the current mean and covariance. This linearization phase is the main difference between the EKF and the KF. As the non-linearity increases, the UKF or particle filters are more suitable choices for position tracking, because the performance of the EKF can be relatively poor in these cases. However, the complexity of calculation increases also with these filters. [69, pp. 101–118]

KF is commonly used implementation of Bayesian filters. Computational efficiency is one of the main advantages of KF, since KF uses only matrix and vector operations on the means and covariances of Gaussian processes. [69, pp. 101–118] KF estimates the state of a linear dynamic system from a series of noisy measurements [87, pp. 324–329].

KF is a recursive estimator, which means that only the estimate from the previous time-step and the current measurement are needed to solve the estimate for the current state [87, pp. 324–329]. KF relies on a state transition model to estimate the current state based on two steps: prediction and update. In the prediction step, the estimation is calculated based on the prior knowledge of previous estimates and the assumed movement model. In the update step, the estimate is updated with the obtained measurements of the current state. [78, pp. 770–772] The prediction step can also be called as *a priori* state and the update step can be called as *a posteriori* [78, pp. 772–775].

EKF is an advanced version of the KF and EKF allows solving non-linear problems [78, pp. 772–775]. In the EKF, the non-linear state transition and observation equations are linearized by the expansions of Taylor series. The linearization is done around the mean of the relevant Gaussian random variable and then the linear KF is used for the linearized model. [87, pp. 324–329]

4.5.2 Structure of Kalman Filter and Extended Kalman Filter

First, we consider the general form of the equations for the state transition model and the observation model (also known as the measurement model). The function \mathbf{f} presents the state transition model and the function \mathbf{h} presents the observation model. The functions can be linear or non-linear, but the both functions must be differentiable. At the time index k , the non-linear equations of the state estimation vector \mathbf{x}_k , and the measurement vector \mathbf{z}_k can be presented as

$$\mathbf{x}_k = \mathbf{f}_{k-1}(\mathbf{x}_{k-1}) + \mathbf{v}_{k-1} \quad (4.27)$$

$$\mathbf{z}_k = \mathbf{h}_k(\mathbf{x}_k) + \mathbf{w}_k, \quad (4.28)$$

where \mathbf{v}_k is the system process noise, and \mathbf{w}_k is the measurement noise. [69, pp. 104–118], [87, pp. 324–329]

Following assumptions about the system model must apply in the classic KF:

- The system process noise $\mathbf{v}_k \sim \mathcal{N}(\mathbf{0}, \mathbf{Q}_k)$ and the measurement noise $\mathbf{w}_k \sim \mathcal{N}(\mathbf{0}, \mathbf{C}_k)$ should be zero-mean Gaussian distributed with the known covariances \mathbf{Q}_k and \mathbf{C}_k .
- The system process noise and the measurement noise should be independent, meaning that they are not correlated with each other or with the state of the system.
- The state transition function $\mathbf{f}_{k-1}(\mathbf{x}_{k-1})$ should be a known linear function of the state estimate \mathbf{x}_{k-1} .
- The measurement function $\mathbf{h}_k(\mathbf{x}_k)$ should be a known linear function of the state estimate \mathbf{x}_k .

In the case of the EKF, the state model and the observation model do not have to be linear functions, but they still have to be differentiable. If the system is non-linear, EKF linearizes the system models around the current estimate. [69, pp. 104–118], [87, pp. 324–329]

Assuming that the state transition model and the observation model are linear, Equation 4.27 and Equation 4.28 for the classic KF can be written as

$$\mathbf{x}_k = \mathbf{F}_{k-1}\mathbf{x}_{k-1} + \mathbf{v}_{k-1} \quad (4.29)$$

$$\mathbf{z}_k = \mathbf{H}_k\mathbf{x}_k + \mathbf{w}_k, \quad (4.30)$$

where \mathbf{F}_k is the state matrix, and \mathbf{H}_k is the measurement matrix. The state matrix contains the linear dependencies between the states of time-steps k and $k - 1$, and the measurement matrix reflects the linear relation between the measurements and the state at time-step k . [69, pp. 104–118]

In the linearization process, the EKF utilizes Jacobian matrices. The term $\mathbf{f}_{k-1}(\mathbf{x}_{k-1})$ is obtained with the Jacobian matrix

$$\mathbf{F}_{k-1} = \frac{\partial \mathbf{f}_{k-1}(\mathbf{x}_{k-1})}{\partial \mathbf{x}_{k-1}}.$$

Similarly, the term $\mathbf{h}_k(\mathbf{x}_k)$ is linearized with the Jacobian matrix

$$\mathbf{H}_k = \frac{\partial \mathbf{h}_k(\mathbf{x}_k)}{\partial \mathbf{x}_k}.$$

In EKF linearization, Jacobian matrices are re-calculated at each time-step because they depend on the previous estimates, and the linearization is always performed around the last updated position estimate. [69, pp. 104–118]

The Kalman filter can be divided into two main steps, prediction and update. The prediction step is often based on physical model, and the update step compares the prediction to measurements. The new estimation is updated in the update step to be used in the next time-step or prediction round. In the Bayesian estimation, prior, posterior, and likelihood information have all Gaussian PDFs and therefore can be represented by means and covariances. Because of this, a simple matrix-vector notation of the estimates can be used. [69, pp. 104–118], [87, pp. 324–329] Next, we will present the general equations for the prediction and update steps.

The first step is the prediction. The state of the current time-step can be calculated using the state of the previous time-step and the knowledge of the state matrix given by \mathbf{F}_k . The estimate of the state prediction is

$$\hat{\mathbf{x}}_{k|k-1} = \mathbf{F}_{k-1} \hat{\mathbf{x}}_{k-1|k-1}, \quad (4.31)$$

where $\hat{\mathbf{x}}_{k-1|k-1}$ is the estimate of the previous time-step. The predicted estimate covariance is also part of the prediction step. The predicted a priori estimate covariance is

$$\hat{\mathbf{P}}_{k|k-1} = \mathbf{F}_k \hat{\mathbf{P}}_{k-1|k-1} \mathbf{F}_k^T + \mathbf{Q}_k, \quad (4.32)$$

where $\hat{\mathbf{P}}_{k-1|k-1}$ is the covariance matrix of the previous time-step. [69, pp. 104–118], [87, pp. 324–329]

The second step is the update. In the update step, the innovation residual vector is

$$\tilde{\mathbf{y}}_k = \mathbf{z}_k - \mathbf{H}_k \hat{\mathbf{x}}_{k|k-1}, \quad (4.33)$$

where \mathbf{z}_k is the observed measurement at the current time-step. Innovation covariance is

$$\mathbf{S}_k = \mathbf{H}_k \hat{\mathbf{P}}_{k|k-1} \mathbf{H}_k^T + \mathbf{R}_k. \quad (4.34)$$

The Kalman gain matrix is

$$\mathbf{K}_k = \hat{\mathbf{P}}_{k|k-1} \mathbf{H}_k^T \mathbf{S}_k^{-1}. \quad (4.35)$$

With the equations presented earlier, the updated (a posteriori) state estimate can be written as

$$\hat{\mathbf{x}}_{k|k} = \hat{\mathbf{x}}_{k|k-1} + \mathbf{K}_k \tilde{\mathbf{y}}_k. \quad (4.36)$$

Updated estimate covariance is

$$\mathbf{P}_{k|k} = (\mathbf{I} - \mathbf{K}_k \mathbf{H}_k) \hat{\mathbf{P}}_{k|k-1}, \quad (4.37)$$

where \mathbf{I} represents the identity matrix. The resulting posterior PDF have the Gaussian distribution. [69, pp. 104–118], [87, pp. 324–329]

We can consider a simple positioning tracking example with KF, and how the associated matrices may look. If we consider the 2D case in position tracking applications, the state vector of KF for the device with unknown position can be presented as

$$\mathbf{x}_k = [x_k, y_k, v_{x,k}, v_{y,k}]^T, \quad (4.38)$$

where x_k is x-coordinate, y_k is y-coordinate, $v_{x,k}$ is velocity in the direction of x-axis, and $v_{y,k}$ is velocity in the direction of y-axis. The expansion for the 3D case is simple, and it is only necessary to add the variables for the third dimension, for example z_k and $v_{z,k}$. Otherwise, the principle is the same. [69, pp. 104–118]

A simple mobility model that can be considered here, is based on the principle of random walk. The state matrix is then presented as

$$\mathbf{F} = \begin{bmatrix} 1 & 0 & \Delta t & 0 \\ 0 & 1 & 0 & \Delta t \\ 0 & 0 & 1 & 0 \\ 0 & 0 & 0 & 1 \end{bmatrix}, \quad (4.39)$$

where Δt is the sampling time. [69, pp. 104–118]

The covariance matrix of the process noise is

$$\mathbf{Q} = \begin{bmatrix} \sigma_{Q,x}^2 & 0 & 0 & 0 \\ 0 & \sigma_{Q,y}^2 & 0 & 0 \\ 0 & 0 & \sigma_{Q,v_x}^2 & 0 \\ 0 & 0 & 0 & \sigma_{Q,v_y}^2 \end{bmatrix} \quad (4.40)$$

which is a diagonal matrix including the variance of the mobility in the x - and y - directions

for the location and velocity. In this model it is implied that the change of the located device is controlled by process noise of a certain variance. This model is really theoretical and simplified and to get more realistic results, the more realistic mobility models should be used. [69, pp. 104–118]

Considering a simple measurement model, it is assumed that a position estimate is available in each time-step. The measurement is performed from the position estimates x and y and no velocity estimates are available. Therefore, the velocity is treated as a hidden state. The measurements also have a linear dependence on the state vector, which is represented by the measurement matrix [69, pp. 104–118]

$$\mathbf{H} = \begin{bmatrix} 1 & 0 & 0 & 0 \\ 0 & 1 & 0 & 0 \end{bmatrix}.$$

5. METHODOLOGY

In this chapter we will present the research methodology. First, we consider how the CRLB estimation can be used with DECT-2020 NR context and numerologies. Then, we provide an overview of the process for selecting optimal anchors to obtain an accurate positioning solution with power consumption optimization.

5.1 Cramér-Rao Lower Bound with DECT-2020 NR Numerologies

We will use the DECT-2020 NR numerologies to calculate CRLB values. The theory of CRLB is presented in Chapter 4. The CRLB results with DECT-2020 NR numerologies will give us an understanding of the best possible accuracy levels to be achieved with different positioning methods. The CRLBs are considered for the ToA and AoA positioning methods and the results are presented in Chapter 6.

As we noted in Chapter 4, the CRLB in ToA is proportional to the transmission bandwidth. Therefore, we need the information about the supported transmission numerologies which are presented in ETSI TS 103 636 Part 3: Physical layer, Table 4.3-1 [66, pp. 9–10]. Table 5.1 presents the main numerologies used in the CRLB calculations.

In Table 5.1, μ is the subcarrier spacing factor, Δ_f^μ is the OFDM subcarrier spacing, β is the Fourier transform scaling factor, $B_{DFT}^{\mu,\beta}$ is the nominal bandwidth, N_{OCC}^β is the number of occupied subcarriers, and $B_{TX}^{\mu,\beta}$ is the transmission bandwidth consisting of the occupied subcarriers and the empty direct current (DC) carrier in the centre of the transmission bandwidth.

For both ToA and AoA CRLB calculations, we need to know the possible SNR values, which can be obtained from ETSI TS 103 636 Part 2: Radio reception and transmission requirements, Table 8.4.3-1. The SNR values of particular interest to consider and evaluate are approximately from -5 dB to 45 dB. [65, p. 23] In addition to the bandwidth information, we also need to know the subcarrier spacing and the number of the subcarriers for the CRLB for ToA. These can be found in Table 5.1. For CRLB for AoA, the number of antenna elements is also needs to be defined, and these can be found in ETSI TS 103 636 Part 3: Physical layer, Table 6.3.2-1. As it is defined in the mentioned technical specification, the possible number of spatial streams is 1, 2, 4 and 8, and it is less

Table 5.1. Supported transmission numerologies in DECT-2020 NR, adapted from [66, pp. 9–10].

	β	$B_{DFT}^{\mu,\beta}$ [kHz]	N_{OCC}^{β}	$B_{TX}^{\mu,\beta}$ [kHz]
$\mu = 1$ $\Delta_f^{\mu} = 27$ kHz	1	1 728	56	1 539
	2	3 456	112	3 051
	4	6 912	224	6 075
	8	13 824	448	12 123
	12	20 736	672	18 171
	16	27 648	896	24 219
$\mu = 2$ $\Delta_f^{\mu} = 54$ kHz	1	3 456	56	3 078
	2	6 912	112	6 102
	4	13 824	224	12 150
	8	27 648	448	24 246
	12	41 472	672	36 342
	16	55 296	896	48 438
$\mu = 4$ $\Delta_f^{\mu} = 108$ kHz	1	6 912	56	6 156
	2	13 824	112	12 204
	4	27 648	224	24 300
	8	55 296	448	48 492
	12	82 944	672	72 684
	16	110 592	896	96 876
$\mu = 8$ $\Delta_f^{\mu} = 216$ kHz	1	13 824	56	12 312
	2	27 648	112	24 408
	4	55 296	224	48 600
	8	110 592	448	96 984
	12	165 888	672	145 368
	16	221 184	896	193 752

than or equal to the number of antenna ports used for channel transmission. [66, p. 28]

5.2 Selecting the Best Anchors for Positioning

In this section, we use the concept of PEB introduced in Section 4.4.4. We present the different principles for selecting the best anchors for positioning. The comparison of the results with different selection methods is based on the simulated PEB values in the assumed DECT-2020 NR environment. The simulated results for anchor selection are presented in Section 6.3.

The position of the user device has some margin of error because the measurements are

never error-free. Therefore, the unknown position of the user device can be represented by a covariance matrix. The covariance matrix represents the error of a multidimensional Gaussian distributed data set as a representation of the variance in multiple dimensions. The error can be visualized as a covariance ellipse, or confidence ellipse, in the coordinate grid. For example, in (x, y) coordinates, the confidence ellipse is a 2D plot of the data set of measurements.

The idea of the confidence ellipse in 2D ToA positioning case is illustrated in Figure 5.1. The confidence ellipse represents the probability for the position of the user device, and the ellipse is formed based on the measurements of the signals between the user device and the anchors using the chosen positioning method. For example, ToA, TDoA, AoA or RSS based methods can be used individually or together. The position approximation can be defined based on the different calculation methods. PEB represents the confidence

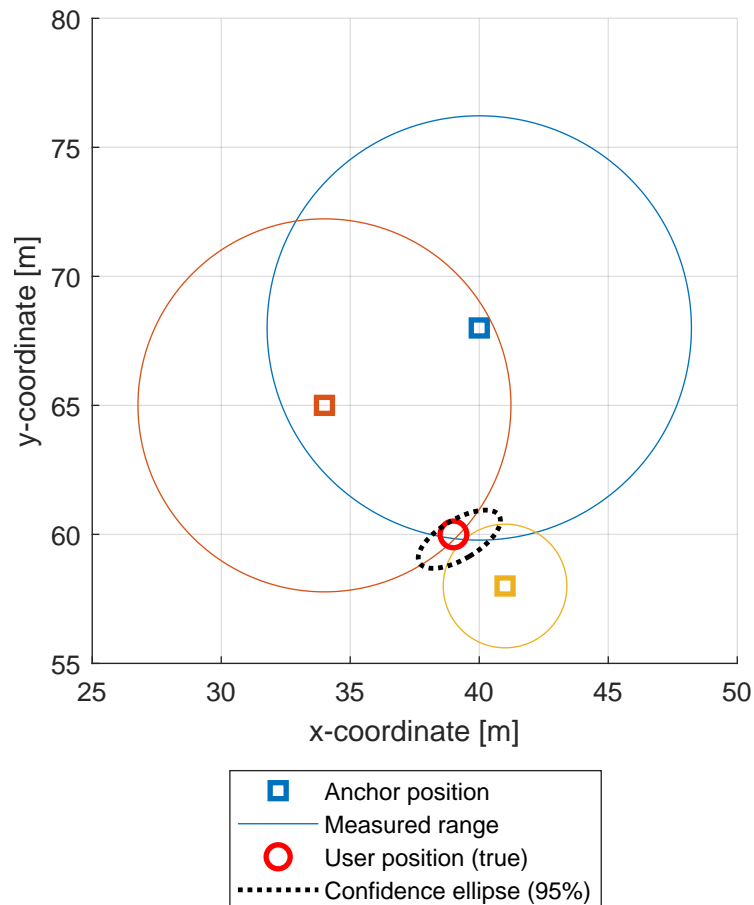


Figure 5.1. Example of a confidence ellipse for positioning using ToA measurements with errors.

ellipse as a more illustrative numerical value. PEB describes the smallest achievable positioning error. As we can see from Equation 4.26, PEB is calculated based on CRLB, and CRLB is the inverse of FIM. PEB could be calculated using a different value than CRLB, but we are often interested in the best possible positioning accuracy, and CRLB defines the lower limit of accuracy.

FIM describes how much information the measurement provides. Since we assume that two random values are independent, that means in this case we have two different measurements from two different anchors, the chain rule can be used. This means that FIM can be calculated individually for the all measurements between the located device and the anchors, or FIM can also be calculated for a scenario with three chosen anchors. The sum of FIMs from three individual anchors is the same as the separately calculated total FIM for the case with the same three chosen anchors. Therefore, the analysis of the different combinations of anchors can be done by calculating the individual FIMs and comparing the different combinations.

In theory, it is always best to use all possible measurements and available information to optimize the positioning performance. However, certain measurements from the certain anchors are more important and provide more information than others. Therefore, if it is possible to determine how to detect and use the most useful anchors for positioning, we can optimize the positioning performance also for the other perspective than just accuracy. In some cases, we may also have a goal for the positioning accuracy, and the goal could be achieved by optimizing the number of measurements, thus saving energy.

Figure 5.2 shows 4 example selections of 3 anchors for positioning. The black squares represents the anchor positions, the blue squares represents the selected anchors for positioning and the user device is represented by the red circle. There are 5 anchors that could be used for positioning in an area of 100 m x 100 m. The AoA positioning method is used in this example, but the same principle works also for ToA positioning, for example. The SNR values for each anchor are shown next to the anchors. The PEB values for each selection are shown in the upper left corner. However, the exact PEB values are not so important here, as they depend on the parameters used, but the differences in PEB between the selections are more interesting. As we can see from Figure 5.2, the geometry has a significant effect on the positioning accuracy. If choose the anchors based on the SNR values, as it is done in the left upper corner in Figure 5.2, the positioning accuracy can be significantly worse than other selections if the geometry is bad.

The selection of the all 5 anchors in the example case is presented in Figure 5.3. In theory, increasing the number of positioning measurements should improve accuracy. We can see from Figure 5.3 that the PEB is smaller and therefore better than all the selections of 3 anchors in Figure 5.2. However, compared to the 2 best selections in Figure 5.2, the difference in PEB value is small. Therefore, we can notice that the good positioning accuracy can be gained with a low number of used anchors if the selection is good.

The appropriate selection of measurements is beneficial for multiple reasons. For example, it is possible to reduce signaling overhead, reduce latency, reduce computational load and improve power efficiency. Our goal is to find a way to select the best measurements from anchors to optimize the positioning performance in terms of acceptable accuracy,

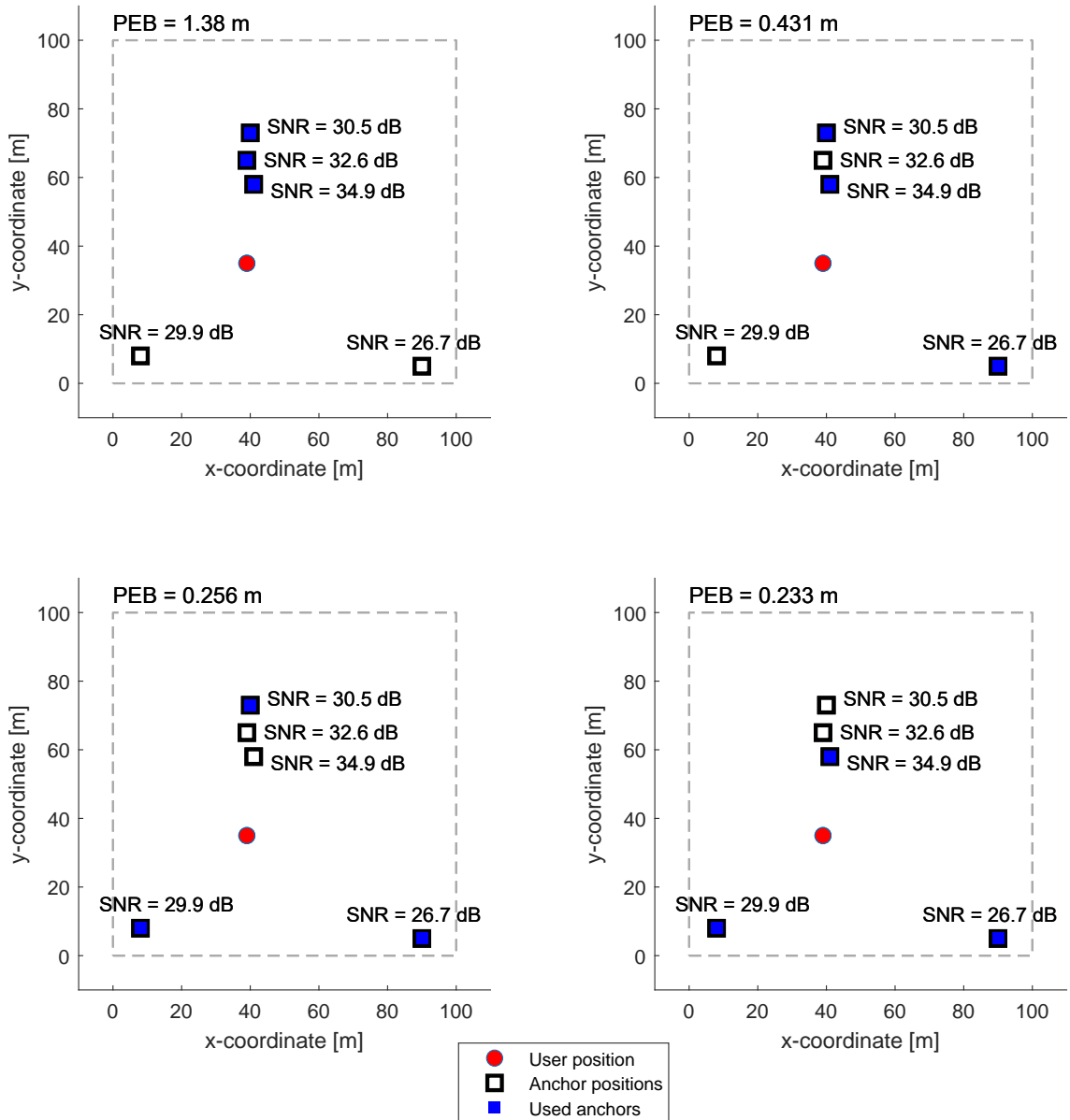


Figure 5.2. Choosing the best anchors in the AoA positioning. Examples of different anchor selections.

but also taking into account the other factors, such as efficiency aspects. We assume that it is possible to select the best anchors for positioning with an algorithm and that the positioning result could meet the best possible accuracy much better than just randomly selecting the anchor measurements.

We investigate the research question 3 using the MATLAB algorithm. We can specify the the size of the observation area in the MATLAB code by defining the edge length of the square grid in meters. With the grid size and the anchor density, we can calculate the total number of anchors within the observation area. Here, we mark the chosen anchors as $N_{a,chosen}$ and all possible anchors as $N_{a,total}$. We will compare the different numbers of chosen anchors for the all possible cases, which could be represented as

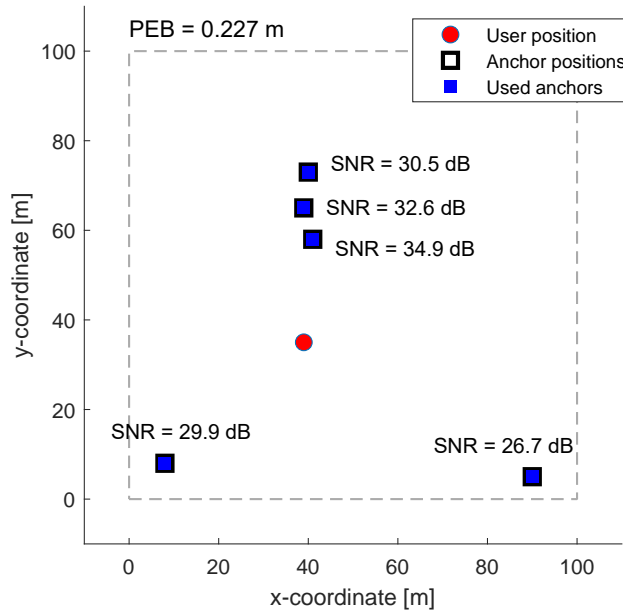


Figure 5.3. Choosing the best anchors in the AoA. All 5 possible anchors selected.

$N_{a,\text{chosen}} \in \{2, \dots, N_{a,\text{total}}\}$, where $N_{a,\text{total}}$ is the total number of anchors in the observation area, and $N_{a,\text{chosen}}$ is the number of chosen anchors used for positioning. The algorithm is built to perform anchor selection in three different ways:

- *SNR-method*: The anchor selection is based on the SNR values. The chosen anchors are the $N_{a,\text{chosen}}$ anchors with the highest SNR values.
- *Norm-method*: The selection is based on the norm of FIM values. The chosen anchors are the $N_{a,\text{chosen}}$ anchors with the highest norm values of FIM.
- *Prior Information -method*: We will make some assumptions or have a priori knowledge about the position of the device as a prior information. Then, we select the anchors based on the prior information and use the anchors that give the most additional information to the knowledge we already have. *PriorInfo-method* is the used abbreviation in the figures for this selection method.

To compare these three different methods, we will also get the reference results for the following methods:

- *All combinations -method*: The selection of the anchors is based on the calculation of all possible combinations and then the combination with the best positioning accuracy is selected. This method should give the ideal positioning accuracy for the used parameters. However, this method has a high computational load, but it is good for obtaining the reference values. *AllCombs-method* is the abbreviation used in the figures.
- *Random-method*: The selection of the $N_{a,\text{chosen}}$ anchors is completely random.

The selection is done by running the algorithm for many rounds (from 1 000 to 100 000)

and each round has a new random scenario, where the locations of the user device and the anchors are random. The direction of the antennas of anchors is also random in each round. The PEB is calculated with all different selection methods mentioned above, and the values are stored. The results of the PEB values are shown in the figures where the x-axis represents the number of chosen anchors $N_{a,\text{chosen}} \in \{2, \dots, N_{a,\text{total}}\}$ and the y-axis represents the average PEB values of all rounds run for all different choosing methods. This way we can see how the PEB changes between the different choosing methods.

After the simulation has run many rounds, the average values for the different choosing methods are calculated. In individual cases, the different methods may give varying results, but as the number of different random cases increases, they tend to follow a Gaussian distribution, and the means of the large number of simulations are more representative of the universal case.

In this work we study the difference of choosing the best measurements in such a way that we know the location of the user device. In this way, we do not have any uncertainty about the position of the user device, and we can obtain results for comparing the anchor selection methods thinking of positioning optimization. The purpose of this study is not to implement the actual positioning algorithm, and that would be a subject of further research. However, when using tracking algorithms such as the Kalman filter, there is always prior information available about the position of the user device with a certain degree of accuracy.

There are different variables that we can study. For example, we can consider different node densities. The density of anchors can be defined as

$$D_a = \frac{N_a}{A}, \quad (5.1)$$

where N_a is the number of anchors in the area and A is the area size. In this work, we have considered the areas of square shape, and therefore, the area can be defined as $A = s^2$, where s is the side length. Other shapes of area would also be possible, for example circular. The total number of the anchors can be calculated based on the anchor density, but alternatively, the area and number of anchors can be specified in the code. Other variables that can be set in the code, are transmit power at different gains, and noise figure at the receiver.

In order to use the prior information method to select the best anchors, we need to define how accurate our knowledge of the user position is. The prior information is defined as the standard deviation of PEB. The algorithm will work with quite low accuracies of prior information. For example, in many cases an accuracy of 1 000 m is sufficient to select the best anchors using this method.

6. RESULTS AND ANALYSIS

Based on the literature review of positioning methods in Chapter 4, ToA and AoA are two potential positioning methods considered to use in DECT-2020 NR networks. In this chapter we will present simulated results for CRLB for ToA and AoA positioning. We will also present the results for selecting the best anchors for positioning based on PEB. We will study the achievable PEB values in the optimal theoretical cases with different anchor selection methods. The theoretical background for the positioning results is presented in Chapter 4. The methodology used to obtain the results is presented in Chapter 5.

6.1 Cramér-Rao Lower Bounds for Time of Arrival

Theoretical CRLB values for ToA distance estimation using DECT-2020 NR subcarrier spacing of 108 kHz are shown in Figure 6.1. The possible DECT-2020 NR bandwidths with the subcarrier spacing 108 kHz are shown in Figure 6.1 as an example case. Other possible DECT-2020 NR subcarrier spacings are 27 kHz, 54 kHz and 216 kHz, as shown in Table 5.1. The logarithmic y-axis represents the standard deviation of the CRLB in meters. The x-axis represents the SNR values in decibels. As we can see in Figure 6.1, the bandwidth has a direct effect on the positioning accuracy. The larger the bandwidth is, the smaller the CRLB is, that means the smaller the possible positioning error. From Figure 6.1 we can also see that a larger SNR value results in a smaller CRLB. For example, we can see from Figure 6.1 that at SNR = 10 dB the CRLB standard deviation is 0.8 m at bandwidth $B = 6.156$ MHz and 0.04 m at bandwidth $B = 48.492$ MHz. However, the case with LoS and without errors is assumed. In reality, the results are much worse and especially in the IoT systems there are so many sources of error that ToA positioning results with low standard deviation cannot be achieved. Nevertheless, the results in Figure 6.1 show us the best possible theoretical CRLB with these numerologies.

CRLB values for ToA positioning with all the different DECT-2020 NR subcarrier spacings are shown in Figure 6.2. There are four different possible DECT-2020 NR subcarrier spacings 27 kHz, 54 kHz, 108 kHz and 216 kHz, as we can see in Table 5.1 presented earlier. There are six different possible transmission bandwidths for each subcarrier. The six possible transmission bandwidths for a subcarrier spacing of 108 kHz are shown in Figure 6.1. Figure 6.2 shows the minimum and maximum bandwidths of each subcarrier

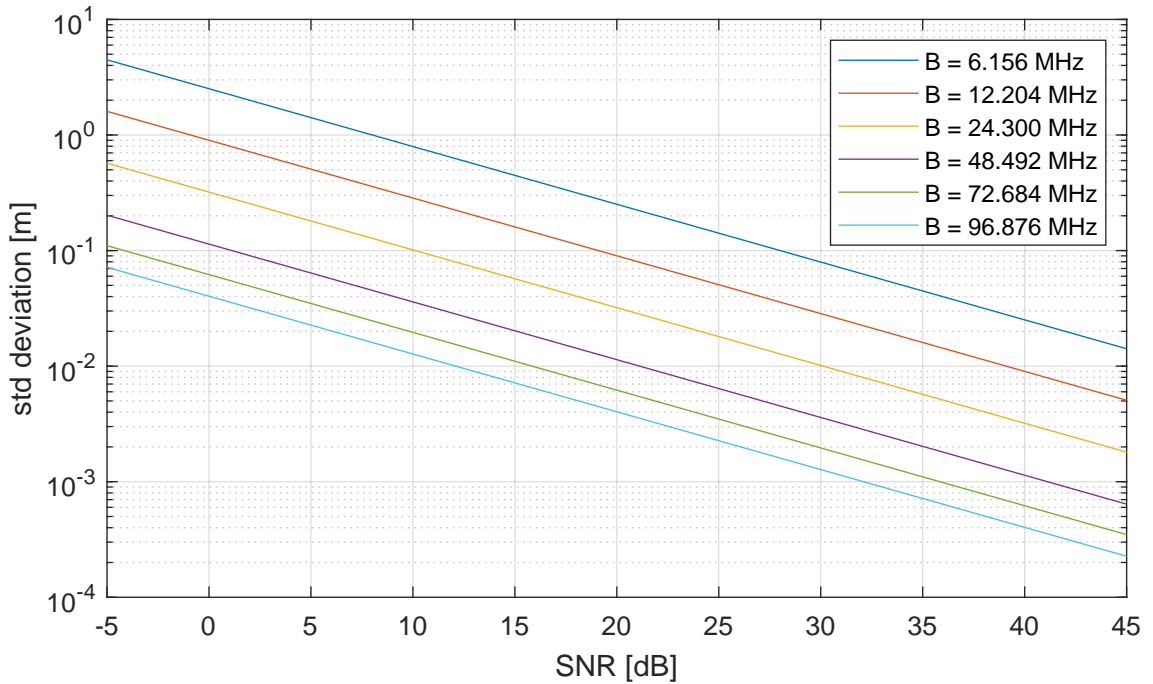


Figure 6.1. CRLBs for ToA based range estimation with DECT-2020 NR subcarrier spacing of 108 kHz.

to illustrate the differences between the cases with different subcarriers. The different subcarrier spacings are shown in different colours. The solid line illustrates the minimum transmission bandwidth and the dashed line shows the maximum transmission bandwidth for each subcarrier. The blue lines in Figure 6.2 are the same as the highest and lowest lines in Figure 6.1.

As we can see from Figure 6.2, larger subcarrier spacings allow higher bandwidths and this leads to smaller CRLB standard deviations and therefore smaller possible positioning errors. However, we can also notice that the subcarrier spacing itself does not have affect the CRLB, but the bandwidth does.

We can see from Figure 6.2 that the CRLB standard deviation value of about 1 meter is achieved with all possible DECT-2020 NR bandwidths if the SNR is higher than 20 dB. For the worse SNR values, the CRLB standard deviation increases and the positioning accuracy decreases even in the theoretical case. According to Figure 6.2, the bandwidth should be around $B = 12$ MHz to obtain accurate results even with lower SNR values.

According to the results here, we can analyze that the good channel conditions with fair SNR allow accurate positioning. As we can see from the results, another important factor in ToA positioning is bandwidth. Higher bandwidths can provide better positioning accuracy for ToA positioning.

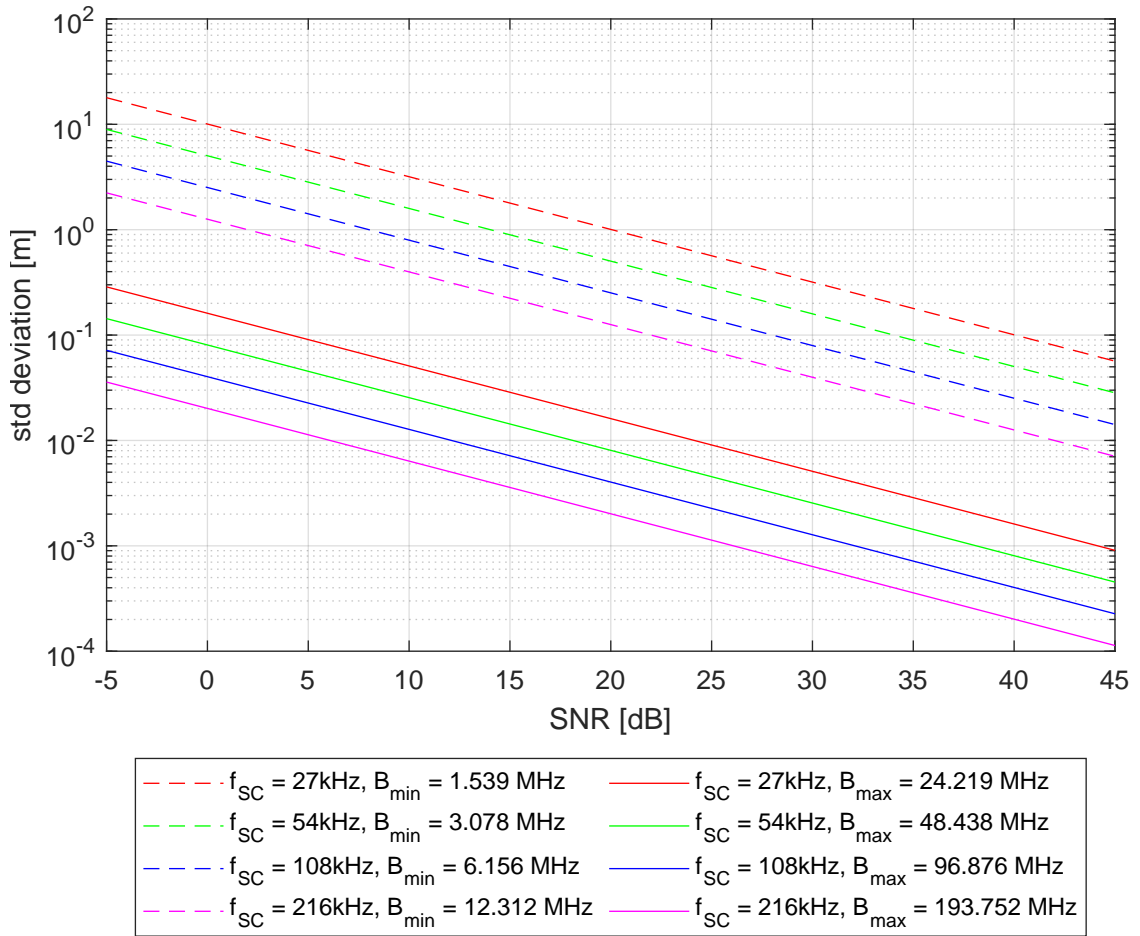


Figure 6.2. Comparison of CRLBs for ToA based range estimation with DECT-2020 NR numerologies.

6.2 Cramér-Rao Lower Bounds for Angle of Arrival

CRLB values for AoA estimation with different number of antenna elements are shown in Figure 6.3. The parameters used for the antenna spacing is $d = \frac{\pi}{2}$ and the antenna direction angle is $\alpha = 60^\circ$. The x-axis represents the observed SNR values and the logarithmic y-axis represents the CRLB standard deviation in degrees.

All three possible numbers of antenna elements 2, 4 and 8 for DECT-2020 NR are presented in Figure 6.3. As we can see in Figure 6.3, the number of antenna elements affects to the CRLB for AoA. The larger the number of antenna elements, the smaller the CRLB standard deviation and the better positioning accuracy. For example, in Figure 6.3 we can see that with SNR = 10 dB the CRLB standard deviation is 1.27 degrees with 8 antenna elements and CRLB standard deviation is 11.6 degrees with 2 antenna elements. The difference is noticeable and with smaller SNR values the difference becomes more pronounced. For a SNR of 35 dB, the corresponding CRLB standard deviation values are 0.66 degrees for 2 antenna elements and 0.070 degrees for 8 antenna elements.

The second studied variable in terms of its effect on CRLB for AoA estimation is the

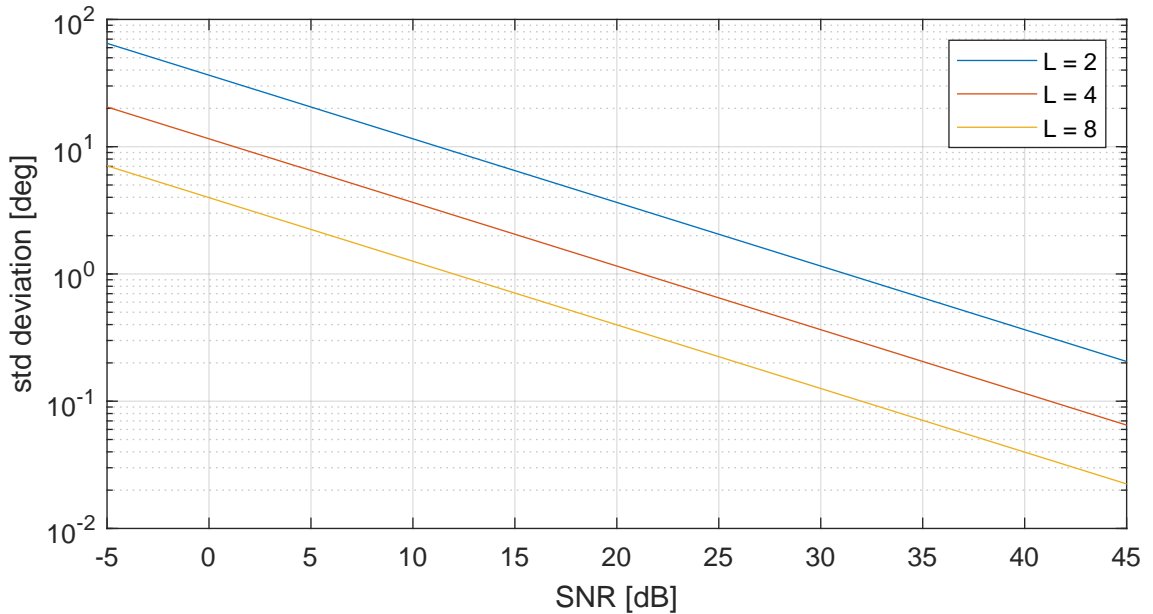


Figure 6.3. CRLBs for AoA based angle estimation with different numbers of antenna elements. Parameters used: antenna spacing $d = \frac{\lambda}{2}$ and antenna direction angle $\alpha = 60^\circ$.

antenna spacing. The antenna spacing values are represented in terms of wavelength. The three different antenna spacing values of $\frac{\lambda}{4}$, $\frac{\lambda}{2}$ and λ are shown in Figure 6.4. The parameters used are the number of antenna elements $L = 4$ and the antenna direction angle $\alpha = 60^\circ$. We observe the same SNR values from -5 dB to 45 dB as in other figures and the SNR values are again plotted on the x-axis. The logarithmic y-axis presents the CRLB standard deviation for the AoA. Here we can see that a larger antenna spacing results in a smaller CRLB standard deviation for the antenna spacing values considered.

The CRLB for AoA estimation with different planar wavefront angles are presented in Figure 6.5. The other changeable parameters used in Figure 6.5 are the number of antenna elements $L = 4$ and the antenna spacing $d = \frac{\lambda}{2}$. As in the case of ToA case, we have observed the results with different SNR values between -5 dB and 45 dB. In Figure 6.5, the logarithmic y-axis represents the standard deviation in degrees.

The antenna direction angle can get values from -180° to 180° or alternatively from 0° to 360° . However, the angle of arrival of the planar wavefront is the determining factor, and therefore, the possible angles of arrival are from 0° to $\pm 90^\circ$. The resulting CRLBs for AoA follows the behaviour of the cosine, which can also be seen from Equation 4.24. Therefore, if we want to think of the antenna directions, the 90° multiples of the antenna directions give the same positioning result. For example, antenna directions of 30° and 120° form similar planar wavefronts, and therefore, the resulting CRLB is the same.

We have chosen to present four different figures with antenna direction angles α between values 0° and 85° . As we can see from Figure 6.5, the smaller the antenna direction

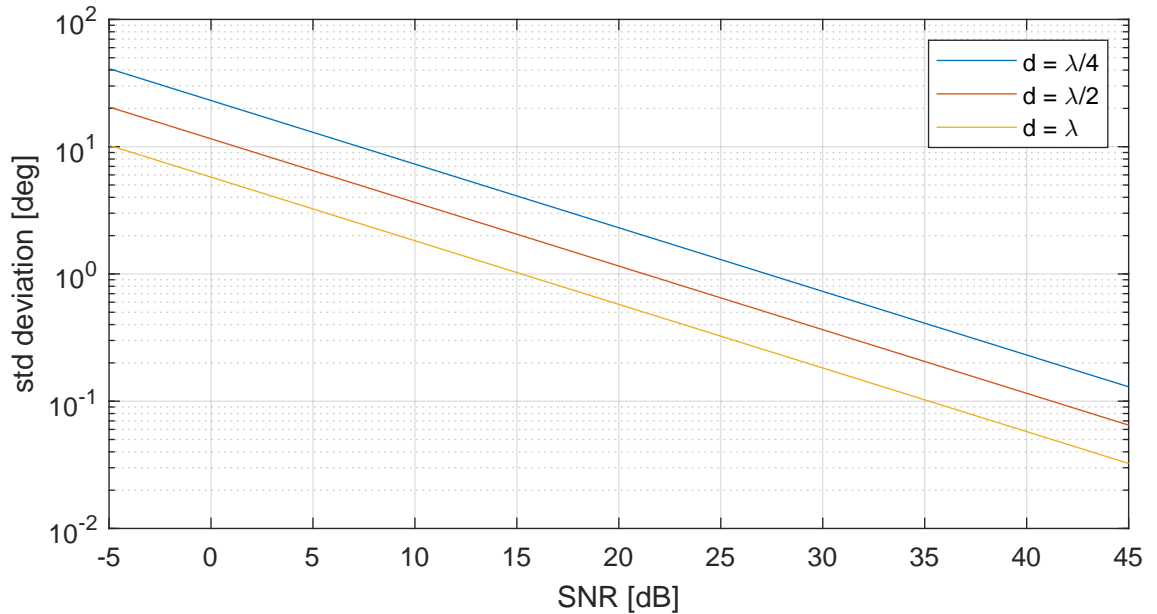


Figure 6.4. CRLBs for AoA based angle estimation with different antenna spacing values. Parameters used: number of antenna elements $L = 4$ and antenna direction angle $\alpha = 60^\circ$

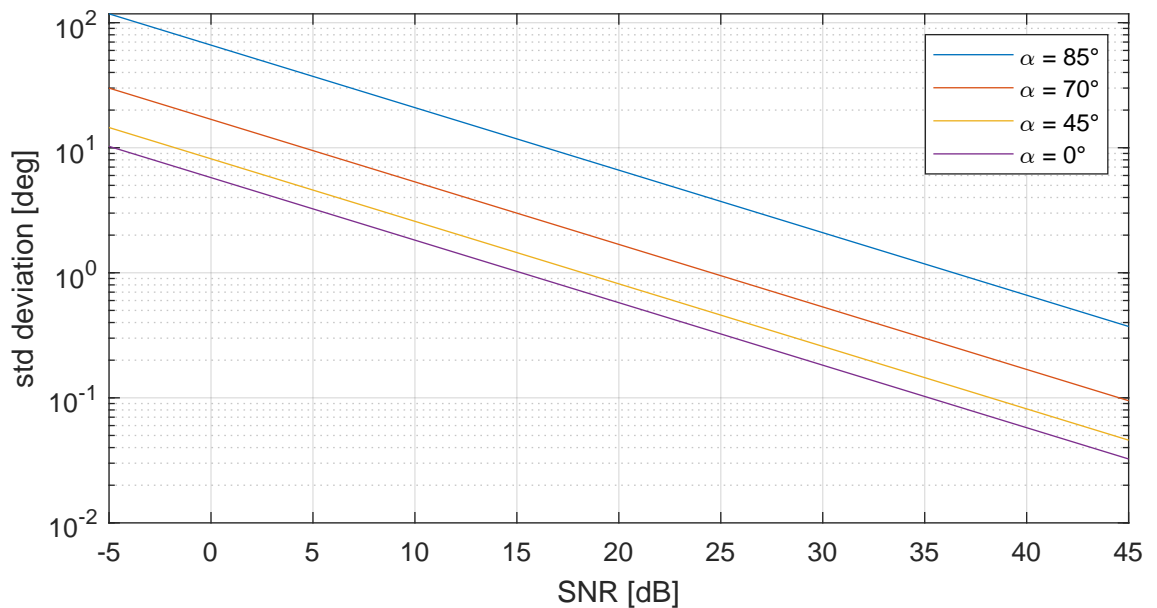


Figure 6.5. CRLBs for AoA based angle estimation with different antenna direction angles. Parameters used: number of antenna elements $L = 4$ and antenna spacing $d = \frac{\lambda}{2}$.

angle, the smaller the CRLB standard deviation. We can also see from Figure 6.5 that a change in the smaller angles α has less effect on the CRLB than a similar angle change near the angle $\alpha = 90^\circ$. For example, the difference of 45 degrees between the angles $\alpha = 0^\circ$ and $\alpha = 45^\circ$ is much smaller than the difference of 15 degrees between the angles $\alpha = 70^\circ$ and $\alpha = 85^\circ$.

As we have seen from the previous figures, there are four variables in AoA positioning

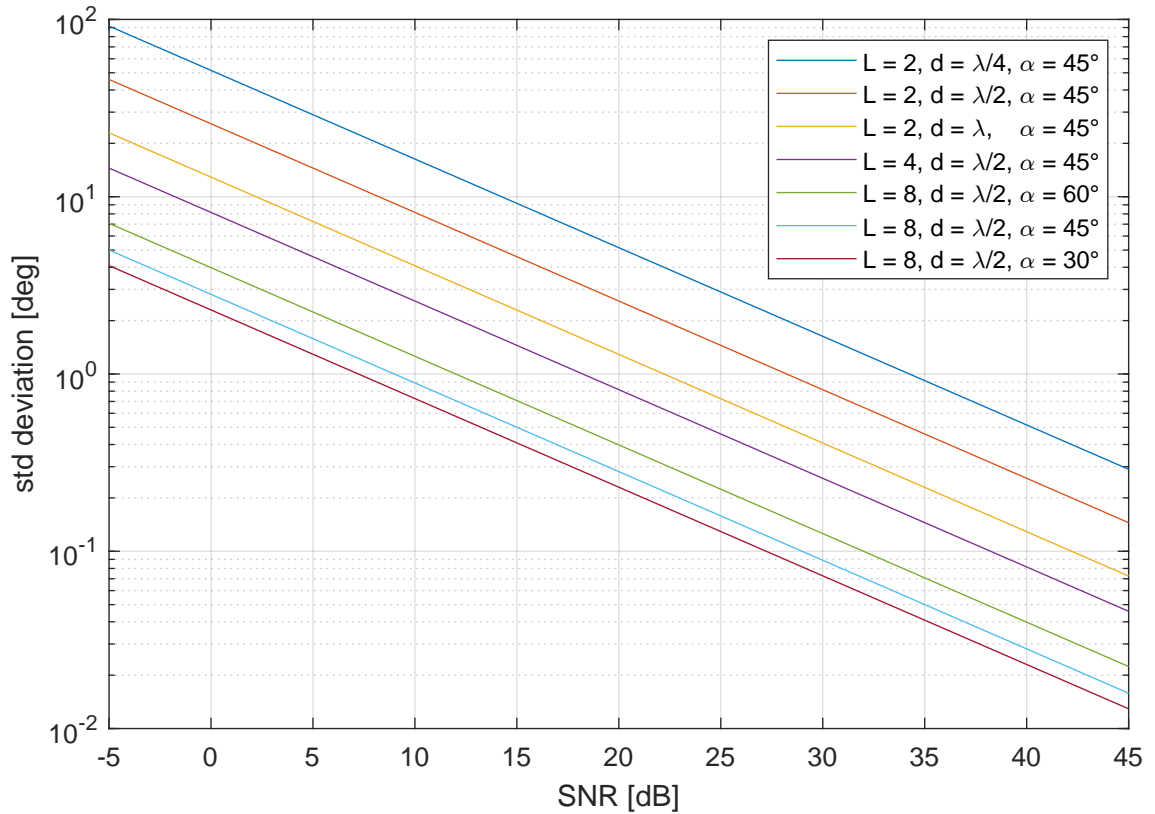


Figure 6.6. CRLBs for AoA based angle estimation with different parameter combinations.

that affect the CRLB values. The number of antenna elements L , the antenna element spacing d , the received angle of a planar wavefront α , and the SNR. One set of CRLBs is presented in Figure 6.6, where the different scenarios are presented with different SNR values between -5 dB and 45 dB. The observed values shown on the logarithmic y-axis are the CRLB standard deviations in degrees.

Figure 6.6 shows the combination of different parameter values. As we can see from Figure 6.6 and the earlier AoA related figures, the greater number of antenna elements results better the potential accuracy. Larger antenna spacing seems to result better potential accuracy. Smaller reception angles give better potential accuracy.

We can also see from Figure 6.6 that by changing the different parameters in different ways, we can achieve relatively similar results with these different combinations. Thus, we can see that it is the overall effect of the parameters that matters. For example, if we reduce the number of antenna elements and want to have similar positioning accuracies, we need to reduce the antenna direction angle α or increase the antenna spacing d .

6.3 Position Error Bound and Selecting the Best Anchors for Positioning

In this section, we will present and analyze the results of selecting the best anchors for positioning using different anchor selection methods. The selection methods used and the principles for the methods are presented in Section 5.2.

We consider the DECT-2020 NR environment in our simulations. Therefore, we have used the values for various parameters based on Table 5.1, and the chosen parameters are presented in Table 6.1, unless otherwise specified later. In each set of results, 1 000 simulation rounds have been used to obtain better generally applicable results. The parameter *Prior information accuracy* in Table 6.1 means how accurate information we have about the user position at the beginning of using the *prior information -method*. In other words, we have defined that we have knowledge with an accuracy of 1 000 m for the potential location of the user device.

Table 6.1. Values used in anchor selection simulations.

Parameter	Value
Carrier frequency	1.9 GHz
Subcarrier spacing	54 kHz
Active bandwidth	24.246 MHz
Number of antennas in anchors	4
Antenna separation	$\lambda/2 = 78.9$ mm
Prior information accuracy	1 000 m

A comparison of methods for selecting the best anchors in AoA is shown in Figure 6.7. In this case, the considered area is a square of size 100 m x 100 m, and there are total of 7 anchors available to use. As we can see from Figure 6.7, the different anchor selection methods produce different position results based on PEB. The PEB values are averaged over 1 000 simulation rounds. The y-axis is logarithmic and represents the PEB values obtained. The x-axis represents the number of anchors selected for positioning. Although the PEB values give us information about the best positioning accuracies achievable with these example values, the actual PEB values are not so important, because there are many parameters that affect the values. However, we are interested in the relative differences, as the differences seem to remain relatively similar regardless of the values chosen. In Figure 6.7, the ideal selection with *all combinations -method*, represented by the cyan line, shows us the average of 1 000 simulation rounds from the minimum PEBs of each simulation round with different number of used anchors and the scenario used. Furthermore, the darker blue line (*AllCombs-method (mean)*) in the figure shows us the average of 1 000 simulation rounds with the average PEB value of each round with this

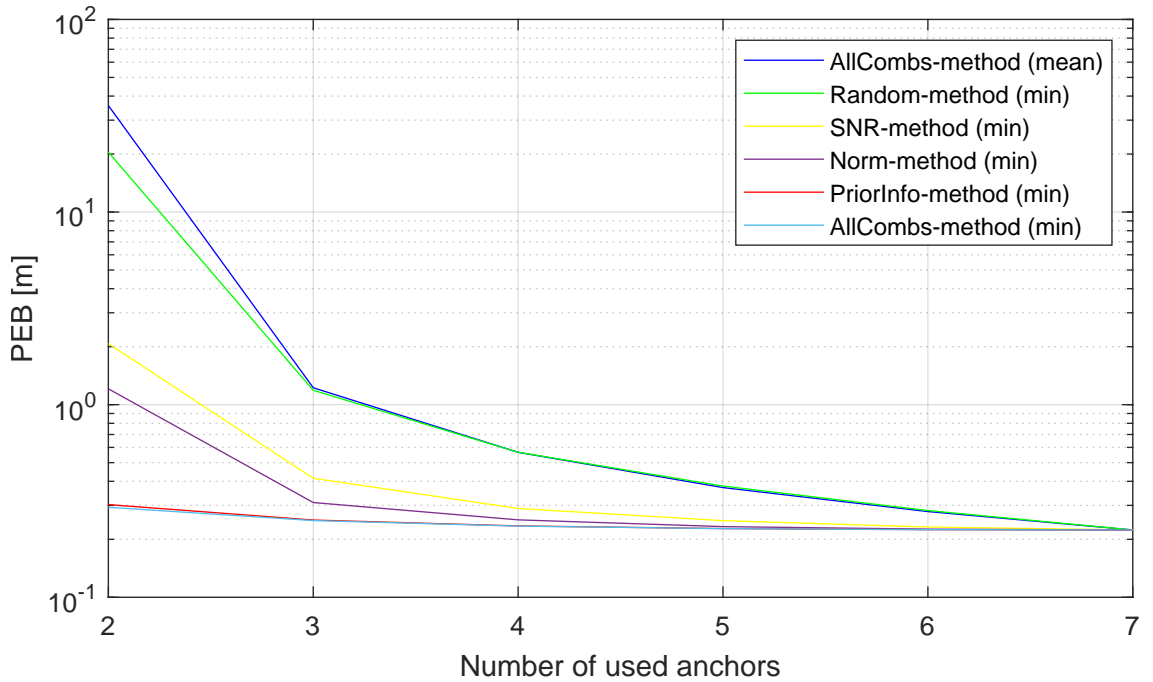


Figure 6.7. Comparison of methods for selecting the best anchors in the AoA positioning. Mean of PEB values from 1 000 simulation rounds. The grid edge length of the observation area is 100 m.

ideal selection method. Therefore, the darker blue line represents the average positioning error from all possible variations, while the other lines represent the best achievable positioning error in an overall picture with the different selection methods. We can see in Figure 6.7 that there are significant differences between the different selection methods when we will select only 2 or 3 anchors for positioning in the 100 m x 100 m area used. Therefore, it can be really important to do selection well and not just randomly select some anchors for positioning.

The 95th percentile of the same measurement data as in Figure 6.7 is shown in Figure 6.8. In other words, the results in Figure 6.8 does not take into account the best 5% of the results from 1 000 simulation rounds of each method. Figure 6.8 shows us better that with the 3 or 4 anchors used, PEB increases a little more with *SNR-method* and *norm-method* than with *prior information -method* if we compare the results in Figure 6.7. Therefore, we can see that there is less variation between the results with the *prior information -method* than with the other two selection methods.

The standard deviations of PEB with the different selection methods from 1 000 simulation rounds are presented in Figure 6.9. Here we can see that the standard deviation of PEB is significantly higher for SNR and norm-based methods, especially when 2 or 3 anchors are used for positioning. Together with Figure 6.8 we can conclude that in this positioning environment with the AoA positioning method, the *prior information* based anchor selection method offers a smaller positioning error than methods based on SNR

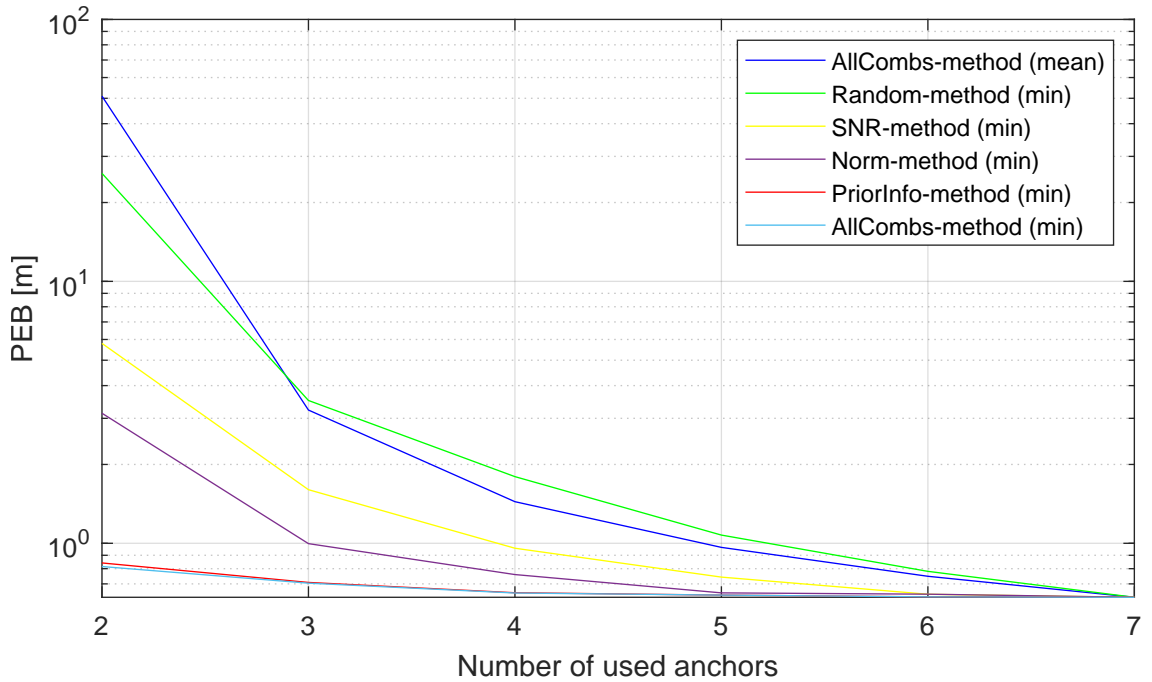


Figure 6.8. Comparison of methods for selecting the best anchors in the AoA positioning. 95th percentile of PEB values from 1 000 simulation rounds. The grid edge length of the observation area is 100 m.

and the distance between the user and anchor (norm), and it also offers better reliability than the methods to being compared because there is not such a large variation between the results. We can also see from Figure 6.7, Figure 6.8 and Figure 6.9, that the *prior information -method* gives really close the same values as the control line calculated from all combinations, and therefore, we can consider that the *prior information -method* can offer good positioning accuracies if we have sufficient prior information and there are no significant effects from any error sources in the positioning environment.

Anchor selection in ToA positioning works on the same principles as in AoA. The PEB results for ToA with the same numerologies as in the previous figures for AoA are shown in Figure 6.10. As we can see from the ToA results, the anchor selection lines look quite similar to those in AoA. The most significant difference in the lines is that the *SNR-method* and *norm-method* give the same results, and this has been seen in all the simulations run with MATLAB, not just the one presented in here. The reason for this is that the SNR depends directly on the distance between the user device and the anchor, because we have an assumption of the free-space path loss in our model. We can also see from Figure 6.10 that the PEB values are significantly better than in AoA with the optimal scenario without errors. However, the impact of errors in ToA based positioning is significant. For example, even very small clock errors can make a big difference in range estimation, because the speed of signal propagation is high, and the effects of clock errors are really difficult to avoid in the IoT environment, where the cost of the nodes should be kept low. Therefore, we will concentrate more on the AoA results because the results for AoA are

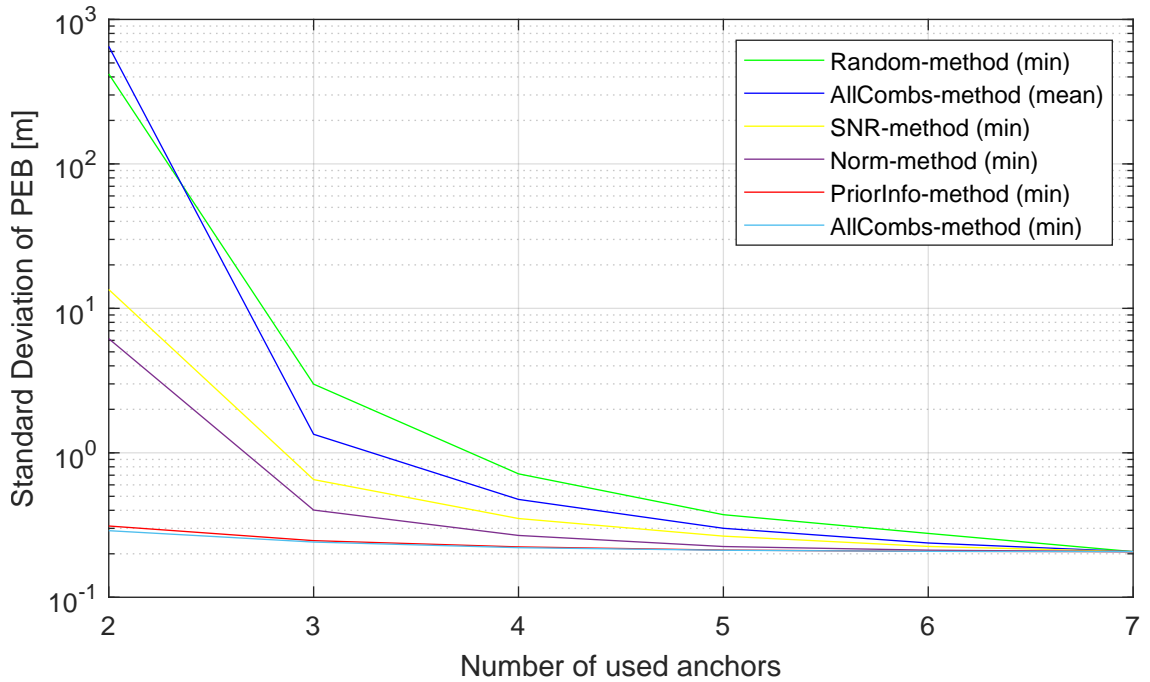


Figure 6.9. Comparison of methods for selecting the best anchors in the AoA positioning. Standard deviation of PEB values from 1 000 simulation rounds. The grid edge length of the observation area is 100 m.

more realistic to achieve and give a more concrete picture. However, the relative differences for the selection of anchors in ToA seem to be quite similar to those in AoA, so the results with AoA will give us some direction also with ToA.

We have considered a square positioning area with an edge length of 100 m. Next, we increase the edge length to 150 m and use approximately the same density of the anchors. In this case, we have 15 anchors available to use for positioning. The simulation results in AoA with this scenario are shown in Figure 6.11. We can see in Figure 6.11 that similar average PEB values are achieved with different methods if we can use higher number of anchors for positioning. For example, if we select 5 or more anchors for positioning, there are no significant differences between *prior information -method*, *norm-method* or *SNR-method*. We can also see that the random selection of anchors gives similar PEB values to the average of all simulations (mean of *all combinations -method*). Even though the *prior information -method* gives better results than the methods based on SNR and norm, all these three methods still perform significantly better than selecting the anchors randomly. If we compare the results in Figure 6.7 with Figure 6.11, where the difference is a larger area, we can see that the random selection becomes even worse the larger the area is. As before, the *prior information -method* works better than SNR- and norm-based methods when only 2 or 3 anchors are selected for positioning. As mentioned in Section 5.2, we are especially interested in having a small number of anchors selected for positioning, for example, to improve the power efficiency and reduce the computational load on the system.

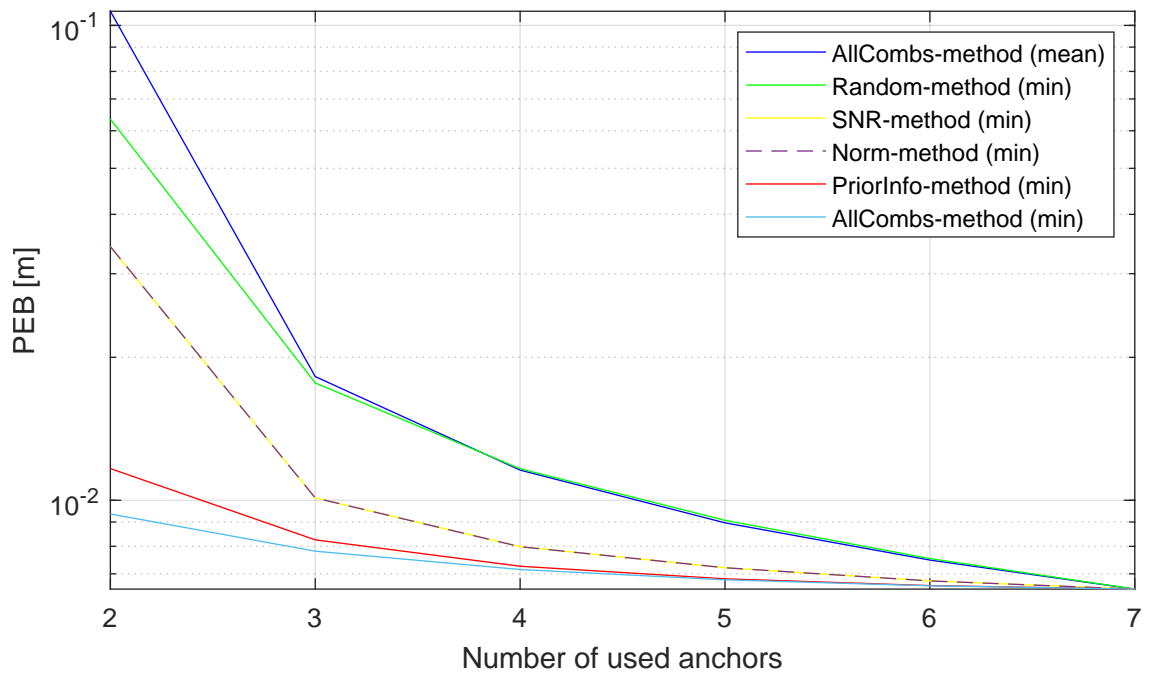


Figure 6.10. Comparison of methods for selecting the best anchors in the ToA positioning. Mean of PEB values from 1 000 simulation rounds. The grid edge length of the observation area is 100 m.

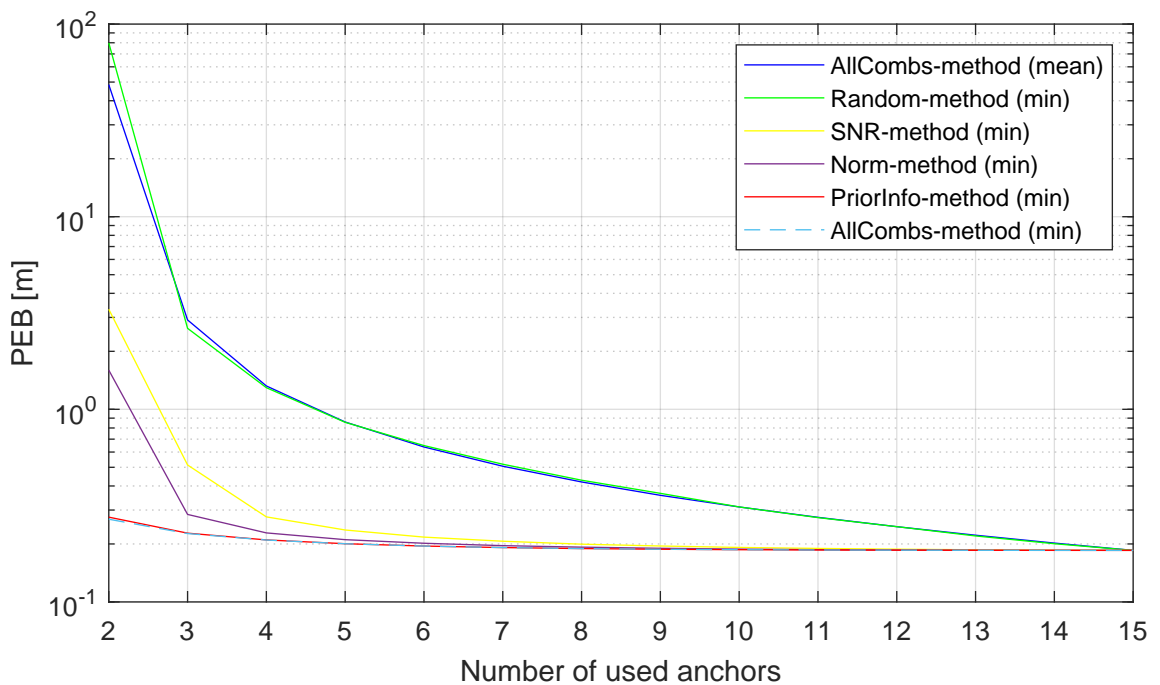


Figure 6.11. Comparison of methods for selecting the best anchors in the AoA positioning. Mean of PEB values from 1 000 simulation rounds. The grid edge length of the observation area is 150 m.

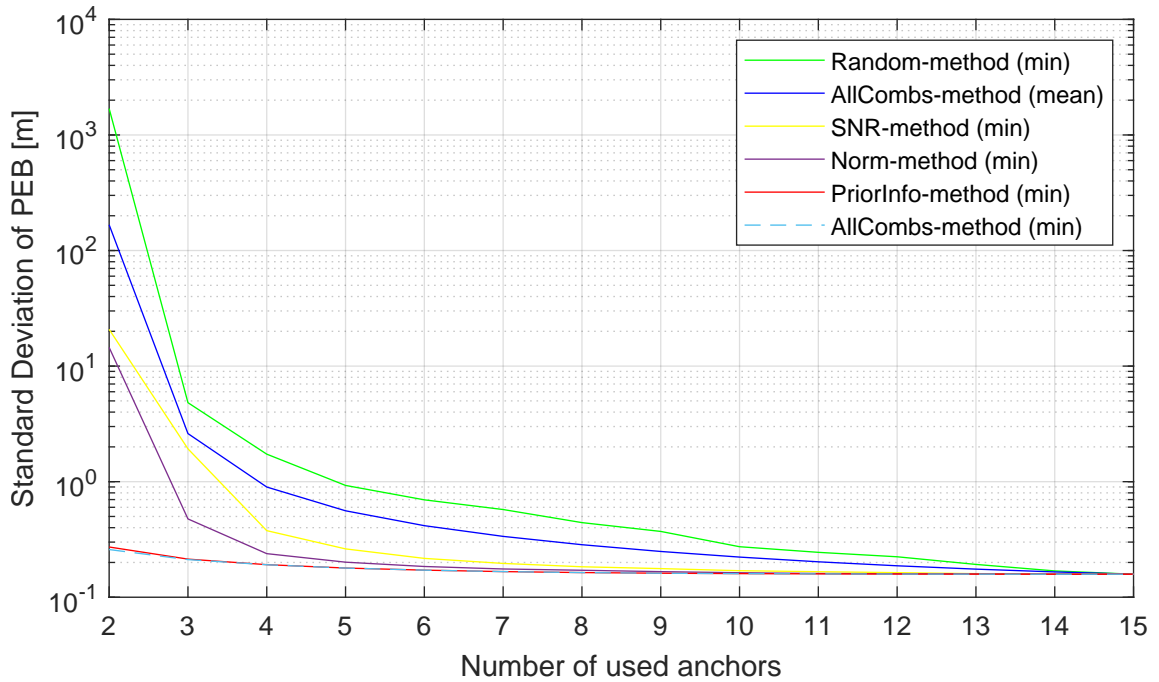


Figure 6.12. Comparison of methods for selecting the best anchors in the AoA positioning. Standard deviation of PEB values from 1 000 simulation rounds. The grid edge length of the observation area is 150 m.

If we look at the standard deviation of PEB in the AoA case with the area grid edge length of 150 m shown in Figure 6.12, we can see that the difference in the standard deviation with 2 or 3 anchors selected for positioning is significant between the *prior information -method* and the other methods to be compared. Here we can see that the standard deviation of PEB with the *prior information -method* is also close to the ideal selection. An interesting detail when comparing Figure 6.9 and Figure 6.12 is that the standard deviation of PEB with *prior information -method* is the same or even slightly better for the larger area (edge length of 150 m) than for the smaller area (edge length of 100 m), but the standard deviation of PEB with SNR- and norm-based methods has a significant increase. Therefore, based on these results in this environment, we could conclude that the *prior information -method* offers a low positioning error and good reliability with the low positioning errors.

So far, we have considered approximately the same density of anchors in the positioning area. Finally, we will consider a positioning case where we reduce the density of anchors. We choose to combine the previous cases and study the case of 7 possible anchors in the area and choose the grid edge length of the observation area to be 150 m. If we have 7 anchors and two cases with different area sizes with side lengths of 100 m and 150 m, based on Equation 5.1, the ratio between the densities is

$$D_1 \div D_2 = \frac{7}{(100 \text{ m})^2} \div \frac{7}{(150 \text{ m})^2} = 2.25.$$

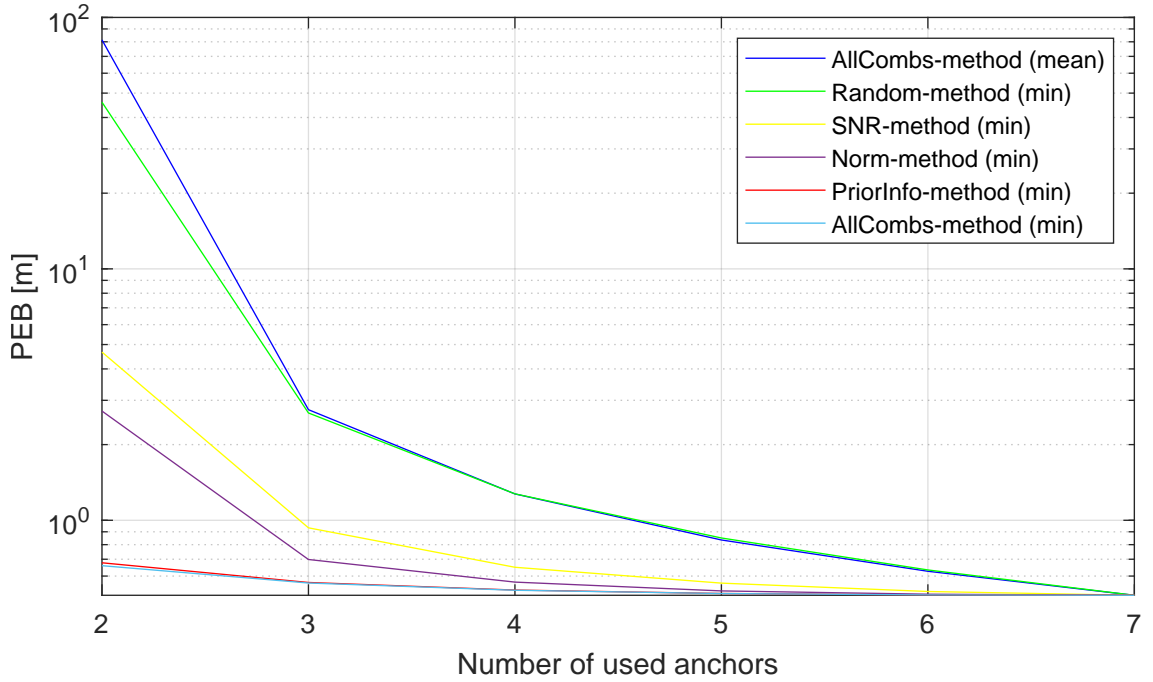


Figure 6.13. Comparison of methods for selecting the best anchors in the AoA positioning. Mean of PEB values from 1 000 simulation rounds. The grid edge length of the observation area is 150 m.

The scenario with 7 anchors in the area with side of 150 m is shown in Figure 6.13. If we compare the results in Figure 6.7 and Figure 6.13, we can see that the PEB increases when the density is lower (150 m side). From the figures we can see that the shapes of the lines are similar. For example, the values of PEB with 3 anchors used for *prior information -method* with 2 different side lengths are 0.25179 m (100 m side) and 0.56582 m (150 m side). If we compare the exact values, we get

$$\frac{PEB_2}{PEB_1} = \frac{0.56582 \text{ m}}{0.25179 \text{ m}} = 2.2471... \approx 2.25.$$

We can see that the density of the anchors has a directly proportional effect on the PEB results. Therefore, the more dense the anchor networks, the lower the PEB that can be achieved. However, the relative differences between the different anchor selection methods remain the same.

Based on all the results, we can say that the exact positioning results and PEB are difficult to present because there are many parameters that can affect to the exact values. However, the relative differences between the anchor selection methods can be presented. In theory, *prior information -method* works really well as an anchor selection method and has better PEB results than SNR and norm-based methods. However, the differences are mainly in the scenarios where the number of anchors used is 2–4. Despite the differences, the other two anchor selection methods could also be potential alternatives to achieve acceptable positioning results.

7. CONCLUSION

In this thesis, considering the research questions in Section 1.2, we have studied potential positioning methods in DECT-2020 NR technology, calculated limits for positioning accuracy with DECT-2020 NR numerologies, and compared different anchor selection methods for AoA and ToA positioning with MATLAB simulations. To gain a comprehensive understanding of the topic, we took also an overview of the IoT and DECT-2020 NR standard from a theoretical perspective. In addition, we studied the basics of positioning theory, such as the principles of different positioning methods, the theoretical basics for positioning bounds, and basic theory of Kalman filter from a position tracking perspective.

Based on the literature review, there are several potential positioning methods that can be used in DECT-2020 NR networks. The positioning methods that we considered in this thesis were ToA, TDoA, AoA, and RSS based methods. The basic principles of these positioning methods are presented in Section 4.3. This section answered for the research question 1. We focused on the ToA and AoA methods in the positioning accuracy and anchor selection simulations.

In the simulation part, we first simulated the best potential positioning accuracy for ToA positioning method based on CRLB with DECT-2020 NR numerologies. We compared the effects of different DECT-2020 NR bandwidths and subcarrier spacings for CRLB. We could see that the bandwidth has a direct effect on the CRLB in ToA positioning. The higher the bandwidth, the lower the CRLB that can be achieved and therefore the better the potential positioning accuracy. Additionally, higher subcarrier spacings allow higher bandwidths. The available bandwidth sets in DECT-2020 NR with different subcarriers partly overlap, which was shown in Figure 6.2.

Next, we produced CRLB results for AoA positioning. For AoA positioning, the considered variables considered were number of antenna elements, antenna spacing, and antenna direction angle. Bandwidth has no effect on CRLB results for AoA. For DECT-2020 NR devices, the possible numbers of multiple antenna elements are 2, 4 and 8. We can see that a lower CRLBs can be achieved with a higher number of antenna elements. Therefore, 8 antenna elements provide better positioning accuracy than 2 or 4 antenna elements. Furthermore, the effect of the antenna spacing was quite simple: the higher the antenna spacing, the lower the CRLB was possible to achieve. The number of antenna

elements was not changed when observing the effect of antenna spacing. The third variable considered was the antenna direction angle, which has an effect on the direction of the planar wavefront. The results showed that the smaller the angle of the wavefront, the smaller CRLB was achieved. However, in this case we could see that the effect of the same variation in the vicinity of the wavefront angle 0° was not as significant as vicinity of the angle 90° . Therefore, the positioning accuracy is significantly reduced as the wavefront angle approaches 90° . At the wavefront angle of 90° , the orientation of the antennas would be perpendicular to the user. If the wavefront angle is between 0° and 45° , there is not so much difference in the results. However, the best results are obtained when the wavefront angle is 0° which means that the antenna is pointing in the same direction as the signal between the user device and the anchor. Overall, we found that there are several factors that influence the CRLB results for AoA, and similar results can be obtained with different combinations of variables.

Based on the CRLB simulation results for ToA, presented in Section 6.1, and AoA, presented in Section 6.2, we obtained numerical positioning accuracy values for these two positioning methods with DECT-2020 NR numerologies. These results provided the answer to the research question 2. We could also see from the theoretical CRLB results that ToA and AoA are potential positioning methods in DECT-2020 NR to achieve good positioning accuracies with the assumptions made. In practice, a major challenge with the ToA method in a IoT environment, such as a DECT-2020 NR network, is the clock errors of the devices. Therefore, the theoretical results with ToA method are too good compared to the realistic situation. However, CRLB shows the best possible positioning accuracy that can be achieved with the signal characteristics used. In practice, the AoA method might be better than ToA.

Finally, we studied the methods for selecting anchors in order to find the best method for the lowest PEB and thus, the best positioning accuracy. The positioning methods studied were AoA and ToA. We considered 3 anchor selection methods which were based on different parameters: SNR, Euclidean distance (norm) and prior information. We also had 2 anchor selection methods as a reference: random selection and ideal selection. We simulated the results with MATLAB and ran 1 000 simulation rounds to obtain generally applicable results. The new scenario was created in each simulation round, which means that the locations of the user devices and anchors were randomly generated in each round. We could see from the anchor selection results that it is possible to get the PEB really close to the ideal results with the prior information based method, considering the assumptions and parameters that were used. The result did not depend on the size of the area or the number of base stations in the area. Besides the average positioning accuracy, the prior information based method also had a low variation between the PEB results in different simulation rounds, and therefore, it can be considered as a method that produces reliable results without significant variation compared to the average PEB. The

SNR and norm-based methods also perform well when compared to the random selection of anchors. However, the simulations show that prior information based method is better, especially when the number of selected anchors is 2–3. Despite the total number of anchors in the area, similar PEB results can be obtained with all methods if there is a possibility to take many positioning measurements. However, since we want to have high energy efficiency, the small number of selected anchors is preferred.

We made some assumptions to avoid the complexity, for example, LoS was assumed in both CRLB and anchor selection simulations. In reality, multipath propagation is a common challenge in wireless communications, and this must be taken into account in real-world implementations. However, the simulated results we have obtained represent the best possible performance with the numerologies used. In any case, the comparison of different selection methods is possible with the assumptions made, and our goal was to find the best method for anchor selection and compare relative performances.

In the anchor selection part, our perspective was to compare the different selection methods, and therefore we had a scenario where the user device position was known. In real positioning cases, the position of user device is not known and this creates a different scenario and new challenges for anchor selection. It should still be possible to perform positioning in this case, but we would need more precise prior information about the position or movements of the user device. The possible solution could be to use some estimation filters, for example, KF presented in Section 4.5. Therefore, the creation of algorithms for the actual positioning solution, including the presented anchor selection method, would require more research and development. We obtained simulated positioning accuracy results for different anchor selection methods in the DECT-2020 NR network, and we compared the results with the ideal selection. We could see the differences with different number of selected anchors. These results answered to the research question 3.

In the end, we got answers to all the research questions, taking into account the necessary assumptions we made. An interesting topic for further research would be to do measurements, for example ToA, AoA, and RSS, in the real DECT-2020 NR network, and compare the results with the theoretical results. Developing the anchor selection methods into a practical system is also an interesting topic for the future. In conclusion, the thesis presents the best performance accuracy bounds for positioning with the AoA and ToA positioning methods in DECT-2020 NR networks. The thesis also includes the study of anchor selection methods to achieve efficient user positioning in DECT-2020 NR networks. The results show that there are significant differences in positioning accuracy results with different combinations of selected anchors. The results are theoretical and certain assumptions have been made. With these assumptions, a suitable method for selecting the anchors for positioning has been presented. This method is computationally efficient, keeps battery consumption low, and gives good positioning results.

REFERENCES

- [1] ETSI. *Digital Enhanced Cordless Telecommunications (DECT)*. URL: <https://www.etsi.org/technologies/dect> (visited on 03/22/2024).
- [2] T. Nihtilä and H. Berg. “Energy Consumption of DECT-2020 NR Mesh Networks”. *2022 Joint European Conference on Networks and Communications & 6G Summit (EuCNC/6G Summit)*. IEEE. 2022, pp. 196–201. DOI: 10.1109/EuCNC/6GSummit54941.2022.9815770.
- [3] K. Ashton. “That ‘internet of things’ thing”. *RFID journal* 22.7 (2009).
- [4] M. Vaezi, A. Azari, S. R. Khosravirad, M. Shirvanimoghaddam, M. M. Azari, D. Chasaki and P. Popovski. “Cellular, Wide-Area, and Non-Terrestrial IoT: A Survey on 5G Advances and the Road Toward 6G”. *IEEE Communications surveys and tutorials* 24.2 (2022), pp. 1117–1174. ISSN: 1553-877X. DOI: 10.1109/COMST.2022.3151028.
- [5] W. E. Zhang, Q. Z. Sheng, A. Mahmood, M. Zaib, S. A. Hamad, A. Aljubairy, A. A. F. Alhazmi, S. Sagar, C. Ma et al. “The 10 research topics in the Internet of Things”. *2020 IEEE 6th International Conference on Collaboration and Internet Computing (CIC)*. IEEE. 2020, pp. 34–43. DOI: 10.1109/CIC50333.2020.00015.
- [6] S. Li, L. D. Xu and S. Zhao. “The internet of things: a survey”. *Information systems frontiers* 17 (2015), pp. 243–259. DOI: 10.1007/s10796-014-9492-7.
- [7] S. C. Mukhopadhyay and N. K. Suryadevara. *Internet of things: Challenges and opportunities*. Springer, 2014. DOI: 10.1007/978-3-319-04223-7_1.
- [8] F. P. G. Márquez. *Internet of Things*. IntechOpen, 2021. ISBN: 1-83968-851-3. DOI: 10.1007/978-3-030-70478-0.
- [9] M. H. Miraz, M. Ali, P. S. Excell and R. Picking. “A review on Internet of Things (IoT), Internet of everything (IoE) and Internet of nano things (IoNT)”. *2015 Internet Technologies and Applications (ITA)* (2015), pp. 219–224. DOI: 10.1109/ITechA.2015.7317398.
- [10] P. Figueiredo e Silva, V. Kaseva and E. S. Lohan. “Wireless positioning in IoT: A look at current and future trends”. *Sensors* 18.8 (2018). DOI: 10.3390/s18082470.
- [11] M. I. Hossain, L. Lin and J. Markendahl. “A Comparative Study of IoT-Communication Systems Cost Structure: : Initial Findings of Radio Access Networks Cost”. *2018 11th CMI International Conference: Prospects and Challenges Towards Developing a Digital Economy within the EU*. 2018, pp. 49–55. DOI: 10.1109/PCTDDE.2018.8624853.

- [12] M. Burhan, R. A. Rehman, B. Khan and B.-S. Kim. "IoT elements, layered architectures and security issues: A comprehensive survey". *sensors* 18.9 (2018). DOI: 10.3390/s18092796.
- [13] S. A. Abdulhussien and S. K. Ibrahim. "Effects of Wireless Sensor Network Topology on Response Time". *2020 International Conference on Electrical, Communication, and Computer Engineering (ICECCE)*. 2020, pp. 1–5. DOI: 10.1109/ICECCE49384.2020.9179353.
- [14] ETSI. *DECT-2020 New Radio (NR); Part 1: Overview*. TS 103 636-1. Version 1.4.1. Jan. 2023. URL: https://www.etsi.org/deliver/etsi_ts/103600_103699/10363601/01_04_01_60/ts_10363601v010401p.pdf (visited on 03/22/2024).
- [15] S. Tayeb, S. Latifi and Y. Kim. "A survey on IoT communication and computation frameworks: An industrial perspective". *2017 IEEE 7th annual Computing and Communication Workshop and Conference (CCWC)*. IEEE. 2017, pp. 1–6. DOI: 10.1109/CCWC.2017.7868354.
- [16] LoRa Alliance. *LoRa Alliance - Homepage*. URL: <https://lora-alliance.org/> (visited on 03/22/2024).
- [17] Sigfox. *Geolocation technologies*. URL: <https://build.sigfox.com/geolocation-technologies> (visited on 03/22/2024).
- [18] Connectivity Standards Alliance. *CSA-IOT - Connectivity Standards Alliance*. URL: <https://csa-iot.org/> (visited on 03/22/2024).
- [19] Z-Wave. *Z-Wave*. URL: <https://www.z-wave.com/> (visited on 03/22/2024).
- [20] Z-Wave Alliance. *Z-Wave Alliance*. URL: <https://z-wavealliance.org/> (visited on 03/22/2024).
- [21] ABI Research. *DECT 2020 NR: Sustainability and Scale for the IoT*. Tech. rep. Sept. 2022.
- [22] Wirepas. *From standard to proof of concept: Wirepas and Nordic Semiconductor demonstrate the world's first non-cellular 5G connection*. URL: <https://www.wirepas.com/news-and-more/from-standard-to-proof-of-concept> (visited on 03/22/2024).
- [23] ETSI. *ETSI Launches DECT-2020: New Radio Interface for IoT*. Oct. 20, 2020. URL: <https://www.etsi.org/newsroom/press-releases/1839-2020-10-etsi-launches-dect-2020-new-radio-interface-for-iot> (visited on 03/22/2024).
- [24] ETSI. *World's first non-cellular 5G technology, ETSI DECT-2020, gets ITU-R approval, setting example of new era connectivity*. Oct. 19, 2021. URL: <https://www.etsi.org/newsroom/press-releases/1988-2021-10-world-s-first-non-cellular-5g-technology-etsi-dect-2020-gets-itu-r-approval-setting-example-of-new-era-connectivity> (visited on 03/22/2024).
- [25] O. Liberg. *The Cellular Internet of Things*. Oct. 24, 2017. URL: <https://www.3gpp.org/news-events/3gpp-news/c-iot> (visited on 03/22/2024).
- [26] M. T. Abbas, K.-J. Grinnemo, J. Eklund, S. Alfredsson, M. Rajiullah, A. Brunstrom, G. Caso, K. Kousias and Ö. Alay. "Energy-saving solutions for cellular internet

- of things—a survey”. *IEEE Access* 10 (2022), pp. 62073–62096. DOI: 10.1109/ACCESS.2022.3182400.
- [27] M. Penner, M. Nabeel and J. Peissig. “URLLC performance evaluation of IMT-2020 candidate technology: DECT-2020 new radio”. *2021 IEEE 94th Vehicular Technology Conference (VTC2021-Fall)*. IEEE. 2021, pp. 1–7. DOI: 10.1109/VTC2021-Fall52928.2021.9625340.
- [28] B. Foubert and N. Mitton. “Long-range wireless radio technologies: A survey”. *Future internet* 12.1 (2020). DOI: 10.3390/fi12010013.
- [29] T. Pedersen, B. H. Fleury and COST Action CA15104, IRACON. *Whitepaper on New Localization Methods for 5G Wireless Systems and the Internet-of-Things*. Tech. rep. Apr. 2018. URL: <http://www.iracon.org/wp-content/uploads/2018/03/IRACON-WP2.pdf> (visited on 03/22/2024).
- [30] X. Lin, J. Bergman, F. Gunnarsson, O. Liberg, S. M. Razavi, H. S. Razaghi, H. Rydn and Y. Sui. “Positioning for the Internet of Things: A 3GPP Perspective”. *IEEE Communications Magazine* 55.12 (2017), pp. 179–185. DOI: 10.1109/MCOM.2017.1700269.
- [31] K. Mekki, E. Bajic, F. Chaxel and F. Meyer. “Overview of cellular LPWAN technologies for IoT deployment: Sigfox, LoRaWAN, and NB-IoT”. *2018 IEEE International Conference on Pervasive Computing and Communications Workshops (PerCom Workshops)*. IEEE. 2018, pp. 197–202. DOI: 10.1109/PERCOMW.2018.8480255.
- [32] Y. Li, Y. Zhuang, X. Hu, Z. Gao, J. Hu, L. Chen, Z. He, L. Pei, K. Chen, M. Wang, X. Niu, R. Chen, J. Thompson, F. M. Ghannouchi and N. El-Sheimy. “Toward Location-Enabled IoT (LE-IoT): IoT Positioning Techniques, Error Sources, and Error Mitigation”. *IEEE Internet of Things Journal* 8.6 (2021), pp. 4035–4062. DOI: 10.1109/JIOT.2020.3019199.
- [33] J. Numminen. “DECT-2020: new radio, new capabilities”. *Connect-World Europe* 1 (2021), pp. 10–11. URL: <https://connect-world.com/dect-2020-new-radio-new-capabilities/> (visited on 03/22/2024).
- [34] M. D. Perez-Guirao, T. Weisshaupt and A. Wilzeck. “DECT NR+: Unveiling the Essentials of a new non-cellular 5G Standard for Verticals”. *Mobile Communication-Technologies and Applications; 26th ITG-Symposium*. VDE. 2022, pp. 1–6.
- [35] R. Kovalchukov, D. Moltchanov, J. Pirskanen, J. S ae, J. Numminen, Y. Koucheryavy and M. Valkama. “DECT-2020 New Radio: The Next Step toward 5G Massive Machine-Type Communications”. *IEEE Communications Magazine* 60.6 (2022), pp. 58–64. DOI: 10.1109/MCOM.001.2100375.
- [36] ITU. *Committed to connecting the world*. URL: <https://www.itu.int/en/Pages/default.aspx> (visited on 03/22/2024).
- [37] ETSI. *About ETSI*. URL: <https://www.etsi.org/about> (visited on 03/22/2024).

- [38] European Commission. *Key Players in European Standardisation*. URL: https://single-market-economy.ec.europa.eu/single-market/european-standards/key-players-european-standardisation_en (visited on 03/22/2024).
- [39] European Union. *Regulation (EU) No 1025/2012 of the European Parliament and of the Council*. 2012. URL: <https://eur-lex.europa.eu/legal-content/EN/TXT/?uri=CELEX:32012R1025> (visited on 03/22/2024).
- [40] ETSI. *Technical Committee (TC) Digital Enhanced Cordless Telecommunications (DECT)*. URL: <https://www.etsi.org/committee/dect> (visited on 03/22/2024).
- [41] DECT Forum. *Organisation*. URL: <https://www.dect.org/organisation> (visited on 03/22/2024).
- [42] DECT Forum. *Mission*. URL: <https://www.dect.org/mission> (visited on 03/22/2024).
- [43] DECT Forum. *NR+ Working Group*. URL: <https://www.dect.org/wg-dect-5g-business> (visited on 03/22/2024).
- [44] A. Samuylov, D. Moltchanov, J. Pirskanen, J. Numminen, Y. Koucheryavy and M. Valkama. "Performance Assessment of DECT-2020 NR and Classic DECT Coexistence Mechanisms". *2023 IEEE 97th Vehicular Technology Conference (VTC2023-Spring)*. 2023, pp. 1–7. DOI: 10.1109/VTC2023-Spring57618.2023.10200362.
- [45] ITU. *Detailed specifications of the radio interfaces of International Mobile Telecommunications-2000 (IMT-2000)*. Recommendation ITU-R M.1457-0. May 2000. URL: https://www.itu.int/dms_pubrec/itu-r/rec/m/R-REC-M.1457-0-200005-S!!PDF-E.pdf (visited on 03/22/2024).
- [46] ITU. *Detailed information about the IMT-family*. URL: <https://www.itu.int/en/ITU-R/study-groups/rsg5/rwp5d/Pages/IMT.aspx> (visited on 03/22/2024).
- [47] ITU. *Minimum requirements related to technical performance for IMT-2020 radio interface (s)*. Report ITU-R M.2410-0. Nov. 2017. URL: https://www.itu.int/dms_pub/itu-r/opb/rep/R-REP-M.2410-2017-PDF-E.pdf (visited on 03/22/2024).
- [48] ITU. *Requirements, evaluation criteria and submission templates for the development of IMT-2020*. Report ITU-R M.2411-0. Nov. 2017. URL: https://www.itu.int/dms_pub/itu-r/opb/rep/R-REP-M.2411-2017-PDF-E.pdf (visited on 03/22/2024).
- [49] ITU. *Guidelines for evaluation of radio interface technologies for IMT-2020*. Report ITU-R M.2412-0. Oct. 2017. URL: https://www.itu.int/dms_pub/itu-r/opb/rep/R-REP-M.2412-2017-PDF-E.pdf (visited on 03/22/2024).
- [50] V. Dhanwani, N. Kumar, A. K. Bachkaniwala, D. Rawal and S. Kumar. "Assessment of Candidate Technology ETSI: DECT-2020 New Radio". *2020 IEEE 3rd 5G World Forum (5GWF)*. 2020, pp. 625–630. DOI: 10.1109/5GWF49715.2020.9221186.
- [51] A. Anttonen, P. Karhula, M. Lasanen and M. Majanen. *Enabling Massive Machine Type Communications with DECT-2020 Standard: A System-Level Performance Study*. Tech. rep. VTT-R-00367-21. 2021. URL: <https://cris.vtt.fi/en/publications/enabling-massive-machine-type-communications-with-dect-2020-stand> (visited on 03/22/2024).

- [52] S. Soni, R. Makkar, T. Singhwi, D. Rawal, N. Sharma and L. Minz. "On Performance of multi-hop assisted mMTC for DECT-2020 New Radio System". *2021 International Conference on Information and Communication Technology Convergence (ICTC)*. 2021, pp. 984–988. DOI: 10.1109/ICTC52510.2021.9620940.
- [53] T. Singhwi, S. Andra, S. J. Seelam, R. Makkar, D. Rawal and N. Sharma. "DECT-2020 New Radio System Level Assessment for Multi-Hop Assisted mMTC usage Scenario". *2021 IEEE International Conference on Advanced Networks and Telecommunications Systems (ANTS)*. 2021, pp. 1–6. DOI: 10.1109/ANTS52808.2021.9936990.
- [54] K. Maliatsos, A. Gotsis and A. Alexiou. "Evaluation of the IMT-2020 Candidate Radio Interface Technology DECT-2020 NR". *2022 14th International Conference on COMmunication Systems & NETworkS (COMSNETS)*. 2022, pp. 889–893. DOI: 10.1109/COMSNETS53615.2022.9668561.
- [55] ITU. *Detailed specifications of the terrestrial radio interfaces of International Mobile Telecommunications-2020 (IMT-2020)*. Recommendation ITU-R M.2150-1. Feb. 2022. URL: https://www.itu.int/dms_pubrec/itu-r/rec/m/R-REC-M.2150-1-202202-S!!PDF-E.pdf (visited on 03/22/2024).
- [56] ITU. *The outcome of the evaluation, consensus building and decision of the IMT-2020 process (Steps 4 to 7), including characteristics of IMT-2020 radio interfaces*. Report ITU-R M.2483-0. July 2020. URL: https://www.itu.int/dms_pub/itu-r/opb/rep/R-REP-M.2483-2020-PDF-E.pdf (visited on 03/22/2024).
- [57] ITU. *Fourth radio interface technology added to 5G standards*. Feb. 24, 2022. URL: <https://www.itu.int/en/mediacentre/Pages/PR-2022-02-24-5G-Standards.aspx> (visited on 03/22/2024).
- [58] ETSI. *ETSI - Welcome to the World of Standards!* European Telecommunications Standards Institute (ETSI). URL: <https://www.etsi.org/> (visited on 03/22/2024).
- [59] ETSI. *Types of standards*. URL: <https://www.etsi.org/standards/types-of-standards> (visited on 03/22/2024).
- [60] ETSI. *TC DECT Activity report 2022*. URL: <https://www.etsi.org/committee-activity/activity-report-dect> (visited on 03/22/2024).
- [61] P. Olanders. "DECT standardisation: status and future activities". *5th IEEE International Symposium on Personal, Indoor and Mobile Radio Communications, Wireless Networks - Catching the Mobile Future*. Vol. 4. 1994, pp. 1064–1069. DOI: 10.1109/WNCMF.1994.529418.
- [62] ETSI. *Digital Enhanced Cordless Telecommunications (DECT); A high level guide to the DECT standardization*. Technical Report (TR) 178. Jan. 1997. URL: https://www.etsi.org/deliver/etsi_etr/100_199/178/02_60/etr_178e02p.pdf (visited on 03/22/2024).
- [63] ETSI. *Digital Enhanced Cordless Telecommunications (DECT); DECT-2020 New Radio (NR) interface; Study on Physical (PHY) layer*. Technical Report (TR) 103

514. Version 1.1.1. July 2018. URL: https://www.etsi.org/deliver/etsi_tr/103500_103599/103514/01.01.01_60/tr_103514v010101p.pdf (visited on 03/22/2024).
- [64] ITU-R Working Party 5D. *Acknowledgement of candidate SRIT submission from ETSI (TC DECT) and DECT Forum under Step 3 of the IMT-2020 process*. Document IMT-2020/17-E. Dec. 16, 2019. URL: <https://www.itu.int/md/R15-IMT.2020-C-0017/en> (visited on 03/22/2024).
- [65] ETSI. *DECT-2020 New Radio (NR); Part 2: Radio reception and transmission requirements*. TS 103 636-2. Version 1.4.1. Jan. 2023. URL: https://www.etsi.org/deliver/etsi_ts/103600_103699/10363602/01.04.01_60/ts_10363602v010401p.pdf (visited on 03/22/2024).
- [66] ETSI. *DECT-2020 New Radio (NR); Part 3: Physical layer*. TS 103 636-3. Version 1.4.1. Jan. 2023. URL: https://www.etsi.org/deliver/etsi_ts/103600_103699/10363603/01.04.01_60/ts_10363603v010401p.pdf (visited on 03/22/2024).
- [67] ETSI. *DECT-2020 New Radio (NR); Part 4: MAC layer*. TS 103 636-4. Version 1.4.1. Jan. 2023. URL: https://www.etsi.org/deliver/etsi_ts/103600_103699/10363604/01.04.01_60/ts_10363604v010401p.pdf (visited on 03/22/2024).
- [68] ETSI. *DECT-2020 New Radio (NR); Part 5: DLC and Convergence layers*. TS 103 636-5. Version 1.4.1. Jan. 2023. URL: https://www.etsi.org/deliver/etsi_ts/103600_103699/10363605/01.04.01_60/ts_10363605v010401p.pdf (visited on 03/22/2024).
- [69] S. Sand, A. Dammann and C. Mensing. *Positioning in Wireless Communications Systems*. Wiley, 2014. ISBN: 9780470770641.
- [70] G. Mao, B. Fidan and B. D. O. Anderson. “Wireless sensor network localization techniques”. *Computer Networks* 51.10 (2007), pp. 2529–2553. DOI: 10.1016/j.comnet.2006.11.018.
- [71] A. Boukerche, H. A. B. F. Oliveira, E. F. Nakamura and A. A. F. Loureiro. “Localization systems for wireless sensor networks”. *IEEE Wireless Communications* 14.6 (2007), pp. 6–12. DOI: 10.1109/MWC.2007.4407221.
- [72] L. Cheng, C. Wu, Y. Zhang, H. Wu, M. Li and C. Maple. “A Survey of Localization in Wireless Sensor Network”. *International Journal of Distributed Sensor Networks* 8.12 (2012). DOI: 10.1155/2012/962523.
- [73] W. Liu, X. Luo, G. Wei and H. Liu. “Node localization algorithm for wireless sensor networks based on static anchor node location selection strategy”. *Computer Communications* 192 (2022), pp. 289–298. DOI: <https://doi.org/10.1016/j.comcom.2022.06.010>.
- [74] P. Tripathy and P. M. Khilar. “An ensemble approach for improving localization accuracy in wireless sensor network”. *Computer Networks* 219 (2022). DOI: 10.1016/j.comnet.2022.109427.
- [75] A. Norrdine. “An Algebraic Solution to the Multilateration Problem”. Apr. 2015. DOI: 10.13140/RG.2.1.1681.3602.

- [76] S. Alyafawi. “Real-Time Localization using Software Defined Radio”. PhD thesis. Universität Bern, Aug. 2015.
- [77] E. S. Lohan, J. Talvitie, P. Figueiredo e Silva, H. Nurminen, S. Ali-Löytty and R. Piché. “Received signal strength models for WLAN and BLE-based indoor positioning in multi-floor buildings”. *2015 International Conference on Localization and GNSS (ICL-GNSS)*. 2015, pp. 1–6. DOI: 10.1109/ICL-GNSS.2015.7217154.
- [78] R. Zekavat and R. M. Buehrer. *Handbook of Position Location: Theory, Practice, and Advances*. 2nd ed. IEEE Series on Digital & Mobile Communication. Wiley, 2019. ISBN: 1119434580.
- [79] J. Hua, Y. Yin, W. Lu, Y. Zhang and F. Li. “NLOS Identification and Positioning Algorithm Based on Localization Residual in Wireless Sensor Networks”. *Sensors* 18.9 (2018). DOI: 10.3390/s18092991.
- [80] S. M. Kay. *Fundamentals of Statistical Signal Processing, Volume I: Estimation Theory*. Prentice-Hall, Inc., 1993. ISBN: 0133457117.
- [81] S. M. Kay. *Fundamentals of Statistical Signal Processing, Volume III: Practical Algorithm Development*. Pearson, 2017. ISBN: 9780132808057.
- [82] F. Qiu and W. Zhang. “Position error vs. signal measurements: An analysis towards lower error bound in sensor network”. *Digital Signal Processing* 129 (2022). DOI: 10.1016/j.dsp.2022.103637.
- [83] S. B. Weinstein. “The history of orthogonal frequency-division multiplexing [History of Communications]”. *IEEE Communications Magazine* 47.11 (2009), pp. 26–35. DOI: 10.1109/MCOM.2009.5307460.
- [84] Z. Abu-Shaban, X. Zhou, T. Abhayapala, G. Seco-Granados and H. Wymeersch. “Error Bounds for Uplink and Downlink 3D Localization in 5G Millimeter Wave Systems”. *IEEE Transactions on Wireless Communications* 17.8 (2018), pp. 4939–4954. DOI: 10.1109/TWC.2018.2832134.
- [85] F. Qiu and W. Zhang. “Efficient cooperative localization method with node selection based on position error bound”. *Signal Processing* 209 (2023). DOI: 10.1016/j.sigpro.2023.109037.
- [86] H. Schulten. “Localization and Posture Recognition via Magneto-Inductive and Relay-Aided Sensor Networks”. Doctoral Thesis. Zurich, 2022. DOI: 10.3929/ethz-b-000574826.
- [87] D. Dardari, M. Luise and E. Falletti. *Satellite and Terrestrial Radio Positioning Techniques - A Signal Processing Perspective*. 1st ed. Elsevier, 2012. ISBN: 0123820847.